Digitized Theses

Digitized Special Collections

1978

# Theoretical And Experimental Studies For Optimization Of The Thermal Performance Of Adiabatic Calorimeters

Fahmy Mahmoud Hussein

Follow this and additional works at: https://ir.lib.uwo.ca/digitizedtheses

## NOTICE

## AVIS

The quality of this microfiche is heavily dependent upon the quality of the original thesis submitted for microfilming Every effort has been made to ensure the highest quality of reproduction possible.

If pages are missing, contact the university which granted the degree.

Some pages may have indistinct print especially if the original pages were typed with a poor typewriter ribbon or if the university sent us a poor photocopy

Previously copyrighted materials (journal articles, published tests, etc.) are not filmed.

Reproduction in full or in part of this film is governed by the Canadian Copyright Act, R.S.C. 1970, c. C-30. Please read the authorization forms which accompany this thesis.

La qualité de cette microfiche dépend grandement de la qualité de la thèse soumise au microfilmage. Nous avons tout fait pour assurer une qualité supérieure de reproduction.

S'il manque des pages, veuillez communiquer avec l'université qui a conféré le grade.

La qualité d'impression de certaines pages peut laisser à désirer, surtout si les pages originales ont ete dactylographiées à l'aide d un ruban usé ou si l université nous a fait parvenir une photocopie de mauvaise qualité.

Les documents qui font déjà l objet d un droit d auteur (articles de revue, examens publiés, etc.) ne sont pas microfilmés.

La reproduction, même partielle, de ce microfilm est soumise à la Loi canadienne sur le droit d'auteur, SRC. 1970, c. C-30. Veuillez prendre connaissance des formules d'autorisation qui accompagnent cette thèse.

## THIS DISSERTATION HAS BEEN MICROFILMED EXACTLY AS RECEIVED

## LA THÈSE A ÉTÉ MICROFILMÉE TELLE QUE NOUS L'AVONS REÇUE

THEORETICAL AND EXPERIMENTAL STUDIES

FOR OPTIMIZATION OF THE THERMAL

PERFORMANCE OF ADIABATIC CALORIMETERS

by

Fahmy M. Hussein

Faculty of Engineering Science

Submitted in partial fulfillment

of the requirements for the degree

of Doctor of Philosophy

Faculty of Graduate Studies

The University of Western Ontario

London, Canada

April 1978

# ABSTRACT

Comprehensive studies have been made on factors (and their principles) affecting the performance of a non-flow adiabatic calorimeter containing a pure substance with co-existing liquid and vapour phases. A systematic study of calorimeter shell strain energy, fluid vapour surface energy, absolute temperature scale, and most importantly the heat leak over a range of temperatures from 100 to 300°C was conducted.

A detailed examination of the parameters affecting the heat leak, (and hence the performance of the calorimeter) was conducted. Detailed studies indicated that the overall parameters affecting the heat leak such as

(i)  the overall average temperature difference between the calorimeter shell and adiabatic shield,

(ii) surface area of the calorimeter shell and adiabatic shield,

(iii) overall heat transfer coefficient,

are themselves functions of the engineering design of calorimeters as well as experimental procedures.

Detailed experimental investigations on light water indicated the respective relative importance of these factors and parameters on the accuracy of the calorimetric measurements

iii

of thermodynamic properties. These investigations further showed that the heat leak is the single most important parameter affecting the final calorimetric measurements. The absolute magnitude of the heat leak is not unique and will be different for different calorimeters.

A mathematical model has been developed for optimizing the performance and for minimizing the heat leak of the calorimeter. This model was verified experimentally and excellent agreement was found between experiment and theory. Based on this theory, the current U.W.O. non-flow adiabatic calorimeter should be operated at the most optimum heating rate of 8°C per hour.

A computer controlled data acquisition system for data storage, analysis and correlation has been designed and developed to facilitate data collection and analysis. Improvements are thus made possible to facilitate

(i) collection of a greater quantity of data at much finer and smaller increments of time and consequently greater description and knowledge of the process.

(ii) more sophisticated techniques of data analysis.

# ACKNOWLEDGEMENTS

# TABLE OF CONTENTS

viii

# LIST OF TABLES

x

## LIST OF FIGURES

xiii

# NOMENCLATURE

| | |
|---|---|
| A | Area |
| A | Numerical constant |
| a | Linear coefficient of thermal expansion |
| B | Numerical constant |
| $r_i$ | Inner radius of the calorimeter |
| $r_o$ | Outer radius of the calorimeter |
| E | Modulus of elasticity |
| h | Specific enthalpy |
| $h_f$ | Specific enthalpy of saturated liquid |
| $h_{fg}$ | Specific enthalpy of vaporization |
| $h_g$ | Specific enthalpy of saturated vapour |
| I | Current through the calorimeter heater |
| M | Mass of the fluid sample |
| $M_H$ | Mass of the fluid sample in the high filling experiment |
| $M_L$ | Mass of the fluid sample in the low filling experiment |
| $m'$ | Mass of saturated liquid |
| $m''$ | Mass of saturated vapour |
| $m_f$ | Mass of the saturated liquid |
| $m_g$ | Mass of the saturated vapour |
| P | Power supplied to the calorimeter |
| P | Saturation pressure |
| $P_i$ | Pressure in the calorimeter |

| | |
|---|---|
| $P_O$ | Pressure outside the calorimeter shell |
| $W$ | Energy added to the calorimeter |
| $W_H$ | Energy added during the high filling constant mass experiment |
| $W_L$ | Energy added during the low filling constant mass experiment |
| $Cp_C \Delta T$ | Heat capacity of the empty calorimeter |
| $q_E$ | Total heat leak to or from the calorimeter |
| $q_{E_H}$ | Total heat leak in the high filling experiment |
| $q_{E_L}$ | Total heat leak in the low filling experiment |
| $W_S$ | Total straining energy on the calorimeter shell |
| $W_{S.E.}$ | Total energy produced by the surface tension effect |
| $W_{S.E._H}$ | Total surface energy during the high filling experiment |
| $W_{S.E._L}$ | Total surface energy during the low filling experiment |
| $\hat{W}_{S_H}$ | Total straining energy on the calorimeter shell during the high filling experiment |
| $W_{S_L}$ | Total straining energy on the calorimeter shell during the low filling experiment |
| $R$ | Radius of curvature |
| $R_e$ | Resistance of the thermometer |
| $T$ | Absolute temperature |
| $t$ | Thickness of the calorimeter shell |
| $U_S$ | Change in internal energy |
| $u_f$ | Specific internal energy of the saturated liquid |

| | |
|---|---|
| $u_g$ | Specific internal energy of the saturated vapour |
| V | Internal volume of the calorimeter |
| v | Voltage across the calorimeter heater |
| v' | Specific volume of saturated liquid |
| v'' | Specific volume of saturated vapour |
| $v_f$ | Specific volume of saturated liquid |
| $v_g$ | Specific volume of saturated vapour |
| y | Height of vapour in the calorimeter |
| dP/dT | Change in total pressure with respect to absolute temperature |
| dT/dτ | Heating rate |
| dV | Element of volume |
| α | Thermal diffusivity |
| α | Thermometer coefficient |
| δ | Temperature scale constant |
| $δ_{48}$ | International Temperature Scale of 1948 constant |
| $δ_{68}$ | International Temperature Scale of 1968 constant |
| ε | Emmissivity |
| γ | Specific weight of the liquid contained in the calorimeter |
| μ | Poisson's ratio |
| σ | Stefan Boltzman's constant |
| σ | Surface tension coefficient |
| τ | Time |

# CHAPTER 1

## INTRODUCTION

### 1.1 GENERAL

In the last few years, especially after the oil embargo of 1973 and the consequent energy crisis, a great interest in new energy sources has developed, with particular emphasis on nuclear energy. As a result, there has been an acceleration in the development of nuclear power stations throughout the world.

However, the problem which arises in the production of nuclear energy is the enrichment of uranium, and since light water has a relatively high absorption cross section for neutron capture (14)*, a critical system can be attained with such water as moderator only if uranium enriched in the fissile isotope is used as fuel.

In this regard, Canada has been engaged in the design and development of heavy water moderated and heavy water cooled nuclear reactors with natural uranium as a fuel. The physical advantages of heavy water ($D_2O$) as a moderator are well known and there has been a great interest in its use with natural uranium reactors. For example, heavy water has

---

*Numbers in parentheses refer to references in the Bibliography.

a satisfactory "slowing down power", a relatively small absorption cross section for neutron capture and an exceptionally high moderating ratio of 21000 as compared to 58 for light water (14). Therefore, it is considered an ideal medium for moderation.

The Candu system is recognized as the most advanced heavy water moderated and heavy water cooled nuclear power system in the world. In the Candu reactor system since the heavy water is used both as a coolant and as a moderator, an exact knowledge of its thermal properties is highly desirable. For example, the enthalpy of heavy water is one of the most important properties affecting the size and capacity of heavy water circulation pumping equipment and heat exchangers. This may be explained with reference to the following equation

$$\dot{Q} = \dot{m} \, C_p \, \Delta T \qquad\qquad (1.1)$$

where

$\dot{Q}$ is the rate of heat removal from fuel bundles,

$\dot{m}$ is the rate of heavy water coolant flow,

$C_p$ is the specific heat of heavy water, and

$\Delta T$ is the temperature rise of the heavy water coolant

From the equation we notice that the product of $\dot{m}$ and $c_p$ is a constant for a constant value of the ratio ($\dot{Q}/\Delta T$). The size of heat exchanger equipment in a Candu nuclear reactor

power station is directly dependent on the mass rate of flow of heavy water as well as the specific heat of heavy water. Furthermore, thermal conductivity, dynamic viscosity, and P-V-T property are important factors in the safe operations of nuclear reactors for: heat removal from fuel bundles, controlling heavy water circulation and as a characteristic of the design and operation of the water pumping equipment respectively.

## 1.2   OBJECTIVE AND SCOPE OF RESEARCH

Since there is little precise information for the thermo-dynamic properties of heavy water, especially at pressures and temperatures corresponding to operating conditions of Candu reactors, it was necessary to study the factors affecting the results of the previous measurements in an attempt to obtain more accurate results.

Therefore, one of the main objectives of the research with which this thesis is concerned was to evaluate the influence of factors affecting the calorimetric measurements of enthalpy of heavy water specifically and of any two phase (vapour liquid) fluid system generally. Those factors which have been under extensive study, both theoretically and experimentally are:  heat leak, calorimeter shell strain energy, vapour liquid surface energy and changing of the absolute temperature scale. From these studies, improvements can be

made to the calorimeter design. Optimzation of the experi-
mental procedure for the operation of apparatus is thus made
possible. For example, minimization of heat leak is es-
pecially important. In turn, this requires studies of the
factors upon which heat leak depends, including heating rate,
temperature variations on both the calorimeter and adiabatic
shield surfaces, overall temperature difference between the
calorimeter and its surroundings, amount of sample contained
in the calorimeter, and experimental time. One of the factors
that might affect the calorimetric measurements is the change
in the calorimeter volume. However, previous investigations
(34) showed that this factor is small and therefore its
effect is negligible especially because the effect is found
as the difference between two values for different calori-
meter charges as will be explained later.

The theory and measurement techniques were tested on light
water and the results obtained by theory and experiments
were gratifying.

# CHAPTER 2

## COMPREHENSIVE LITERATURE REVIEW ON
## CALORIMETRIC THEORY AND TECHNIQUES.

### 2.1  GENERAL

Several techniques of varying degrees of sophistication
and accuracy have been used for the calorimetric measurements
of the thermodynamic properties of fluids.  These techniques
are:  (i) adiabatic calorimetry, (ii) non-adiabatic calori-
metry, and (iii) comparison techniques in which a material
of known heat capacity is taken as a standard and is compared
with the material of unknown heat capacity.

Some forty years ago, Osborne et al. (44, 45, 46, 47,
48, 49) of the U.S. Bureau of Standards proposed, developed
and utilized a unique adiabatic calorimeter method in their
highly noteworthy calorimeter investigations on light water
under conditions of coexisting liquid and vapour.  The re-
sults on light water from these pioneer investigations still
serve as an international standard.

The Osborne adiabatic calorimetric method was further
developed at the University of Western Ontario by a team of
graduate students under the direction of Professor E.S.
Nowak (7,8,32,35,36,37).  The U.W.O. calorimeter was somewhat
more sophisticated insofar as a spherical geometry was

5

utilized and two internal heaters were distributed through-
out the entire volume of the calorimeter.

The above apparatus and method was utilized in the re-
search of this thesis. Instead of internal heaters, capsule
and surface heaters were utilized in the investigations of
this research. Also, the calorimeter surface was in a highly
tarnished and oxidized condition.

A comparison technique was used by Baker (14) for the
determination of the heat capacity of heavy water. In these
investigations, the apparatus was calibrated using light
water as a standard.

The problem of zero heat leak between the calorimeter
and its surroundings has received differing treatments. In
most cases, the calorimeter system was designed in such a
way that the zero heat leak was very small and therefore was
neglected since it has no effect on the results (42, 44, 69).
For example, in reference (44), the total zero heat leak in
the range of between 200 and 250°C was found to be 7.7 Joules
as compared to a total energy added of 146112.6 Joules, from
which we find that the percentage of heat leak to total
energy added is 0.005%.

## 2.2. ADIABATIC·CALORIMETER TECHNIQUES

Osborne et al. at the U.S. Bureau of Standards, performed two experiments under the same conditions in order to elimi‐ nate the necessity of evaluating the energy expended in straining the calorimeter shell. The previously mentioned zero heat leak was evaluated using data from special measure‐ ments of heat exchange. These experimental corrections for heat leak were used in the data reduction leading to the final results of the different thermodynamic properties (48, 49). In all cases, it would appear that the heat leak did not exceed 0.01% of the total electrical energy added.

Osborne (47) mentioned that for confining energy, the calorimeter should be well insulated from the influence of external sources of heat. In his apparatus, the metal calo‐ rimeter shell C with dimensions of 14 cm by 6.3 cm (Figure 2.1) contained besides the water sample, small internal elec‐ tric heater H located at the bottom of the calorimeter and a system of radial silver plates D for diffusing heat. The calorimeter shell is suspended within a thermally controled inclosure or envelope E, the function of which is to oppose heat leak to or from the calorimeter system and to provide a means for determining the correction of the small unavoidable heat leak. This inclosure consists of two coaxial cylindrical silver shells with flat ends, the inner shell designated as
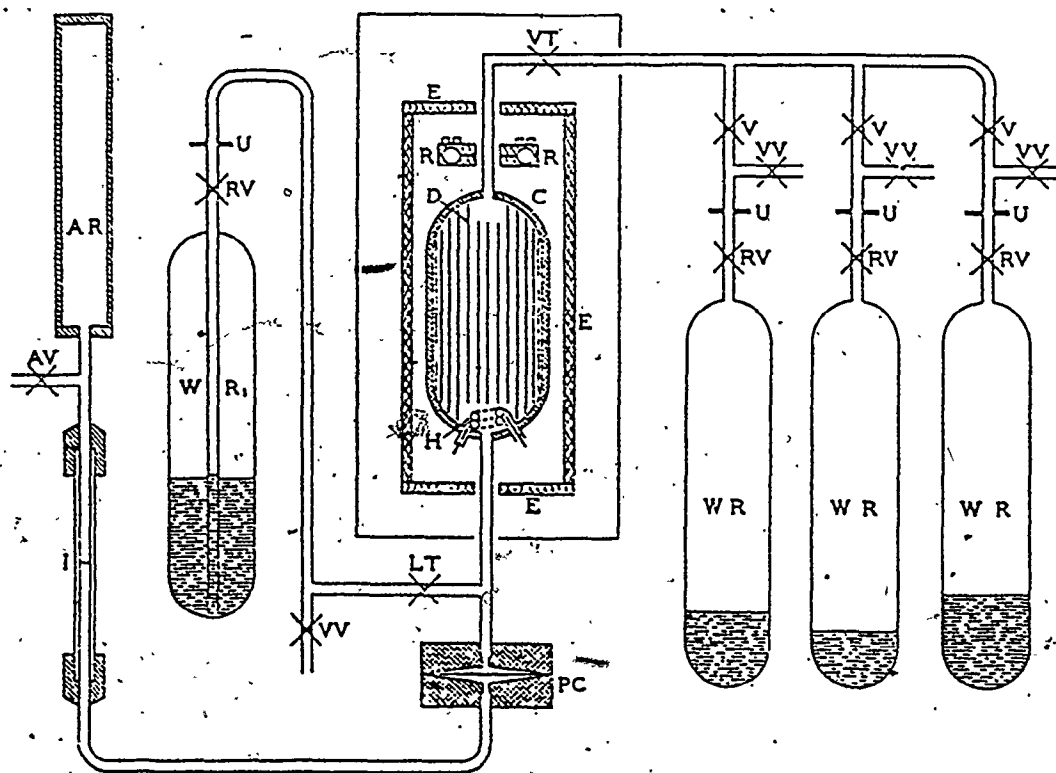
FIGURE 2.1  Schematic diagram of calorimeter equipment

C   Calorimeter shell
H   Electric heater
D   Heat-diffusion system
VT  Vapor throttle
LT  Liquid throttle
V   Shut-off valve
RV  Receiver valve
WR  Water receiver

U   Union
VV  Vaccum valve
I   Pressure indicator
PC  Pressure transmission cell
AR  Air receiver
R   Reference block
AV  Air valve

the "envelope" and the outer one the "guard". The dimensions of the envelope are 22.6 cm by 10 cm and its wall thickness is 6.3 mm while the dimensions of the guard are 26.3 cm by 12.6 cm and its wall thickness is 3.2 mm. In the space outside the guard, two thin aluminum shields of 0.06 mm thickness are placed to impede the loss of heat from the guard by radiation and convection.

Osborne also pointed out that for promoting temperature equalization in the calorimeter, the 30 flat plates of silver, 0.5 mm thick were shaped to conform closely to the vertical profile of the shell.

He mentioned that in the experiments, the zero heat leak was made small by instrumental and experimental precautions such as the use of numerous differential thermoelements to indicate the temperature differences between points on the calorimeter and points on its immediate surroundings. These temperature difference indications were observed and summed algebraically to give integrated heat-leak factors. These factors, when multiplied by an experimentally determined heat leak coefficient, gave the zero heat leak corrections. For example, results of a typical experiment between 200 and 210°C, Osborne (.47) had a zero heat leak factor of 5 microvolt-minutes and a heat leak coefficient of 0.129 Joules/microvolt-minutes. Therefore, the total zero heat leak in that experiment was found to be 0.6 Joules.

This magnitude of zero heat leak amounted to less than
0.002% of the total energy added.

In the non-flow adiabatic calorimetric method used for
the first time by Osborne, a fluid sample in two phase region
is placed in calorimeter.  Electrical energy is added to the
system for performing measurements on various types of thermo-
dynamic processes.  The first is a constant mass experiment
in which a fixed amount of fluid sample is contained in the
calorimeter and receives electrical energy which changes it
from an initial to a final saturation state.  The enthalpy
of saturated liquid is thus found in this type of experiment (7).
The second type is known as the isothermal liquid withdrawal
test, in which electrical energy is added to the contents of
the calorimeter and a measured amount of saturated liquid is
withdrawn at a constant temperature.  The third type is the
isothermal vapour withdrawal test, in which a definite
portion of the contents of the calorimeter is withdrawn as
saturated vapour at the calorimeter temperature which is
maintained constant during the experiment.

In the constant mass experiments, two experiments are
performed over the same temperature interval with different
amounts of mass in the calorimeter in order to eliminate the
necessity of evaluating the energy expended in straining the
calorimeter shell.

With the application of the First Law of Thermodynamics, Osborne obtained the following equation for the energy addition process in the constant mass experiments

$$-W_e = M[h_f - Tv_f \frac{dP}{dT}]_1^2 + (T V \frac{dP}{dT} - PV)_1^2 + M_c c_{p_c} \Delta T - q_{\delta T=0} \qquad (2.1)$$

where

$-W_e$ is the electrical energy added,

$q_{\delta T=0}$ is the zero heat leak ,

$M_c$ is the calorimeter mass, and

$c_{p_c}$ is the specific heat capacity of the empty calorimeter.

In order to determine the enthalpy of the fluid under investigation, Osborne obtained two equations for different calorimeter charges as follows,

$$-W_{e_H} = M_H [h_f - Tv_f \frac{dP}{dT}]_1^2 + (T V \frac{dP}{dT} - PV)_1^2$$

$$+ M_c c_{p_c} \Delta T - (q_{\delta T=0})_H \qquad (2.2)$$

$$-W_{e_L} = M_L [h_f - Tv_f \frac{dP}{dT}]_1^2 + (T V \frac{dP}{dT} - PV)_1^2$$

$$+ M_c c_{p_c} \Delta T - (q_{\delta T=0})_L \qquad (2.3)$$

where

$-W_{e_H}$ and $-W_{e_L}$ are the electrical energies added to the system when charged with masses $M_H$ and $M_L$ respectively, and

$(q_{\delta T=0})_H$ and $(q_\delta T=0)_L$ are the heat leaks corresponding to the two masses of $M_H$ and $M_L$ respectively.

When equations 2.2 and 2.3 are subtracted from one another, Osborne obtained the following equation for determining the enthalpy of saturated fluid and applied it to his system.

$$W_{e_L} - W_{e_H} = \alpha[M_H - M_L] - (q_{\delta T=0})_H + (q_{\delta T=0})_L$$

In spite of the fact that the zero heat leak for either low or high filling was virtually insignificant, Osborne painstakingly utilized experimental data to obtain extremely minute corrections for $(q_{\delta T=0})_H$ and $(q_{\delta T=0})_L$.

West and Ginnings (68) stated that their calorimeter is accurate to 0.1 percent in measuring the heat capacity of $Al_2O_3$ up to $500^\circ C$. They mentioned that in order to attain this accuracy, a number of factors were considered. Firstly, the evaluation of electric energy input to 0.01 percent was relatively easy to accomplish. Secondly, the use of a platinum resistance thermometer for measurement of the temperature change in the calorimeter yielded an accuracy comparable with that of the electric energy.

In their measurements, the procedure West and Ginnings used was the same as Osborne. That is to perform two types of experiments, one with the calorimeter filled with the sample and one with an empty calorimeter (or with a small amount of sample). They mentioned that this is one of the best procedures to eliminate heat leak errors and certain other errors which have the same absolute value in the two types of experiments. However, they said, this procedure does not eliminate heat leak errors which are different in the two types of experiments. This is because the very existence of the sample in the calorimeter during the heating interval makes the temperature distribution in the full calorimeter different from that in the empty calorimeter. Therefore, they mentioned that for high accuracy, it is essential to design a calorimeter having essentially the same temperature distribution over its outer surface in the two types of experiments. Furthermore, they stated that this has been accomplished in their calorimeter by using a series of thin silver shields.

In their apparatus, the calorimeter consisted of two main parts (i) a sample container (Figure 2.2) made from aluminum alloy 1100 in the form of a cylinder 5 cm high and 5 cm in diameter with a stainless-steel cover screwed on the bottom; (ii) a shield system consisting of a silver ring of 0.8 cm$^2$ in cross section to reduce temperature gradients due

Shield lid — Calorimeter lid

Support tube

Shield ring

Calorimeter ring

Thermometer

Container

Silver cups

Inner guard

Outer guard

1 inch
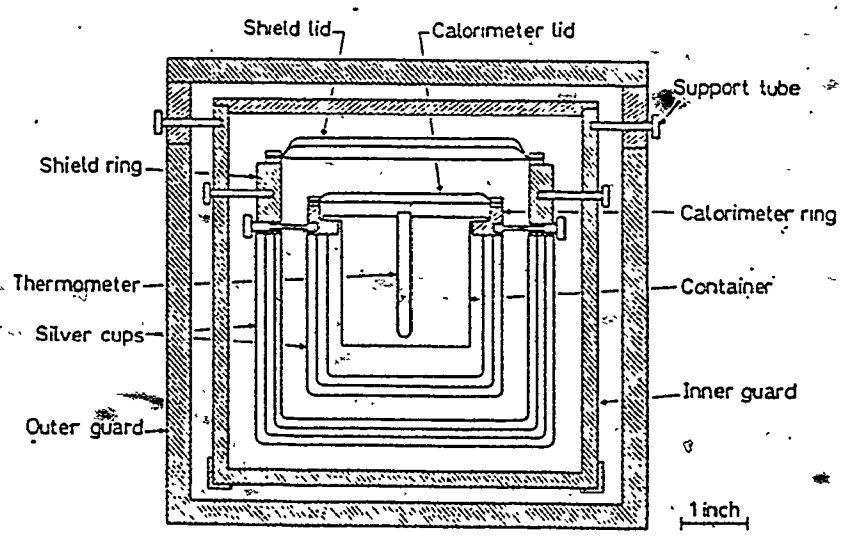
FIGURE 2.2   Schematic vertical section of the adiabatic calorimeter and associated thermostat

to circumferential heat flow. Silver soldered to the ring
are three silver shields each 0.25 mm thick. The function
of the shields is to provide an external surface on which the
effect of the gradients on the sample container and between
the sample container and the ring is greatly attenuated.
West and Ginnings calculated the attenuation by one shield
as a factor of about 8. They said, therefore, that the at-
tenuation by three shields should be about 500. This may be
looked at as follows; if the attenuation factor is $x$ and the
number of shields is $n$, then the total attenuation is $(x)^n$.
Surrounding the calorimeter is the adiabatic jacket which
consists of the silver shield ring to which silver shield
cups and silver shield lid are attached. The main purpose
of the adiabatic jacket is to minimize heat transfer from the
calorimeter. In order to accomplish this, they mentioned
that both the heat transfer coefficient and the temperature
difference between the jacket and the calorimeter are made
small. However, they mentioned, this requires equality of
the effective temperature of the jacket to that of the calo-
rimeter which is hard to maintain. They stated therefore,
that in place of effective temperature equality, the more
feasible requirement has been substituted that temperature
inequalities and the corresponding small heat losses be the
same in the two experiments - one with the calorimeter full
and one with it empty. If this substitute requirement is

satisfied, then, when the heat capacity of the empty calori-
meter is subtracted from the full heat capacity, allowance is
automatically made for those small heat losses which are the
same in the two types of experiments. The uncertainty in the
equality of these small heat losses is the chief limitation
on the accuracy of the measurements.

Between the jacket ring and the calorimeter ring are
two ten-junction thermopiles which indicate the vital tempera-
ture difference between the calorimeter and its jacket.
Surrounding the jacket is a 2 cm thick aluminum guard whose
temperature is controlled a few tenths of a degree below
that of the jacket to reduce the power required in the jacket
and the consequent temperature gradients. It also guards
the jacket from effects of changes in ambient conditions and
in the temperature gradients in the glass fiber which is used
for thermal insulation of the apparatus.

West and Ginnings used a platinum resistance thermometer
for their temperature measurements. Also inserted in the
top of the sample container are three coils of the calori-
meter heater. They mentioned that this placement of the
heaters permits observation of the calorimeter temperature
within a few hundredths of a degree while heating. The tem-
perature differences on the surface of the sample container
are significant only during the heating interval. They

calculated them to be not greater than 0.02°C when empty and 0.04°C when full.

West and Ginnings evaluated the heat transfer coefficient and found its mean value to be 0.23 watts/°C at 400°C. Thus, they said the zero heat leak was equivalent to 0.08% of the heat capacity of the $Al_2O_3$. This magnitude of zero heat leak though still small is about an order of magnitude larger than that in the experiments of Osborne et al.

West (69) described the heat flow in adiabatic calorimeters of various shapes and materials in terms of linear partial differential equations. He stated that well established techniques for measuring electrical energy and temperature differences are accurate enough that the most likely source of the differences is in accounting for the heat exchange between the calorimeter and its surroundings.

West also pointed out that small temperature differences which exist on the surfaces of the calorimeter and adiabatic shield during the heating period produce a corresponding rate of heat leak exchange which is approximately proportional to the heating rate, i.e. $dq/d\tau \propto dT/d\tau$. More specifically, there is a zero heat leak even though the temperature difference between a particular point on a calorimeter and a particular point on the shield as measured by a differential thermocouple is maintained essentially at and around "zero"

during the heating period. Since the time required to raise the sample through a given temperature interval is inversely proportional to the heating rate, West concluded that the net zero heat leak is the product of the rate of heat leak exchange and the time, and thus he further concluded that the zero heat leak is practically the same for all heating rates i.e. $\dot{q}_{\delta T=0} = C\tau \, dT/d\tau$. Furthermore, he mentioned that this unknown net heat exchange could be accounted for by making it the same in the experiments with the full and the empty calorimeter. However, he pointed out, due to the transient effects, there is a difference in the unknown heat exchange between measurements with the full and the empty calorimeter and this difference is a cause of systematic deviations.

West stated that the rate of change or drift of the calorimeter temperature in the equilibration periods immediately prior to or after an experiment is usually non-zero, indicating that the temperature variation found on the adiabatic shield is not perfectly matched to that of the calorimeter even when the controlled temperature difference is zero (since the temperature difference between the two is sensed at only one or more points on the surface by means of a differential thermocouple). He called the heat exchange indicated by this temperature change the "residual heat leak"

Also, West mentioned that whenever thermal energy is supplied to the calorimeter or the adiabatic shield, it must

flow from the heater to a surface where it is lost to other surfaces or to some volume where it raises the temperature. This thermal energy sets up gradients throughout the body which have components along the surface. Since the temperature of the calorimeter and shield can be observed at only a relatively few points, it follows that the observed temperature differs from the average over the surface. Consequently, there is heat exchange between the calorimeter and the shield whenever power is supplied to either of them, even though the controlled temperature difference is zero. It is possible and often practicable to distribute heaters and thermocouples to make this heat exchange small. However, West mentioned that it does not appear possible to satisfy exactly the requirements that a shield heater, for example, should be distributed so as to generate at each point at equilibrium the heat lost from that point to the environment and that the same distribution should supply both heat lost and heat required to raise the shield temperature during the heating period without gradients along the surface.

In discussing the heat leak problem, West mentioned that he was analyzing the apparatus for a heat leak correction which was a small part of the total heat added in an experiment. Therefore, he said that he used approximations which affect the heat leak by only a small percentage of itself. In order to obtain linear equations, approximations were made

that the heat capacities per unit volume, the heat transfer coefficients, and the thermal conductivities of all materials in the calorimetric apparatus are independent of temperature over the small temperature interval of the experiment. He also assumed heat transfer by convection was negligible.

West called the procedure used by Osborne a good practice, i.e. performing two measurements with the calorimeter full and empty (or with large and small samples) reproducing the gradients on the surfaces of the calorimeter and shield in order to allow for the unknown heat-transfer during the heating period. But, he said, placing a sample in the calorimeter alters the time required for heat to reach the surface, so that the transients for the full calorimeter differ from those for the empty and he demonstrated this by having two cases of empty and full calorimeter in which he found the relationship between the temperature difference and time for different heating rates as given in Figure 2.3.

The following equation was given by West for the total zero heat leak Q from the calorimeter.

$$Q = q_{\delta T = 0} \cdot \tau_f + q_R \cdot \tau_r \tag{2.4}$$

where $q_R$ is the residual heat leak which exists prior to and after the heating period

$\tau_r$ is the time elapsed between the initial and the final temperature readings (sec)
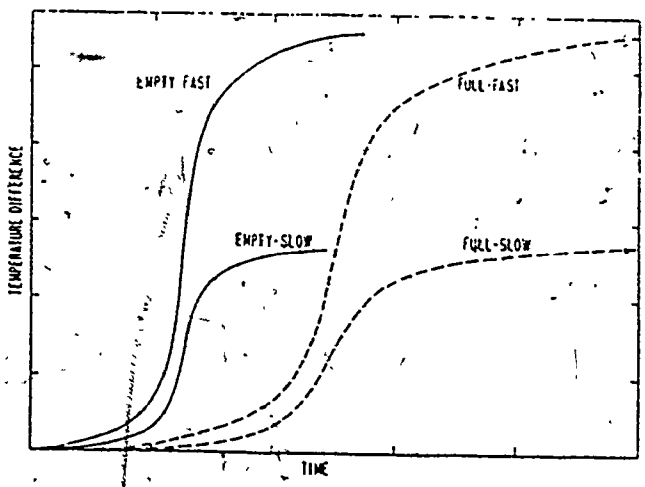
FIGURE 2.3  Schematic of temperature difference between two points on the surface of the calorimeter as a function of time for different heating rates and loading conditions

$q_{\delta T=0}$   is the heat leak due to gradients set up during the heating period

$\tau_f$   is the time required to heat through the temperature range $T_f - T_o$

$T_f$   is the final temperature of the system ($^0$C)

$T_o$   is the initial temperature ($^0$C).

Also, West pointed out that in the equation there is nothing to indicate the sign of the residual heat leak, and, in most apparatus, heat probably flows from the calorimeter at some points and to it at others. The net effect depends on the relative locations of the shield heater and the control thermocouple if there is no parasitic emf in the control circuit.

Chan (7) mentioned that in his apparatus, the temperature distribution over the metal surfaces of the calorimeter and adiabatic shield in the high and low filling experiments is essentially the same and consequently, that heat leaks in these two types of experiments are practically identical. He also mentioned that the temperature difference between the calorimeter and the adiabatic shield in his experiments for vapour and liquid withdrawal was 0.02°C which he said is extremely small. Therefore, heat leak is negligible in both cases.

The apparatus designed by Chan and used in this research

consists of the following parts (Figure 2.4):

(i)   An Inconel high pressure calorimeter which contains
      the sample and consists of a spherical, thin-walled
      metal shell in the form of two hemispheres having a
      radius of 6.35 cm and a wall thickness of 0.63 cm.

(ii)  A copper thin-walled adiabatic shield which surrounds
      the calorimeter and is made in the form of two hemis-
      pheres having a diameter of approximately 18 cm and a
      wall thickness of approximately 0.3 cm.  The function
      of the adiabatic shield is to minimize the heat ex-
      change to or from the calorimeter.

(iii) A thick-walled copper outerguard which encloses the
      calorimeter and the adiabatic shield and is made in the
      form of two thick-walled hemispheres with 22 cm inter-
      nal diameter and 24.5 cm outside diameter.  The func-
      tion of the outerguard is to prevent changes in the
      temperature of the environment from influencing the
      adiabatic shield and calorimeter.  It also provides a
      high vacuum space to minimize the heat transfer between
      the calorimeter and its surroundings.  Furthermore, it
      supplies most of the heat which is lost to the outside.

Two heaters are employed in the calorimeter as surface
heaters, each having a total resistance of 105 ohms.  Also,
there are two heaters on the surface of the adiabatic shield,

## LEGEND TO FIGURE 2.4

| ITEM | |
|------|--|
| 1 | Inconel 600 Calorimeter Shell |
| 2 | Copper Adiabatic Shield |
| 3 | Copper Outer Guard |
| 4 | Ceramic Support |
| 5 | Liquid Withdrawal Tube |
| 6 | Vacuum Tube |
| 7 | Nut |
| 8 | Nipple |
| 9 | Vacuum Connection Box |
| 10 | Conax Seals |
| 11 | Water Cooling Tubes |
| 12 | Support Frame |
| 13 | Silver Heat Diffusion System |
| 14 | Micrometering Valves |
| 15 | Resistance Thermometer |
| 16 | Vapour Withdrawal Tube |
| 17 | Adiabatic Shield Heater |
| 18 | Outer Guard Heater |
| 19 | Vacuum Metal "V" Seal |
| 20 | Calorimeter Heater |
| 21 | Diatomaceous Earth |
| 22 | Aluminum Enclosure |
| 23 | Vacuum Rubber Seal |
| 24 | Tube Heaters |
| 25 | Thermocouple Junctions |
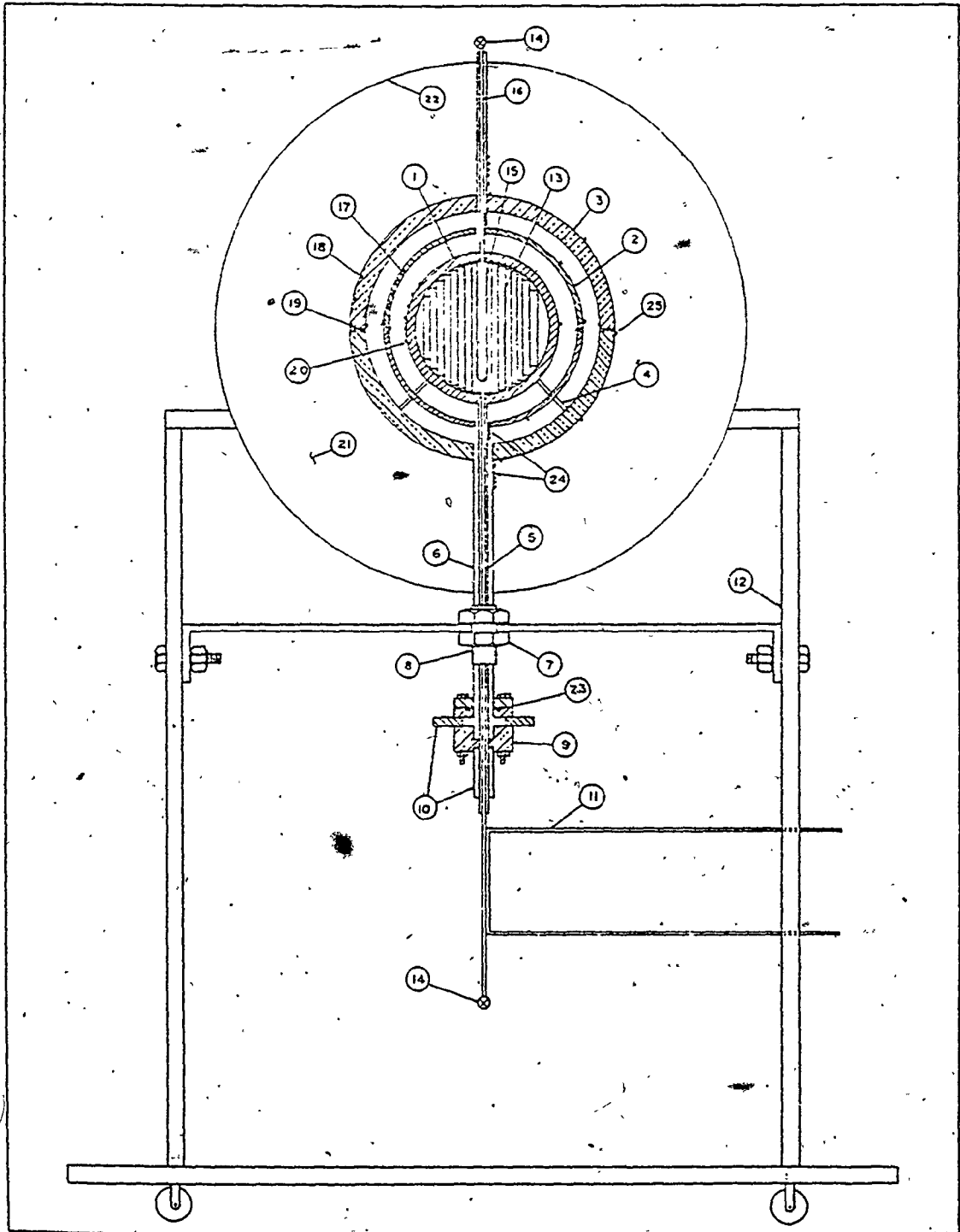
FIGURE 2.4 THE NON FLOW ADIABATIC CALORIMETER APPARATUS

each having a total resistance of approximately 50 ohms and they are used to maintain a uniform surface temperature of the adiabatic shield. Four outerguard heaters are employed on the outerguard surface; each has a length of 25 cm and a total resistance of approximately 25 ohms.

Chan applied the same experimental method as Osborne. However, Chan used a different approach in deriving his general energy equation but obtained the same equation as Osborne. He also performed two experiments for different calorimeter fillings, and obtained two equations which, when combined, resulted in a general equation for determination of the enthalpy of saturated liquid. In his results, Chan assumed that the difference between the zero heat leaks for large and small fillings was negligible compared to the net electrical energy added. Also, he considered the strain energy to be the same in both cases and therefore neglected its effect. Furthermore, neither Osborne nor Chan took into account the effect of the surface energy on the measurements.

When Chan applied his results for the determination of the heat capacity of the empty calorimeter from the constant mass experiments, he neglected both the zero heat leak under high filling and the effect of strain energy. Therefore, in the following equation for the heat capacity determination from constant mass experiments,

$$(-W_e)_M = M[h_f - Tv_f \frac{dP}{dT}]_1^2 + (T V \frac{dP}{dT} - PV)_1^2$$

$$+ M_c c_{p_c} \Delta T - (q_{\delta T=0})_M + (W_S)_M \qquad (2.5)$$

where

$(-W_e)_M$ is the electric energy added to the calorimeter and contents

$(q_{\delta T=0})_M$ is the zero heat leak when the calorimeter is charged with a certain mass M, and

$(W_S)_M$ is the strain energy on the calorimeter shell with a mass M.

Chan neglected the last two terms in the equation. However, Chan, in conducting direct heat capacity measurements on the empty calorimeter, applied the following equation,

$$(-W_e)_o = M_c c_{p_c} \Delta T - (q_{\delta T=0})_o \qquad (2.6)$$

where

$(-W_e)_o$ is the electric energy added to the empty system, and

$(q_{\delta T=0})_o$ is the zero heat leak of the empty system.

Chan accounted for the zero heat leak of the empty system which he found to increase with temperature and represents 1.1% of the total electrical energy added for a temperature range between 250 and 300°C. The zero heat leak values

utilized by Chan (7) are given in Table 2.1.*

The following equation was also obtained by Chan for the determination of the enthalpy of saturated liquid:

$$-\frac{W_{e_H} - W_{e_L}}{M_H - M_L} = \Delta(h_f - Tv_f \frac{dP}{dT}) \qquad (2.7)$$

where

$-W_{e_H}$ and $-W_{e_L}$ are the total electrical energies added for both high and low calorimeter fillings respectively, and

$M_H$ and $M_L$ are the masses of liquid in both high and low filling cases.

## 2.3 COMPARISON TECHNIQUES

Baker (1) used the comparison technique, in which a material of known heat capacity is compared with the material in question, to determine the heat capacity of deuterium oxide. Normal water was used as the comparison material since heat capacity values for it are well known over a wide temperature range.

---

*It is evident that the zero heat leak from the U.W.O. calorimeter is an order of magnitude larger than that in the West and Ginnings apparatus. Part of the reason for this poorer performance is no doubt due to the fact that the U.W.O. calorimeter is three times larger than the West and Ginnings apparatus.

## TABLE 2.1

### ZERO HEAT LEAK VALUES FOR THE EMPTY CALORIMETER

### OF CHAN'S APPARATUS

| Temperature Interval °C | | Zero Heat Leak (Joules) | Total Energy Added (Joules) | % Heat Leak |
|---|---|---|---|---|
| From | To | | | |
| 50 | 100 | -330.1 | 80502.0 | 0.41 |
| 100 | 150 | -462.9 | 82771.8 | 0.56 |
| 150 | 200 | -757.2 | 84990.9 | 0.89 |
| 200 | 250 | -881.8 | 87190.0 | 1.01 |
| 250 | 300 | -1019.9 | 89332.2 | 1.14 |

Baker mentioned that the comparison technique offers a
fairly simple method for determining heat capacities.
Further, he said, the comparison method offers the advantage
of balancing heat losses so that these heat losses need
not be known absolutely but only minimized as much as pos-
sible (analysis of this argument will be seen later).

The apparatus which Baker used in his research is a
stainless-steel flanged top vessel as the calorimeter, and
was used for a temperature range of 100 to 200°C.  The
flanged cover contained a heater well (in which a 50 ohm
resistor is wound on a ceramic spool) and two small wells to
receive thermistors as temperature sensing elements (Figure
2.5).

The calorimeter was suspended by Teflon strips from the
cover of a second cylinder which served to maintain a vacuum
around the calorimeter.  The outer cylinder was also a stain-
less steel flanged vessel.  The cover of the outer cylinder
contained an outlet through which lead wires to the cell
heater and thermistors were placed.  Agitation in the cell
was provided by a Teflon-coated bar magnet driven by a spinning
magnet located outside the outer cylinder.  The assembled
calorimeter was immersed in an oil bath which was maintained
at a prescribed temperature to a precision of ±0.001°C
control.

CALORIMETER

FIGURE 2.5
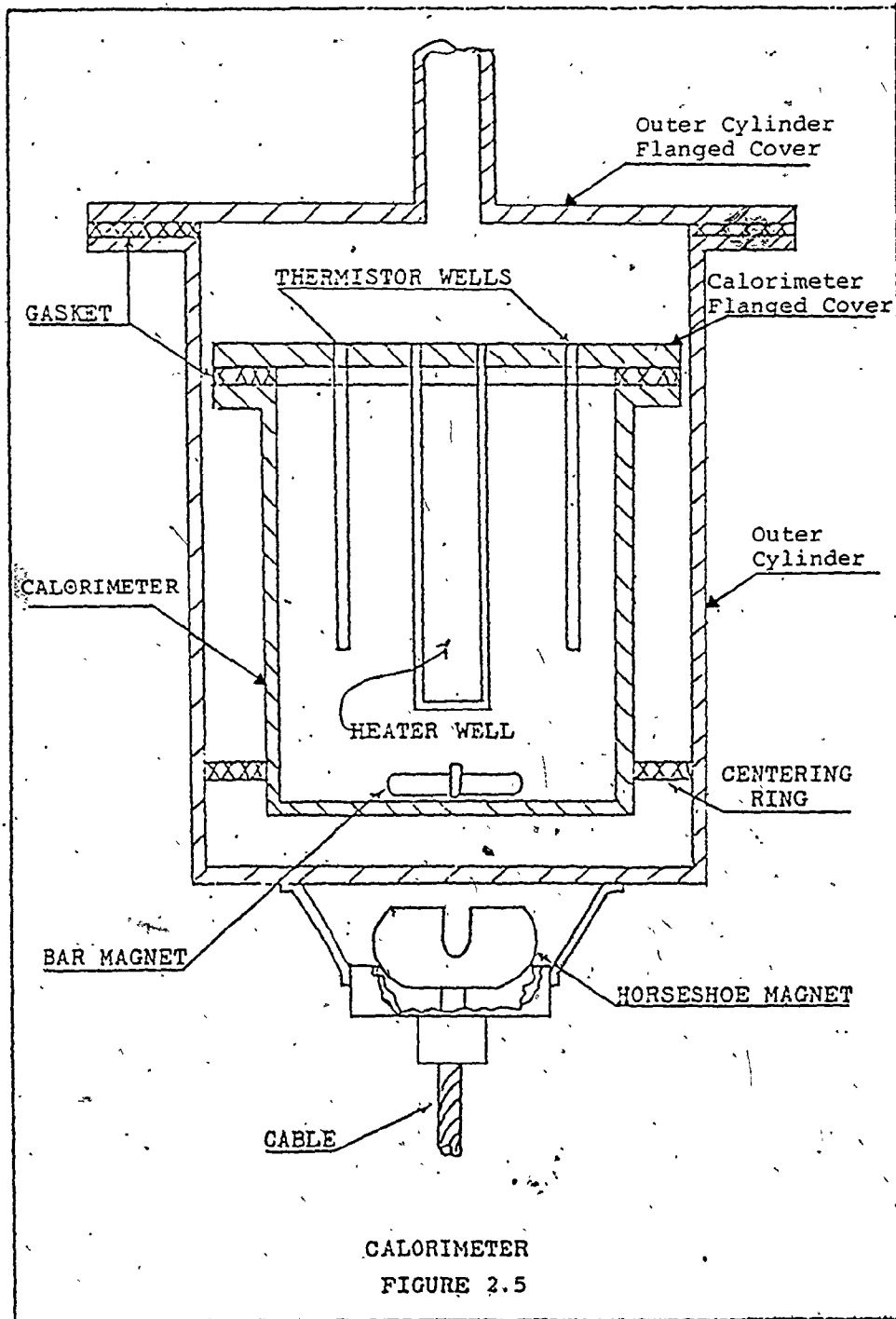
Baker mentioned that after the calorimeter was charged, it was then fastened to the cover of the outer cylinder by Teflon supports. With the thermistors and heater in place, the calorimeter was then centred inside the outer cylinder by a Teflon ring. The outer cylinder was sealed by its flanged cover. Vacuum connections were made to the outer cylinder. The entire assembly was placed in a 50 gallon oil bath. The annulus between the calorimeter and outer cylinder were evacuated to 10 to 15 mm Hg. The temperature of the contents of the calorimeter and the bath were allowed to come to equilibrium.

Baker obtained the heat gain by the calorimeter and its contents by first allowing the temperature of the calorimeter to come to equilibrium with the oil bath temperature. The bath temperature was then raised 0.7°C. The agitator was started and the temperature of the contents of the calorimeter allowed to slowly rise until the resistances of the thermistors indicated the temperature to be precisely 0.5°C below the bath temperature. The cell heater was then turned on for a period long enough to give a one degree centrigrade temperature rise.

Baker explained how he obtained the heat capacity of deuterium oxide as follows: by subtracting the heat gain of the water from the heat gain of the calorimeter with water, the heat gain of the calorimeter alone was found. Then, by

subtracting the heat gain of the calorimeter from the heat gain of the calorimeter containing deuterium oxide, the heat gain of the deuterium oxide was determined. From the weight of the deuterium oxide in the calorimeter and the heat gain per degree of temperature, the specific heat of deuterium oxide was calculated.

Baker claimed that the enthalpy values of saturated liquid deuterium oxide up to 400°F are believed to be accurate to within 1.5%. However, this accuracy may be affected by the fact that Baker considered his heat leaks to be balanced and therefore he said that compensation for the heat transfer between the bath and the calorimeter during the heating period was possible by having the cell temperature 0.5°C less than the bath before heating and then allow it to reach a 0.5°C above that of the bath during the heating period. This may be explained by Figure 2.6. Therefore, Baker said if $Q_1$ is the heat leak from outside to the calorimeter where the temperature of the bath is higher than the temperature of the calorimeter and $Q_2$ is the heat leak from the calorimeter to the outside when the temperature of the calorimeter is now higher, then $Q_1$ will be equal to $Q_2$ and therefore the net heat leak is zero. This does not seem to be the case because after heating is stopped, certain time is elapsed before the final equilibrium temperature is obtained and therefore an extra amount of heat is transferred
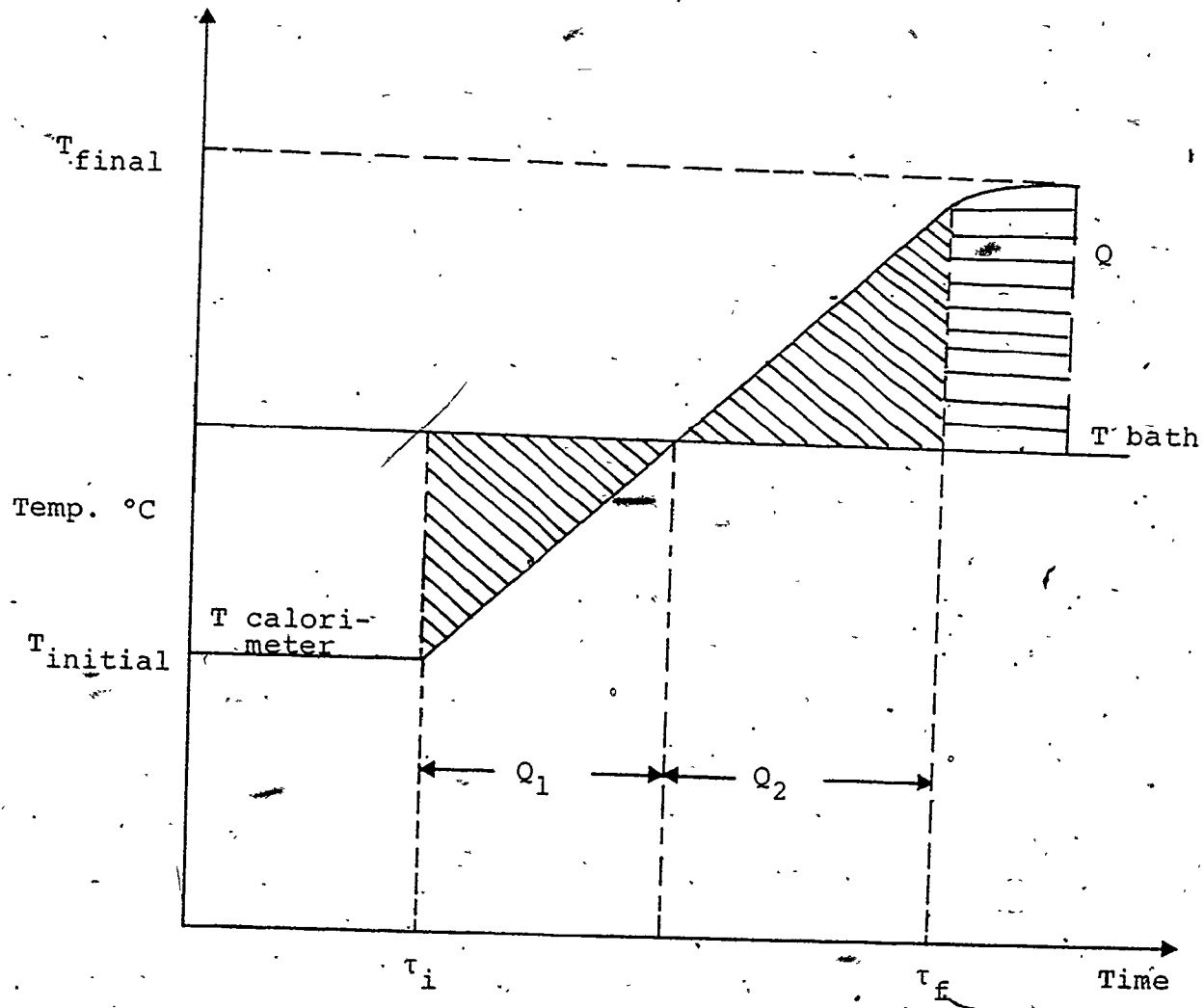
FIGURE 2.6  Relation between the calorimeter and
bath temperature with time during the
heating period

from the system to the outside.  This heat leak is not compensated for as may be seen from Figure 2.6.

## 2.4  APPLICATION OF CALORIMETRIC TECHNIQUES TO THE PRESENT STUDY

The experimental method employed by Chan produced the only other results which were in excellent accord with the internationally recognized standard values of Osborne.  Thus, the experimental apparatus of Chan was employed in this research.

The general energy equation was derived here using an approach similar to both of Osborne and Chan, and the same equation was obtained with the difference that both the zero and incremental heat leaks were considered different for different cases of calorimeter charges.*  Also, the strain energy was considered different for different mass fillings. Furthermore, the surface energy was taken into consideration and added as a term in the general equation.  Moreover, in this research, the effect of changing the absolute temperature scale on the results was considered.  As a result, the following equation was obtained for the determination of the enthalpy of saturated liquid.

---

* The incremental heat leak was zero in the Osborne and Chan investigations.  The present investigation of zero heat leak, though conducted on an inferior apparatus, showed the direction of the zero heat leak is influenced by the charge.

$$\frac{-W_{e_H} - W_{e_L}}{M_H - M_L} = \Delta(h_f - Tv_f \frac{dP}{dT}) - \frac{(q_{\delta T=0} + q_{\delta T})_H - (q_{\delta T=0} + q_{\delta T})_L}{M_H - M_L}$$

$$+ \frac{W_{S_H} - W_{S_L}}{M_H - M_L} + \frac{W_{S.E._H} - W_{S.E._L}}{M_H - M_L} \tag{2.8}$$

where

$(q_{\delta T=0})_H$ and $(q_{\delta T=0})_L$ are the zero heat leaks for both high and low filling cases respectively,

$(q_{\delta T})_H$ and $(q_{\delta T})_L$ are the incremental heat leaks for mass charges of $M_H$ and $M_L$ respectively,

$W_{S_H}$ and $W_{S_L}$ are the strain energies for the two masses, and

$W_{S.E._H}$ and $W_{S.E._L}$ are the surface energies for the two masses $M_H$ and $M_L$ respectively.

Details of the derivation of equation 2.8 may be found in Appendix A.

Equation 2.8 was thus used for determination of the enthalpy of saturated liquid with the correction terms applied.

# CHAPTER 3

## DIGITAL COMPUTER AND DATA ACQUISITION

## SYSTEM DESIGN

### 3.1  HIGH SPEED DIGITAL COMPUTER AND ITS APPLICATION TO CALORIMETRIC DATA

The derivation of thermophysical properties from raw experimental data involves much tedious repetitive computation. The process is therefore much expedited by a high speed digital computer and with fewer errors.

Measurements in this research were performed by using manual methods and with conventional measuring instruments. Although very accurate, the measurements were made with large time intervals. Only a few measurements were taken during the experiment. The computer can process large quantities of data to obtain a few selected values. For example, it is possible to calculate a table of thermodynamic properties from smoothed heat capacities. The computer program used to obtain the energy and temperature properties of the system under investigation is largely dependent on the instrumentation of the laboratory and the procedures that are followed in the measurements. Before assembling such a program, a detailed step-by-step ordered arrangement of the measurement and calculation procedures should be charted or diagrammed. Details of the flow chart and the program for the measurements and calculation

for the data collected in this research may be found in
Appendix B.

The laboratory measurement procedures often become
better systemized and organized when subjected to the need
for interfacing them with a computer program.

## 3.2 COMPUTER-SYSTEM CONNECTION

It was required that the Leeds and Northrup Precision
Digital Voltmeter and Scanner be controlled remotely by a
PDP-11 computer. The Precision Digital Voltmeter (PDVM) is
an Analog to Digital Converter (A/D) whose function is to
convert the data (collected in the form of analog signals)
to digital numbers which are then fed to the computer in the
form of a signed five-and-one-half digit number in binary-
coded decimal-BCD (8,4,2,1) format. The PDVM can be set to
measure various functions, i.e. voltage, current and resis-
tance. The input range is also a variable, unless the unit
is placed in auto-range mode, whereby it will automatically
adjust its gain to accommodate the input. The scanner can
accept up to thirty analog input lines and present the sig-
nals one at a time to the PDVM. The number of lines may be
expanded to 100. The scanner may be loaded with a two-digit
(BCD) address or incremented to the next address.

For the computer to operate with the system, the input

data should be fed to the scanner as analog signals from the
calorimeter system. These are the outputs of the different
thermocouples for temperature difference and temperature
variation measurements, the output of the resistance thermo-
meter for the absolute temperature measurements and the out-
put of the calorimeter heaters for power measurements.
Furthermore, the power and temperature outputs from the adia-
batic shield, outerguard as well as tube heaters are fed as
analog signals to the scanner for temperature and power con-
trol. Appendix B (taken from reference (66)) describes in
detail the outputs from different regions in the apparatus.

An interface between the computer and the system is
necessary in order to transform the analog signals to digital
ones and enable the computer to deal with the data. Figure
3.1 (taken from reference (66)) is a schematic diagram of
the circuit showing the interface signals.

In the calorimetric study, three different types of ex-
periments are performed; constant mass experiments, liquid
withdrawal experiments and vapour withdrawal experiments.
For each type, a flow chart was drawn for the experiment in
three steps:

1.  The first step is the measurement and recording of the
    absolute temperature, temperature differences and tem-
    perature variations as well as pressure until the system
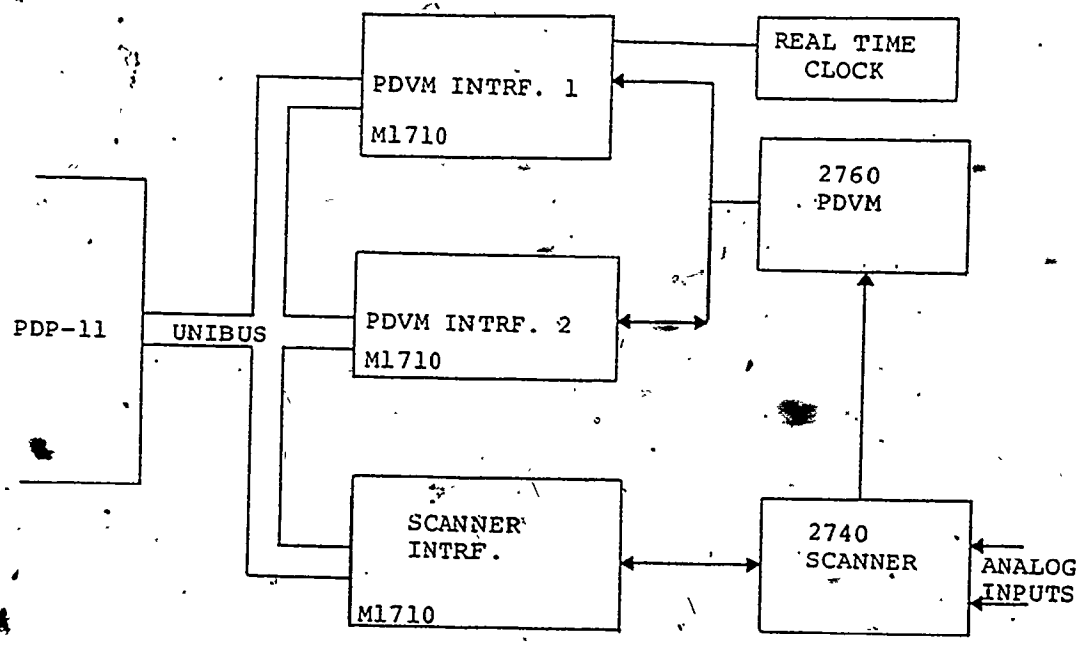
FIGURE 3.1   System block diagram

is brought to the initial equilibrium state.

2. The second step involves the measurement, printing and storage of the absolute temperature, temperature differences and temperature variations on the calorimeter surface, pressure and input power added to the system throughout the experiment.

3. The third step is the measurement and recording of the absolute temperature, temperature differences and temperature and pressure variations until the final equilibrium state is reached.

Also, a detailed program embodying all the steps and calculations for each of the three different types of experiments was written. The flow charts and the computer-scanner-layout are given in Appendix B. Based on the flow charts and the detailed layout, the hardware part of the interface was built and tested by the computer centre of The University of Western Ontario to fulfill the requirements of the system. The PDVM interface diagram with its description and the PDVM test program are given in Appendix B. A diagram and description of the scanner interface may also be found there.

In order to choose a computer system with software and hardware suitable for operating the calorimetric system, a layout of the interface and scanner was first necessary. Figure 3.2 is a photograph of the computer and the Leeds and Northrup (L/N) facility. Based on the scanner layout, the
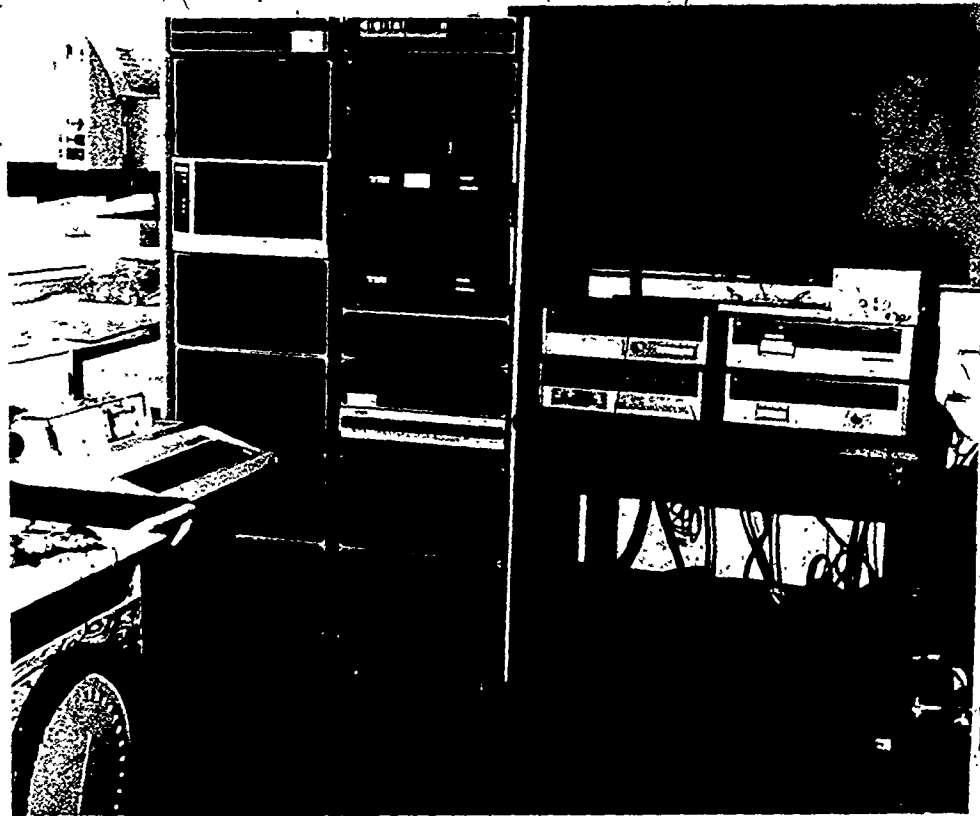
FIGURE 3.2   View of the PDP 11/10 computer and data
acquisition system

hardware was assembled and fulfilled all the requirements when tested.

Initially, it was intended that the computer be used in this research, however the software program was not available at the time of performing the experiments. Therefore, the computer was not used in the research of this thesis. However, comparison of the results obtained in this research with those obtained with the aid of the computer when in operation will be possible.

# CHAPTER 4

## ABSOLUTE TEMPERATURE SCALE

Since the absolute temperature of the water sample is a critical factor in the data reduction, a standard platinum resistance thermometer was used for temperature measurements because of its high accuracy.

As mentioned in Appendix C, the capsule thermometer was calibrated against the primary standard platinum resistance thermometer which in turn was calibrated by the National Research Council of Canada. The calibration of the thermometer was carried out according to the specifications of the International Temperature Scale of 1948. The primary standard thermometer was calibrated at the triple point of water, the boiling point of water (or steam point) and the sulphur point based on the 1948 International Temperature Scale specifications (7).

Recent gas thermometry shows significant discrepancies between the values measured on the Thermodynamic Scale and the corresponding values on the International Practical Temperature Scale of 1948 (IPTS-48). Furthermore, the IPTS-48 has a lower limit at the boiling point of oxygen, so there was a pressing need for an agreed temperature scale at lower temperatures. Because of these defficiencies, the new International Practical Temperature Scale of 1968 (IPTS-68) was

44

introduced.

The IPTS-48 is based on six reproducible temperatures (defining fixed points) to which numerical values are assigned. These defining points are given in reference (.62) as:

(i)     oxygen point (-182.97°C),

(ii)    triple point of water (0.01°C),

(iii)·  the steam point (100°C),

(iv)    the sulfur point (444.6°C),

(v)     the silver point (960.8°C), and

(vi)    the gold point (1063°C).

On the other hand, the corresponding defining fixed points on the IPTS-68 are given in reference (63) as:

(i)     oxygen point (-182.962°C),

(ii)    triple point of water (0.01°C),

(iii)   the steam point (100°C),

(iv)    the freezing point of zinc (419.58°C),

(v)     the freezing point of silver (961.93°C), and

(vi)    the freezing point of gold (1064.43°C).

Therefore, the International Practical Temperature Scale of 1968 is different from the International Practical Temperature Scale of 1948 in the following ways:

(i)  the lower limit of the scale is 13.81°K instead of 90.18°K.

(ii) the values assigned to the defining fixed points are modified where necessary to conform as closely as possible to the thermodynamic temperatures. The only points remaining unchanged are the triple point of water, being permanently fixed by definition, and the boiling point of water.

The temperature, according to the IPTS-68 is defined by the following equation for the range from 0°C to 630.74°C which covers the temperature range used in this research and is given in reference (63):

$$t_{68} = t' + 0.045 \left(\frac{t'}{100}\right)\left(\frac{t'}{100} - 1\right)\left(\frac{t'}{419.58} - 1\right)\left(\frac{t'}{630.74} - 1\right) °C \qquad (4.1)$$

where t' is defined by the following implicit equation, as given in reference (63):

$$t' = \frac{1}{\alpha}\left[\frac{R(t')}{R(0)} - 1\right] + \delta_{68} \left(\frac{t'}{100}\right)\left(\frac{t'}{100} - 1\right) \qquad (4.2)$$

where

> R is the resistance of the thermometer,
>
> $\alpha$ is the thermometer coefficient, and
>
> $\delta$ is the scale constant.

On the other hand, the defining equation for temperature on the IPTS-48 is given also in reference (63) as:

$$t_{48} = \frac{1}{\alpha}\left[\frac{R(t_{48})}{R(0)} - 1\right] + \delta_{48} \left(\frac{t_{48}}{100}\right)\left(\frac{t_{48}}{100} - 1\right) \qquad (4.3)$$

The constants R(0), $\alpha$ and $\delta$ are determined by measurements of the resistance of the thermometer at the triple point of

water, the boiling point of water (or the freezing point of
Tin) and the freezing point of zinc.

It is evident that the new scale differs from the old
one because of a change in the temperature assigned to the
freezing point of zinc and because of the addition of the
second term in the Right Hand Side of equation 4.1. For
convenience, this term may be denoted by $f(t')$, i.e. equa-
tion 4.1 may be written as follows:

$$t_{68} = t' + f(t') \tag{4.4}$$

Since the platinum resistance thermometer used in this re-
search was calibrated according to the 1948 scale, correc-
tions were required to determine the new constants based on
the 1968 scale.

From equations 4.1, 4.2 and 4.3, an explicit expression
for $(t_{68} - t_{48})$ may be found. The result is again given in
reference (63) as:

$$t_{68} - t_{48} = f(t') + \frac{t_{48}(t_{48}-100)(\delta_{68}-\delta_{48})}{\delta_{68}(100-2t_{48}) + 10^4} +$$

$$\tag{4.5}$$

$$\frac{\delta_{68}[t_{68}-t_{48}-f(t')]^2}{\delta_{68}(100-2t_{48}) + 10^4}$$

From equation 4.5, it is evident that at the zinc point, the
term $(t_{68}-t_{48})$ is independent of the thermometer (since it

does not contain the resistance ratio or the $\alpha$ coefficient
which are properties of the thermometer) and is defined to
be 0.075°C. Also, we notice that $\alpha$ does not depend on the
scale against which the thermometer is calibrated. Further-
more, it can be seen from equations 4.1 and 4.4 that at the
zinc point (419.58°C), $f(t') = 0$. Therefore, at the zinc
point, $t' = t_{68}$. Consequently, $(\delta_{68} - \delta_{48})$ may be calculated
using a value of $\delta_{48}$ for any thermometer.

The values for $\delta_{48}$ and $\alpha$ may be found from the following
relations as given in reference (63);

$$A_{48} = \alpha (1 + \frac{\delta_{48}}{100}) \qquad (4.6)$$

$$B_{48} = -10^4 \alpha \, \delta_{48} \qquad (4.7)$$

where $A_{48}$ and $B_{48}$ are the constants in the internationally
recognized resistance-temperature relationship

$$R/R_o = 1 + AT + BT^2 \qquad (4.8)$$

and their values are found from the calibration of the ther-
mometer.

Using the facts drawn from equation 4.5, i.e. $f(t') = 0$,
$t' = t_{68}$ and $t_{68} - t_{48} = 0.075°C$ and substituting for the
values of $A_{48}$ and $B_{48}$ which are obtained from the thermometer
calibration and given in reference (7) as,

$$A_{48} = 3.98478 \times 10^{-3}$$

$$B_{48} = -5.8568 \times 10^{-7}$$

the following relation between $\delta_{68}$ and $\delta_{48}$ was derived

$$\delta_{68} = 0.9995867 \, \delta_{48} + 5.591 \times 10^{-3} \qquad (4.9)$$

Dividing equation 4.6 by equation 4.7 results

$$\frac{A_{48}}{B_{48}} = \frac{-100(100 + \delta_{48})}{\delta_{48}} \qquad (4.10)$$

and upon substitution of $A_{48}$ and $B_{48}$, the following value was obtained for $\delta_{48}$.

$$\delta_{48} = 1.491544366$$

With the substitution of this value for $\delta_{48}$ in equation 4.9, $\delta_{68}$ was found to have the value

$$\delta_{68} = 1.496521058$$

and with the substitution back in equation 4.7, the following value was obtained for $\alpha$

$$\alpha = 3.926199 \times 10^{-3}$$

However, $\alpha$ does not depend on the scale, therefore substituting the above values of $\delta_{68}$ and $\alpha$ in the following equations for $A_{68}$ and $B_{68}$ and which are similar to equations 4.6 and 4.7;

$$A_{68} = \alpha \ (1 + \frac{\delta_{68}}{100}) \hspace{3cm} (4.11)$$

$$B_{68} = -10^4 \ \alpha \ \delta_{68} \hspace{3cm} (4.12)$$

numerical values for $A_{68}$ and $B_{68}$ are obtained as

$$A_{68} = 3.9849553 \times 10^{-3}$$

$$B_{68} = -5.87563948 \times 10^{-7}$$

which in turn are used for the resistance-temperature con-
version.

Using the calculated values of $A_{68}$ and $B_{68}$, the diffe-
rences between the temperatures derived from the IPTS-68 and
the IPTS-48 are computed. These are summarized in Table 4.1
and are in perfect agreement with the results obtained be-
fore (Table 4.1a). Figure 4.1 is a computer plot of the re-
lation between the temperature difference of the two scales
and the absolute temperature based on the 1948 scale. From
the curve, the following can be deduced:

(i) The difference between the IPTS-68 and the IPTS-48 values
is negative for low temperatures and becomes positive only
for temperatures higher than $100°C$.

(ii) The difference has its maximum value at about $510°C$.

(iii) In one part of the temperature range, the difference
is negative while in the other it is positive, thereby in-
creasing the uncertainty in the results based on the IPTS-48.

(iv) The rate of increase in the differences is quite

TABLE 4.1a  (IPTS-68)-(IPTS-48)— IN KELVIN

| t, °C | 0 | -10 | -20 | -30 | -40 | -50 | -60 | -70 | -80 | -90 | -100 |
|---|---|---|---|---|---|---|---|---|---|---|---|
| -100 | 0.022 | 0.017 | 0.003 | -0.000 | -0.013 | -0.013 | -0.005 | 0.007 | 0.012 | (0.005 at O, point) | 0.022 |
| -0 | 0.000 | 0.000 | 0.012 | 0.018 | 0.024 | 0.029 | 0.032 | 0.031 | 0.033 | 0.020 | 0.022 |

| t, °C | 0 | 10 | 20 | 30 | 40 | 50 | 60 | 70 | 80 | 90 | 100 |
|---|---|---|---|---|---|---|---|---|---|---|---|
| 0 | 0.000 | -0.001 | -0.007 | -0.009 | -0.010 | -0.010 | -0.010 | -0.008 | -0.004 | -0.003 | 0.000 |
| 100 | 0.000 | 0.001 | 0.007 | 0.012 | 0.018 | 0.020 | 0.025 | 0.029 | 0.034 | 0.038 | 0.013 |
| 200 | 0.013 | 0.017 | 0.051 | 0.054 | 0.053 | 0.001 | 0.004 | 0.007 | 0.069 | 0.071 | 0.073 |
| 300 | 0.073 | 0.074 | 0.075 | 0.070 | 0.077 | 0.074 | 0.074 | 0.077 | 0.077 | 0.077 | 0.079 |
| 400 | 0.070 | 0.075 | 0.075 | 0.035 | 0.074 | 0.074 | 0.074 | 0.075 | 0.076 | 0.077 | 0.079 |
| 500 | 0.130 | 0.105 | 0.065 | 0.050 | 0.001 | 0.100 | 0.108 | 0.053 | 0.126 | 0.151 | 0.150 |
| 600 | 0.39 | 0.42 | 0.45 | 0.47 | 0.50 | 0.53 | 0.28 | 0.31 | 0.31 | 0.30 | 0.39 |
| 700 | 0.07 | 0.70 | 0.72 | 0.75 | 0.78 | 0.81 | 0.81 | 0.58 | 0.01 | 0.04 | 0.67 |
| 800 | 0.95 | 0.98 | 1.01 | 1.04 | 1.07 | 1.10 | 1.12 | 0.87 | 0.59 | 0.02 | 0.95 |
| 900 | 1.24 | 1.27 | 1.30 | 1.33 | 1.30 | 1.39 | 1.42 | 1.14 | 1.18 | 1.21 | 1.24 |

TABLE 4.1   (IPTS-68)-(IPTS-48) IN KELVINS

| TEMP. DEG.C | 0.0 | 10.0 | 20.0 | 30.0 | 40.0 | 50.0 | 60.0 | 70.0 | 80.0 | 90.0 |
|---|---|---|---|---|---|---|---|---|---|---|
| 0.0 | 0.000000 | -0.004030 | -0.006031 | -0.008814 | -0.009987 | -0.009957 | -0.009133 | -0.007522 | -0.005525 | -0.002754 |
| 100.0 | 0.000000 | 0.003718 | 0.007606 | 0.011665 | 0.016086 | 0.020480 | 0.025039 | 0.029569 | 0.034071 | 0.038353 |
| 200.0 | 0.042608 | 0.046835 | 0.050657 | 0.054454 | 0.057851 | 0.061037 | 0.064016 | 0.066602 | 0.068984 | 0.070981 |
| 300.0 | 0.072778 | 0.074196 | 0.075236 | 0.076086 | 0.076565 | 0.077036 | 0.077144 | 0.077070 | 0.076815 | 0.076381 |
| 400.0 | 0.075940 | 0.075516 | 0.075263 | 0.074833 | 0.074580 | 0.074506 | 0.074776 | 0.075218 | 0.076179 | 0.077469 |
| 500.0 | 0.079443 | 0.000000 | 0.000000 | 0.000000 | 0.000000 | 0.000000 | 0.000000 | 0.000000 | 0.000000 | 0.000000 |
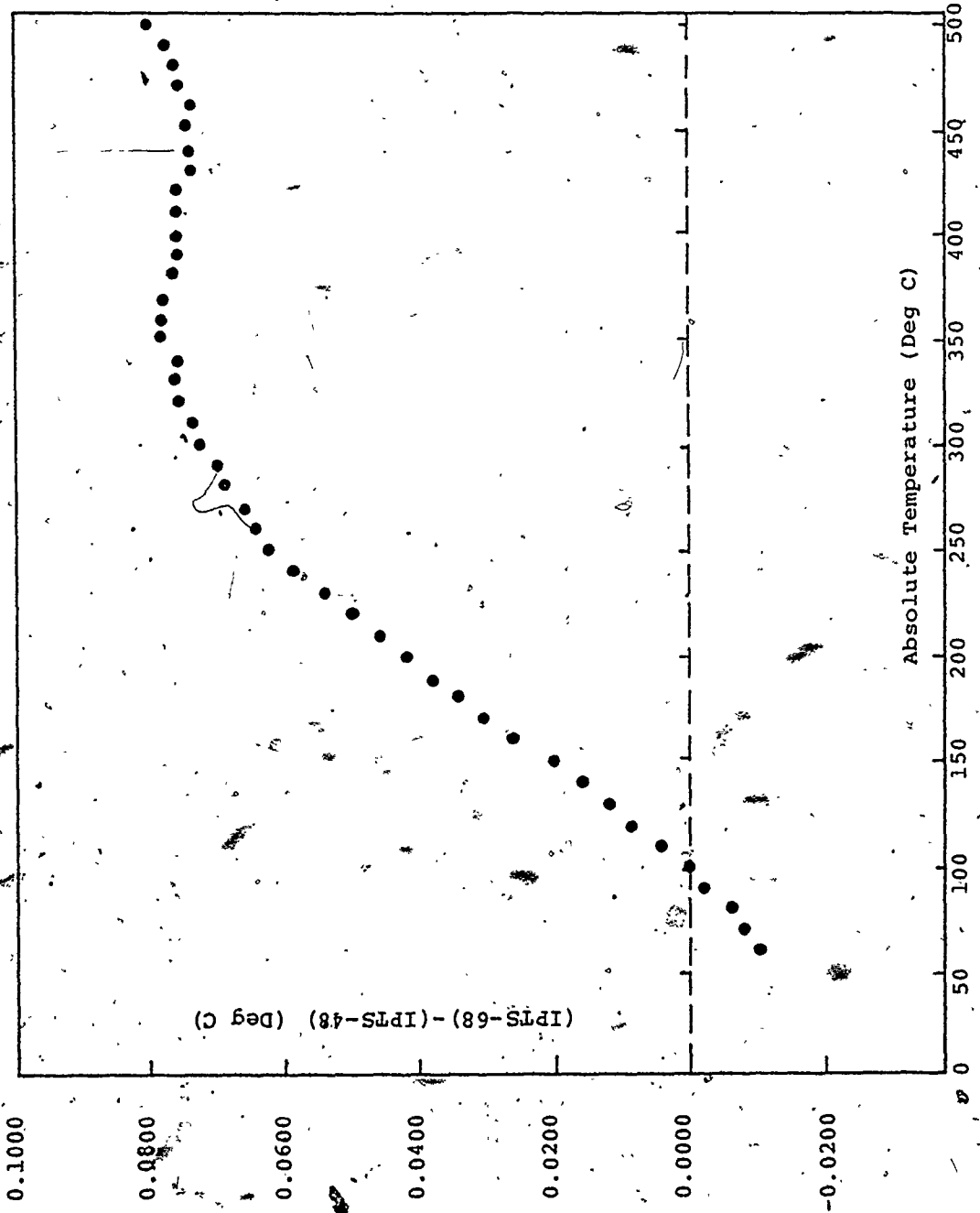
FIGURE 4.1  Temperature difference (degree C) vs absolute temperature (degree C)

large between approximately 100 and 300°C, while above 330°C this rate tends to become smaller.

Since there is a difference between the temperature values based on the IPTS-48 and those based on the IPTS-68, it was believed that this difference might cause some deviations in the calorimetric results. Therefore, derivation of the temperature conversion equations and computations of the temperature values were performed. An example of the problems arising due to the two temperature scales is illustrated in the following analysis:

The total energy added to the system is calculated from the product of the average input power and the experimental time; in other words

$$-W_e = i^2 R_e \tau$$

$-W_e$ is the electrical work added to the system

$R_e$ is the heater resistance

$\tau$ is the time

As this electrical energy is absorbed by the fluid sample and from the energy balance, the following equation may be written:

$$i^2 R_e \tau = m(c_p \Delta T)_{48} \qquad (4.13a)$$
$$= m(c_p \Delta T)_{68} \qquad (4.13b)$$

Since the electrical energy added is constant, the following relation is valid;

$$(c_p \Delta T)_{48} = (c_p \Delta T)_{68}$$

Therefore, different $c_p$ values will be obtained since the $\Delta T$ values are different for the two different scales. On the other hand, since $c_p$ is constant, the total electrical energy added to the system will be different if the temperature difference is calculated with the IPTS-68 than when its calculation is based on the IPTS-48. Tables 4.2 and 4.3 give the results of the total energy in the constant mass experiments for both high and low fillings, based on the IPTS-48 in one case and on the IPTS-68 in the second case. The results of these calculations are shown in the third and fourth columns of Tables 4.2 and 4.3. The last column in these tables shows the percentage deviation between the results obtained from the two scales in each case.

The following conclusions may be drawn from these tables:

1. The effect of changing the absolute temperature scale is very small and, in fact, negligible.

2. The effect increases with temperature up to 200°C and then decreases.

3. The percentage deviation is the same in both high and low fillings at all temperatures. This indicates that

## TABLE 4.2

### EFFECT OF CHANGING THE TEMPERATURE SCALE ON THE EXPERIMENTAL RESULTS (HIGH FILLING)

| Initial Temp. °C | Final Temp. °C | Total Energy Added Based on 1948 Scale | Total Energy Added Based on 1968 Scale | % Deviation |
|---|---|---|---|---|
| 100 | 150 | 216579.0371 | 216491.6101 | -0.040 |
| 150 | 200 | 223822.548 | 223722.853 | -0.045 |
| 200 | 250 | 232985.7287 | 232899.6971 | -0.037 |
| 250 | 300 | 248184.014 | 248126.326 | -0.023 |

## TABLE 4.3

### EFFECT OF CHANGING THE TEMPERATURE SCALE ON THE EXPERIMENTAL RESULTS (LOW FILLING)

| Initial Temp. °C | Final Temp. °C | Total Energy Added Based on 1948 Scale | Total Energy Added Based on 1968 Scale | % Deviation |
|---|---|---|---|---|
| 100 | 150 | 131519.575 | 131465.614 | -0.041 |
| 150 | 200 | 138577.143 | 138515.218 | -0.045 |
| 200 | 250 | 148542.084 | 148487.479 | -0.037 |
| 250 | 300 | 161760.298 | 161722.568 | -0.023 |

the effect of changing the temperature scale does not depend on the mass of liquid contained in the calorimeter. This can be shown analytically with reference to equations 4.13a and 4.13b above when they are applied to high and low fillings where the ratio of energy added to mass will be the same for the same temperature rise.

Based on previous results, computer programs were written for temperature conversion of the thermometer resistance and referenced in the Thermodynamic Laboratory of the University of Western Ontario. The results obtained from these programs are reproduced in IPTS-48 and IPTS-68, and are at 0.001°C temperature intervals within the 25°C to 400°C temperature range. The differences between the results based on the two scales are also given. The results appear in 15 documents, each containing 380 pages and has the conversion for a 25°C temperature range in order to simplify any future work with the existing platinum resistance thermometer.

# CHAPTER 5

## CALORIMETER SHELL STRAIN ENERGY

When a liquid sample is contained in the calorimeter and the temperature of the calorimeter is raised, an amount of work is done on the calorimeter shell due to the fluid. This work is termed the calorimeter shell straining energy.

In order to find a general equation which describes the strain energy, three factors were taken into consideration for the derivation of such a general equation.

(i)   the effect of temperature on the calorimeter shell.

(ii)   the effect of pressure on the calorimeter shell.

(iii) the effect of strain due to the weight of fluid sample contained in the calorimeter.

The above three factors are combined and affect one another, however, in this analysis, the effect of each one has been taken separately and the principle of superposition was applied to find the total effect resulting from the three factors.

## 5.1   THE STRAIN ENERGY DUE TO THE TEMPERATURE EFFECT ONLY

The state of thermal stress in a sphere due to temperatures which vary only with the radial coordinate is well known. Equations expressing the relation between the stresses

57

and temperature in the hollow thin sphere of radii $r_i$ and $r_o$ were derived using Hook's law. The general strain energy equation due to temperature effect only was obtained and written in the following form:

$$W_{ST} = \frac{2\pi E}{1-\mu} \int_{r_i}^{r_o} [\frac{2}{r^3} \frac{2\mu r^3 - r_i^3(1+\mu)}{(1-\mu)(r_o^3 - r_i^3)} \, a \, T \int_{r_i}^{r_o} a \, T \, r^2 \, dr$$

$$- \frac{3}{r^3} \frac{1+\mu}{1-\mu} aT \int_{r_i}^{r} aTr^2 \, dr + \frac{5}{r^6} \frac{1+\mu}{1-\mu} (\int_{r_i}^{r} aTr^2 \, dr)^2$$

$$+ \frac{8r^6(1-2\mu) - 2r_i^3 r^3(2-\mu) + 5r_i^6(1+\mu)}{r^6(1-\mu)(r_o^3 - r_i^3)^2} (\int_{r_i}^{r_o} aTr^2 \, dr)^2$$

$$+ \frac{10r_i^3(1+\mu) - 2r^3(2-\mu)}{r^6(1-\mu)(r_o^3 - r_i^3)} (\int_{r_i}^{r_o} aTr^2 \, dr)(\int_{r_i}^{r} aTr^2 \, dr)] r^2 dr \quad (5.1)$$

Details of the derivation of equation 5.1 may be found in Appendix D. It may be seen from this equation that the strain energy due to the temperature effect only is a function of the material from which the calorimeter is constructed (it contains the modulus of elasticity E, and the linear coefficient of thermal expansion for the calorimeter material $\mu$), the dimensions of the calorimeter and the heating rate. Application of the relation between temperature and heating rate into equation 5.1 and substituting the values for the constants results in numerical values for the strain energy at different temperatures. These results are summarized in Table 5.1. From the table, we may notice that the strain energy value does not change very much with temperature rise.

## TABLE 5.1

### THE STRAIN ENERGY FROM TEMPERATURE EFFECT ONLY

| Initial Temperature (°C) | Final Temperature (°C) | Strain Energy (Joules) |
|---|---|---|
| 100 | 150 | -15.873 |
| 150 | 200 | -16.100 |
| 200 | 250 | -16.354 |
| 250 | 300 | -16.917 |

Also, the numerical value of the strain energy is small.
Furthermore, we notice that the strain energy has a negative
sign. This indicates work being done on the system.

## 5.2 THE STRAIN ENERGY DUE TO THE PRESSURE EFFECT ONLY

A major component of the strain energy is due to the
pressure effect. If a sphere of constant wall thickness is
subjected to uniform internal and external pressures, the
deformation produced is symmetrical around the centre and
changes only with the radius. Consequently, a strain energy
is produced due to stresses in both the radial and tangential
directions. The total strain energy produced as a result of
the pressure effect only may therefore be given by the
following general equation:

$$W_{SP} = \frac{2\pi P_i^2 r_i^6}{E(r_i^3 - r_o^3)^2}[\frac{2}{3}(1-2\mu)(r_o^3 - r_i^3) - \frac{r_o^3}{2}(2-\mu)\ln\frac{r_o}{r_i}$$

$$- \frac{5}{12}(1+\mu)\frac{r_o^6}{r_o^3 - r_i^3}] \qquad (5.2)$$

Complete derivation of equation 5.2 may be found in Appendix
D.

It is clear from this equation that the strain energy
due to the pressure effect alone is a function of the material
of the calorimeter shell. It also depends on the dimensions
of the calorimeter as well as the internal pressure of the

calorimeter vessel.

Substituting the values of constants in equation 5.2 at different saturation pressures results in numerical values for the strain energy at corresponding saturation temperatures. The results are summarized in Table 5.2. From this table, we conclude that:

(i) the strain energy values which result from the pressure effect alone are very small at small pressures. However, the absolute value of strain energy is increasing steeply with pressure.

(ii) at low temperatures, the strain energy produced by the pressure effect is smaller than that produced by the temperature effect, while at high temperatures it becomes larger. This may be attributed to the fact that the strain energy is proportional to the pressure squared in the second case.

(iii) Also, we notice that the strain energy has a negative sign. This indicates work being done on the system.

5.3 THE STRAIN ENERGY FROM THE MASS EFFECT ONLY

The calorimeter is attached to the adiabatic shield by three ceramic supports at angles of 120 degrees from each other as seen in Figure 5-1. When the calorimeter is charged with fluid, there result stresses on the calorimeter shell.

## TABLE 5.2

### THE STRAIN ENERGY PRODUCED
### BY PRESSURE EFFECT

| Initial Temp. (°C) | Final Temp. (°C) | Initial Pressure (Bar) | Final Pressure (Bar) | Strain Energy (Joules) |
|---|---|---|---|---|
| 100 | 150 | 1.013 | 4.760 | − 0.07 |
| 150 | 200 | 4.760 | 15.549 | − 0.80 |
| 200 | 250 | 15.549 | 39.777 | − 5.36 |
| 250 | 300 | 39.777 | 85.928 | −25.41 |
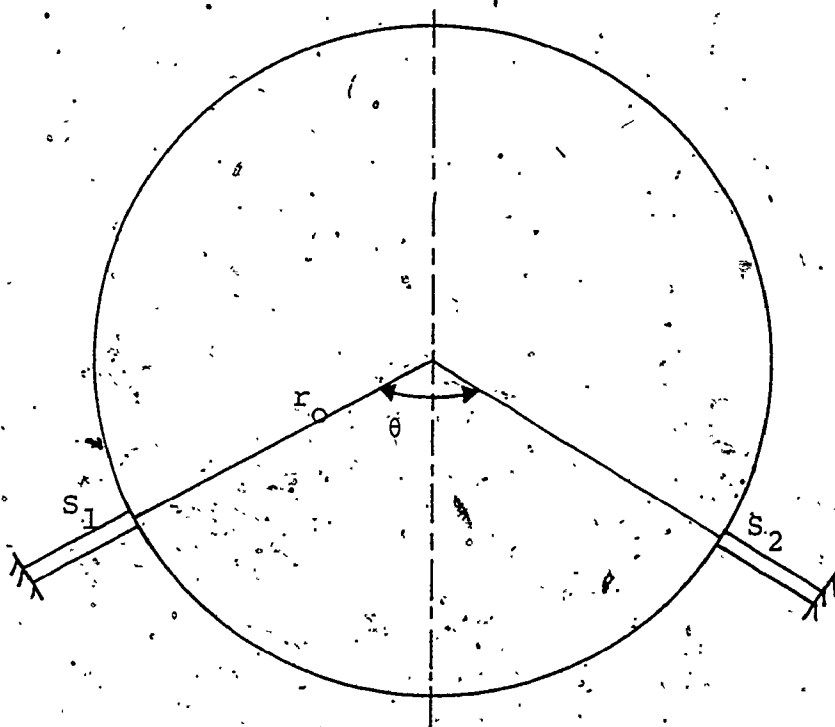
FIGURE 5.1  Location of the calorimeter supports

The stresses along the calorimeter surface are represented by a step function due to the existence of the supports. As a result of these stresses, there will be a strain energy or straining work on the calorimeter shell.

The total strain energy due to the liquid effect only is given by the following general equation:

$$W_{SM} = \frac{2\gamma^2\pi y^2}{27 r_o^2 t^2 E}(3r_o - y)[\frac{81}{16} r_o^6 (1-\mu) - \frac{27}{16} r_o^5 y(2-5\mu) - \frac{9}{8} r_o^4 y^2 (3+4\mu)$$

$$+ \frac{3}{4} r_o^3 y^3 (2-\mu) + 2r_o^2 y^4 (1+\mu) - \frac{2}{3} r_o y^5 (2+\mu) + \frac{2}{9} y^6]$$

$$+ \frac{5\gamma\pi r_o^5}{72 t^2 E}[\frac{3P^2}{2\gamma} (1-\mu) + P(\frac{3}{4}y - \frac{4}{3}r_o)(2-\mu) + \gamma(\frac{3}{8}y^2 - \frac{4}{3}y \cdot r_o + \frac{32}{27}r_o^2)]$$

$$+ \frac{5\gamma^2\pi r_o^5}{54 t^2 E}[(\frac{4}{3}r_o - \frac{3}{4}y)^2 (1+2\mu) - \frac{3P\mu}{\gamma}(\frac{4}{3}r_o - \frac{3}{4}y)] \tag{5.3}$$

Detailed derivation of equation 5.3 is given in Appendix D. Although this equation seems to be complicated, it is based on the basic and simple mathematical relationships and does not involve much calculation to yield numerical values. Furthermore, it may be seen from the equation that the strain energy is a function of the total mass, since it is a function of y which in turn is a direct function of the total mass of liquid contained in the calorimeter.

Numerical values for the strain energy which results

from the effect of mass alone can then be obtained by substitution of the constants in equation 5.3. Data for the values obtained at different temperatures is given in Table 5.3. From the table, we may notice that the numerical values of strain energy due to mass effect alone are very small. Also, we notice that strain energy increases slightly with temperature for different cases of high and low fillings. Furthermore, we find that strain energy value for high filling case is double that for low filling case at all temperatures. This interesting phenomena calls for a very important property. This property is that the relation between strain energies for different fillings may be represented by the following empirical equation:

$$\frac{W_1}{W_2} = (\frac{m_1}{m_2})^x \tag{5.4}$$

where $W_1$ and $W_2$ are the strain energies for fillings of masses $m_1$ and $m_2$ respectively. For the special case of the fillings used in this research, x was found to be 0.79.

Therefore, for the purpose of comparison between strain energies, one can use equation 5.4 instead of equation 5.3 which may be used only to calculate the absolute values of strain energy.

From the previous discussion and, as might be clear

## TABLE 5.3

### STRAIN ENERGY PRODUCED BY
### MASS EFFECT ONLY FOR HIGH AND LOW FILLINGS

| Initial Temp. (°C) | Final Temp. (°C) | Strain Energy for Low Filling (281.2213 gram) Joules | Strain Energy for High Filling (678.5554 gram) Joules |
|---|---|---|---|
| 100 | 150 | 3.44 | 6.878 |
| 150 | 200 | 3.48 | 6.958 |
| 200 | 250 | 3.50 | 6.998 |
| 250 | 300 | 3.52 | 7.038 |
| 300 | 350 | 3.56 | 7.118 |

from Tables 5.1, 5.2 and 5.3, the strain energy resulting
from the temperature effect alone is the greatest at low tem-
peratures. As temperature increases, the strain energy re-
sulting from the pressure effect alone increases until it
becomes the dominant factor.

## 5.4 THE TOTAL STRAIN ENERGY

As mentioned in the beginning of this chapter, the prin-
ciple of superposition is applied to find the total strain
energy in the calorimeter $W_s$ as the sum of the strain energies
resulting from the temperature effect alone, the pressure
effect alone and the mass effect alone as given by equations
5.1, 5.2 and 5.3.

The effect of the strain energy on the results obtained
for constant mass experiments in both high and low fillings
is shown in Tables 5.4 and 5.5. It can be seen from the two
tables that the numerical values of the total strain energy
are very small in comparison with the total electrical energy
added to the calorimeter. Therefore, the effect of strain
energy on the experimental values of enthalpy and other ther-
mophysical properties of fluids obtained from calorimetric
measurements is negligible. We may notice also from the
tables that the effect of strain energy on the results of low
filling experiments is nearly double the effect on the re-
sults obtained for high filling experiments.

## TABLE 5.4

### EFFECT OF TOTAL STRAIN ENERGY ON THE RESULTS OF THE CONSTANT MASS EXPERIMENTS

### (High filling case - 678.5554 grams)

| Initial Temp. (°C) | Final Temp. (°C) | Total Energy Added Joules | Actual Energy Added Joules | % Deviation |
|---|---|---|---|---|
| 100 | 150 | 216579.0371 | 216570.215 | 0.004 |
| 150 | 200 | 223822.548 | 223812.766 | 0.004 |
| 200 | 250 | 232985.7287 | 232971.1367 | 0.006 |
| 250 | 300 | 248184.014 | 248148.802 | 0.014 |

## TABLE 5.5

### EFFECT OF TOTAL STRAIN ENERGY ON THE RESULTS OF THE CONSTANT MASS EXPERIMENTS

### (Low filling case - 281.2213 grams)

| Initial Temp. (°C) | Final Temp. (°C) | Total Energy Added Joules | Actual Energy Added Joules | % Deviation |
|---|---|---|---|---|
| 100 | 150 | 131519.575 | 131507.195 | 0.009 |
| 150 | 200 | 138577.143 | 138563.803 | 0.01 |
| 200 | 250 | 148542.084 | 148523.934 | 0.012 |
| 250 | 300 | 161760.298 | 161721.528 | 0.024 |

# CHAPTER 6

## SURFACE ENERGY

### 6.1 GENERAL

If the sample contained in the calorimeter is partly liquid and partly vapour (i.e. a two phase system), there will exist a surface of separation between the two phases. At the surface, each atom is only partly surrounded by other atoms. On bringing an atom to the surface from the interior, bonds must be broken or distorted, and consequently there is an increase of energy. This will be termed the "surface energy" in this thesis. It is thus defined as the increase in free energy per unit area of new surface formed. If the normal distance between the displaced and undisplaced surfaces is denoted by dh and the radii of the surface areas at initial and final states are denoted by $R_1$ and $R_2$ respectively, the surface energy is then found from the basic equation (22):

$$W_{S.E.} = \sigma \, \pi (R_1^2 - R_2^2) \tag{6.1}$$

where

$W_{S.E.}$ is the change in surface energy (Joules), and

$\sigma$ is the surface tension coefficient (N/m).

## 6.2 SURFACE ENERGY EQUATION

A general equation for the surface energy is derived when a fixed amount of fluid and vapour contained in a spherical container undergoes a given temperature change. Figure 6-1 illustrates the volume changes as the liquid is taken from an initial saturation state at temperature $T_1$ to a final saturation state at temperature $T_2$. In this figure, $h_1$ is the height of vapour at initial state and $h_2$ is the height of vapour at the final saturation state.

In order to find $W_{S.E.}$, $R_1^2$ and $R_2^2$ are found first. The following expressions were found for $R_1^2$ and $R_2^2$.

$$R_1^2 = R^2 [1-4\cos^2\{ \tfrac{1}{3} \cos^{-1}(1 - 2\tfrac{V_{g_1}}{V}) + \tfrac{4\pi}{3}\}] \qquad (6.2)$$

$$R_2^2 = R^2 [1-4\cos^2\{ \tfrac{1}{3} \cos^{-1}(1 - 2\tfrac{V_{g_2}}{V}) + \tfrac{4\pi}{3}\}] \qquad (6.3)$$

where   R is the radius of the calorimeter (cm)

$V_{g_1}$ is the volume of saturated vapour at initial temperature, and is given by,

$$V_{g_1} = M\, v_{g_1}\, \frac{v-v_{f_1}}{v_{g_1}-v_{f_1}} \qquad (6.4)$$

$V_{g_2}$ is the total volume of saturated vapour at final temperature, and the same filling and is given by,
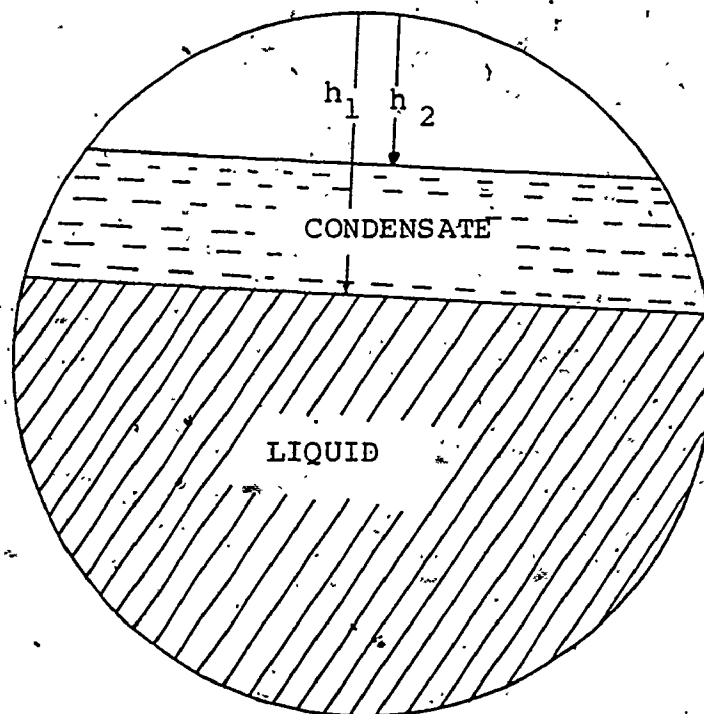
FIGURE 6.1  Process of vapour condensation as calorimeter
contents are allowed to increase in saturated
temperature

$$V_{g_2} = M \, v_{g_2} \, \frac{v - v_{f_2}}{v_{g_2} - v_{f_2}} \qquad\qquad (6.5)$$

M is the total mass and is constant for a particular filling,

v is the specific volume ($v = \frac{V}{M}$), defining the hetero-genous two phase system and is constant for a particular filling,

$v_f$ and $v_g$ are the specific volumes of the saturated liquid and saturated vapour respectively.

Upon substitution of equations 6.2 and 6.3 back into equation 6.1, the following general surface energy equation was obtained for a particular filling:

$$\frac{W_{S.E.}}{4\pi R^2 \sigma} = \{ [\cos^2\{\tfrac{1}{3} \cos^{-1}(1 - \frac{2V_{g_2}}{V}) + \frac{4\pi}{3}\}]$$

$$- [\cos^2\{\tfrac{1}{3} \cos^{-1}(1 - \frac{2V_{g_1}}{V}) + \frac{4\pi}{3}\}]\} \qquad (6.6)$$

The expression in the brackets in equation 6.6 gives the non-dimensional change in surface energy between the initial and final saturation states respectively.

For the purpose of determination of enthalpy and other thermodynamic properties, the difference in the change of surface energy for high and low filling cases is used rather than using the absolute values of surface energies. Consequently, the following general equation was obtained for the

net change of surface energy for high and low-filling cases:

$$\frac{W_{S.E.}}{4\pi R^2 \sigma} = \{[\cos^2\{\tfrac{1}{3}\cos^{-1}(1 - \frac{2V_{g_2}}{V}) + \frac{4\pi}{3}\}]$$

$$- [\cos^2\{\tfrac{1}{3}\cos^{-1}(1 - \frac{2V_{g_1}}{V}) + \frac{4\pi}{3}\}]$$

$$- [\cos^2\{\tfrac{1}{3}\cos^{-1}(1 - \frac{2V_{g_4}}{V}) + \frac{4\pi}{3}\}]$$

$$+ [\cos^2\{\tfrac{1}{3}\cos^{-1}(1 - \frac{2V_{g_3}}{V}) + \frac{4\pi}{3}\}]\} \tag{6.7}$$

where

$$V_{g_1} = M_H \, v_{g_1} \frac{v - v_{f_1}}{v_{g_1} - v_{f_1}} \tag{6.8}$$

$$V_{g_2} = M_H \, v_{g_2} \frac{v - v_{f_2}}{v_{g_2} - v_{f_2}} \tag{6.9}$$

$$V_{g_3} = M_L \, v_{g_3} \frac{v - v_{f_3}}{v_{g_3} - v_{f_3}} \tag{6.10}$$

$$V_{g_4} = M_L \, v_{g_4} \frac{v - v_{f_4}}{v_{g_4} - v_{f_4}} \tag{6.11}$$

Complete details of the derivation of equation 6.6 may be found in Appendix E. We notice from the equation that the surface energy is a function of only the mass of liquid contained in the calorimeter and the temperature of the sample which is characterized by the liquid and vapour specific volumes.

## 6.3 NUMERICAL CALCULATIONS OF THE SURFACE ENERGY

Since the value for σ is given only at 20°C for water, the following equation was given in reference (51) and used to calculate its value at different temperatures:

$$\frac{\sigma_2}{\sigma_1} = (\frac{T_C - T_2}{T_C - T_1})^{1.2} \tag{6.12}$$

where $T_1$ is the initial temperature (20°C),

$T_2$ is the temperature at which σ is required, and

$T_C$ is the critical temperature of the material.

For the purpose of comparison, numerical values for the surface energy in both high and low fillings are given in Table 6.1. Also, the net surface energy is given in the last column of the table. The table indicates that the net surface energy is extremely small compared to the total electrical energy added to the system. It may be concluded therefore that the effect of surface energy on the results of the calorimetric measurements is negligible.

TABLE 6.1

SURFACE ENERGY FOR HIGH AND LOW FILLINGS
AND NET SURFACE ENERGY

| Initial Temperature °C | Final Temperature °C | Surface Energy for High Filling (664.3845 grams) $\times10^{-7}$ Joules | Surface Energy for Low Filling (211.6122 grams) $\times10^{-7}$ Joules | Net Surface Energy $\times10^{-7}$ Joules |
|---|---|---|---|---|
| 100 | 150 | 1639.83 | 1266.06 | 373.77 |
| 150 | 200 | 1575.06 | 1236.75 | 338.31 |
| 200 | 250 | 1481.36 | 1200.54 | 280.82 |
| 250 | 300 | 1358.97 | 1139.01 | 219.96 |

# CHAPTER 7

## EXPERIMENTAL PROCEDURES

Three different types of experiments were performed in this research. These were:

(i)     heat leak experiments,

(ii)    tare energy experiments,

(iii)   constant mass experiments.

## (i) Heat Leak Experiments

Before the actual experiment was started, energy was electrically added to the calorimeter heater until the calorimeter filled with the sample was brought to a pre-established initial temperature. The power was then adjusted until the calorimeter reached the initial equilibrium state (where the reading of the platinum resistance thermometer was constant for about 30 minutes and the readings of the differential thermocouples over the calorimeter and adiabatic shield surfaces were consant for nearly the same period). The initial temperature of the system was then accurately measured just prior to starting the experiment. Constant electrical power was then supplied to the calorimeter heaters and adjusted in order to have a given heating rate. Power to the adiabatic shield, outerguard and tube heaters was adjusted in such a way that a desired constant

temperature difference between the calorimeter and the adiabatic shield was reached. Also, provision was made that the temperature of the outerguard matched that of the adiabatic shield. Adjustments of the power to both top and bottom tube heaters as well as to the supporting tube of the outerguard were made in order to compensate for conductive heat loss from these tubes.

After a certain rise in temperature was obtained, power to both calorimeter and adiabatic shield was turned off, allowing the calorimeter to reach its final equilibrium state. The final temperature of the system was then measured.

(ii) Tare Energy Experiments

Tare energy experiments were performed in order to find the heat capacity of the empty calorimeter experimentally. This was also required in order for comparison between calorimeter heat capacity obtained experimentally and those calculated from constant mass experiments.

In the tare energy experiments, the empty calorimeter was brought to equilibrium at a given absolute temperature. The initial temperature of the system was then accurately measured just prior to starting the experiment. Electrical energy was then added to the calorimeter heaters and power to both adiabatic shield and outerguard was adjusted in such a

2
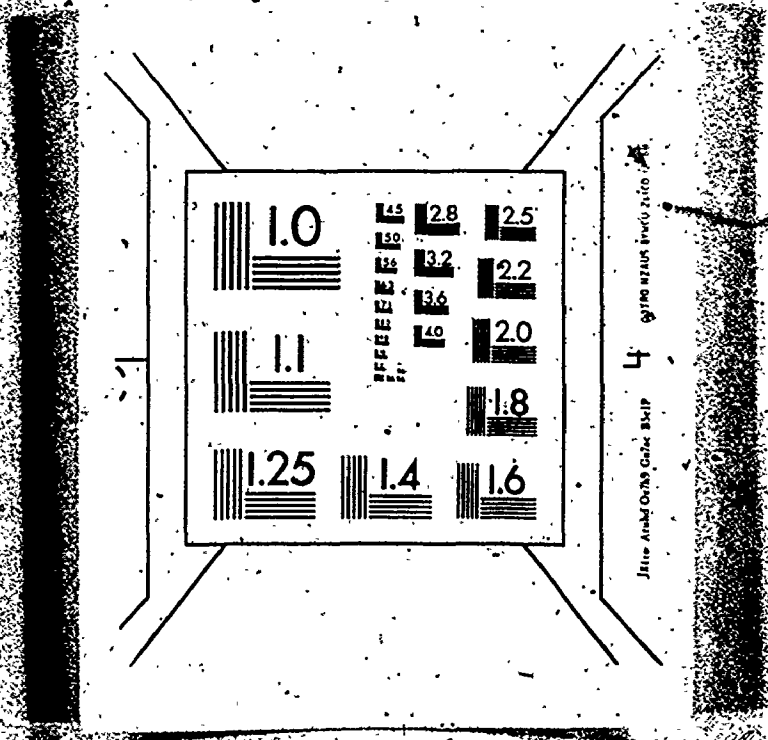
way as to keep the temperature of the adiabatic shield the same as that of the calorimeter in order to prevent heat from transferring from or to the calorimeter. Powers to all the tube heaters were adjusted in order to compensate for heat transfer by conduction.

After a certain temperature rise was obtained, power to both the calorimeter and adiabatic shield was turned off allowing the calorimeter to reach its final equilibrium state. The final temperature of the calorimeter was then measured.

(iii)   Constant Mass Experiments

The procedure used in the constant mass experiments was similar to that used in the heat leak experiments with the exception that in the constant mass experiments, the power to the adiabatic shield is adjusted so that its temperature always matches that of the calorimeter. The power is thus adjusted during the experiment to keep the temperature difference zero, as indicated by the control thermocouple. Usually, the rate of change of the calorimeter temperature in the equilibration period is not zero, indicating that the temperature of the adiabatic shield is not perfectly matched to that of the calorimeter even though the controlled temperature difference is zero. Whenever energy is supplied to the calorimeter or the adiabatic shield, it must flow from the heater to a surface where it is either lost to other surfaces

or to some volume, thereby raising the temperature. This
energy creates temperature gradients throughout the body
which have components only along the surface. Since the
temperatures of the calorimeter and adiabatic shield are
observed at only a relatively few points, it follows that the
observed temperature differs slightly from the average tem-
perature over the surface. In the constant mass experiments,
ligh water was used. Before the water was transferred to the
calorimeter, it was purified and degassed. The procedure
for filling the calorimeter, purifying and degassing the
water is explained in detail in Appendix F.

# CHAPTER 8

## RADIATIVE HEAT LEAK EVALUATION UTILIZING
## SURFACE TEMPERATURE VARIATIONS

### 8.1 INTRODUCTION

Insofar as the rate of thermal energy transfer within a calorimeter will be proportional to the temperature difference, it is extremely difficult to design a calorimeter to operate under ideal adiabatic conditions (zero thermal energy transfer between the calorimeter and the surroundings). The reason for this difficulty is the impossibility of completely matching at all times the temperature variations on the calorimeter surface to those on the adiabatic shield surface.

Existence of the heat exchange between the calorimeter and the surroundings is principally due to non-matching transient temperature distribution on the shield and calorimeter surfaces. The heat exchange mode is convection and radiation for a gaseous path and by conduction for a solid path.

The net amount of heat leak depends on the following factors:

(i)    the overall temperature difference between the calorimeter and the adiabatic shield;

(ii)   the overall heat transfer coefficient between the

calorimeter and its surroundings, and

(iii)   the overall temperature variations on the surfaces of

both the calorimeter and the adiabatic shield.

## 8.2   ERRORS IN HEAT LEAK EVALUATION

In order to control and evaluate the heat leak, it is

essential for a large number of differential thermocouples

to be installed on the surfaces of the calorimeter and adia-

batic shield in order to evaluate the transient temperature

distributions.   If sufficient number of thermocouples is not

employed, this will result in an incomplete knowledge of the

surface temperature variations which could lead to errors in

heat leak evaluation.   Another error in heat leak evaluation

will be due to erroneous thermocouple signals caused by stray

e.m.f. due to inhomogenities in metal composition along the

thermocouple leads.

The most difficult problem in measuring and evaluating

heat leak is to measure the effective temperature differences

along the various paths for heat flow between the calorimeter

and its surroundings.

## 8.3   RADIATION HEAT LEAK EQUATION

An equation is derived for heat leak by radiation; this

is probably the most serious factor in heat leak since the rate of radiative heat loss in the calorimeter is greatly increased at high temperatures, even for small temperature differences between the calorimeter and adiabatic shield. This might be clear from Figure 8-1 for the relation between the radiation heat transfer coefficient and absolute temperature for the case of a temperature difference $(T_1 - T_2)$ of 1°C, and the heat transfer coefficient $(h_r)$ is calculated from the following equation:

$$q = \sigma A(T_1^4 - T_2^4) \tag{8.1}$$

which is reduced to

$$q \equiv h_r A\sigma(T_1 - T_2)$$

and $h_r = (T_1^3 + T_1^2 T_2 + T_1 T_2^2 + T_2^3)$ \hspace{1cm} (8.2)

Derivation of the heat leak equation is based on the fact that heat leak is a function of absolute temperature, temperature difference between the calorimeter and adiabatic shield and temperature variations on the calorimeter surface as well as on the adiabatic shield surface.

The general equation, with reference to Figure 8-2 is now derived.

Since the calorimeter and adiabatic shield surfaces are not isothermal, it is necessary to divide them into isothermal
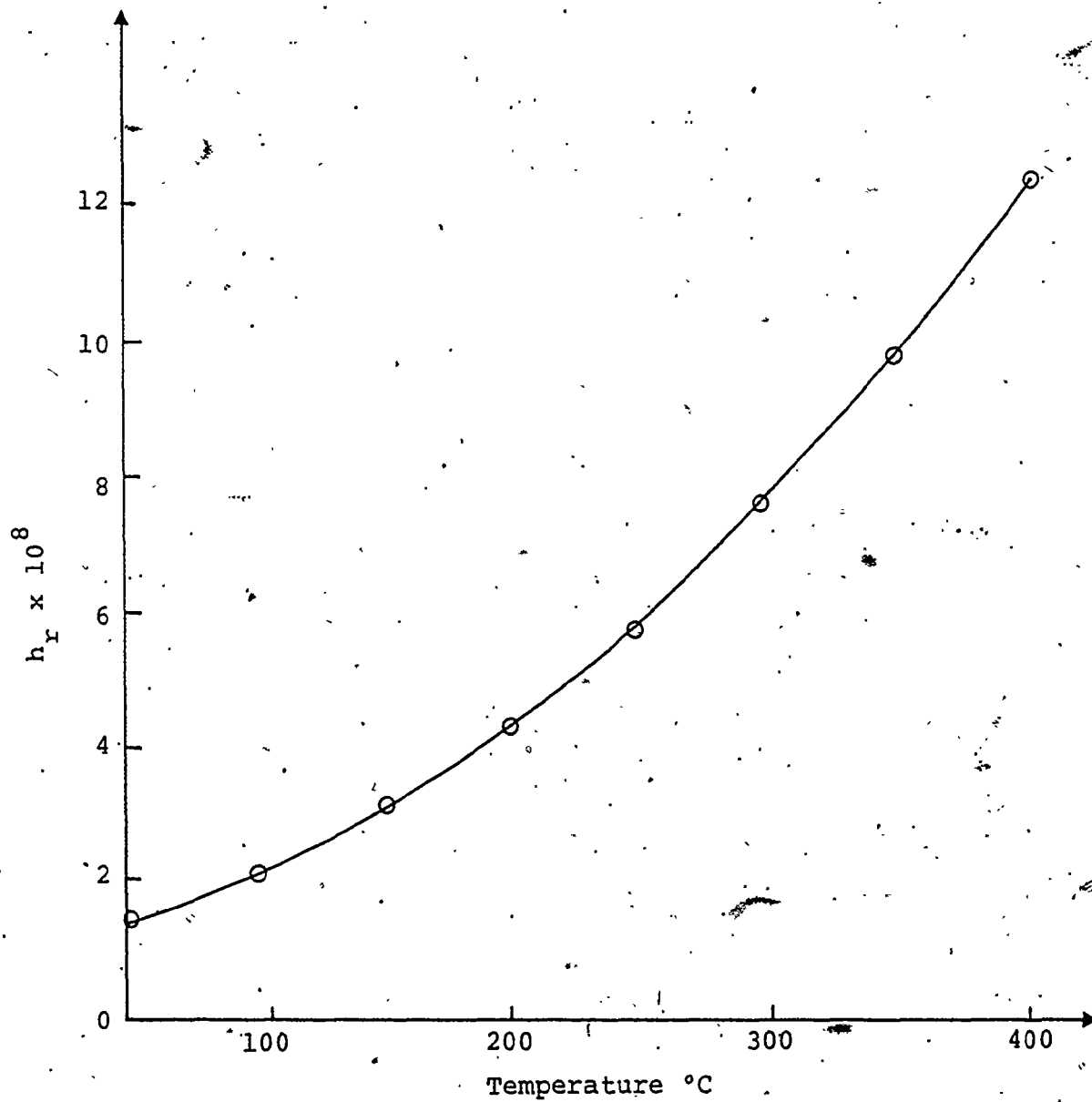
FIGURE 8,1 Relation between the radiation heat
transfer coefficient and absolute
temperature
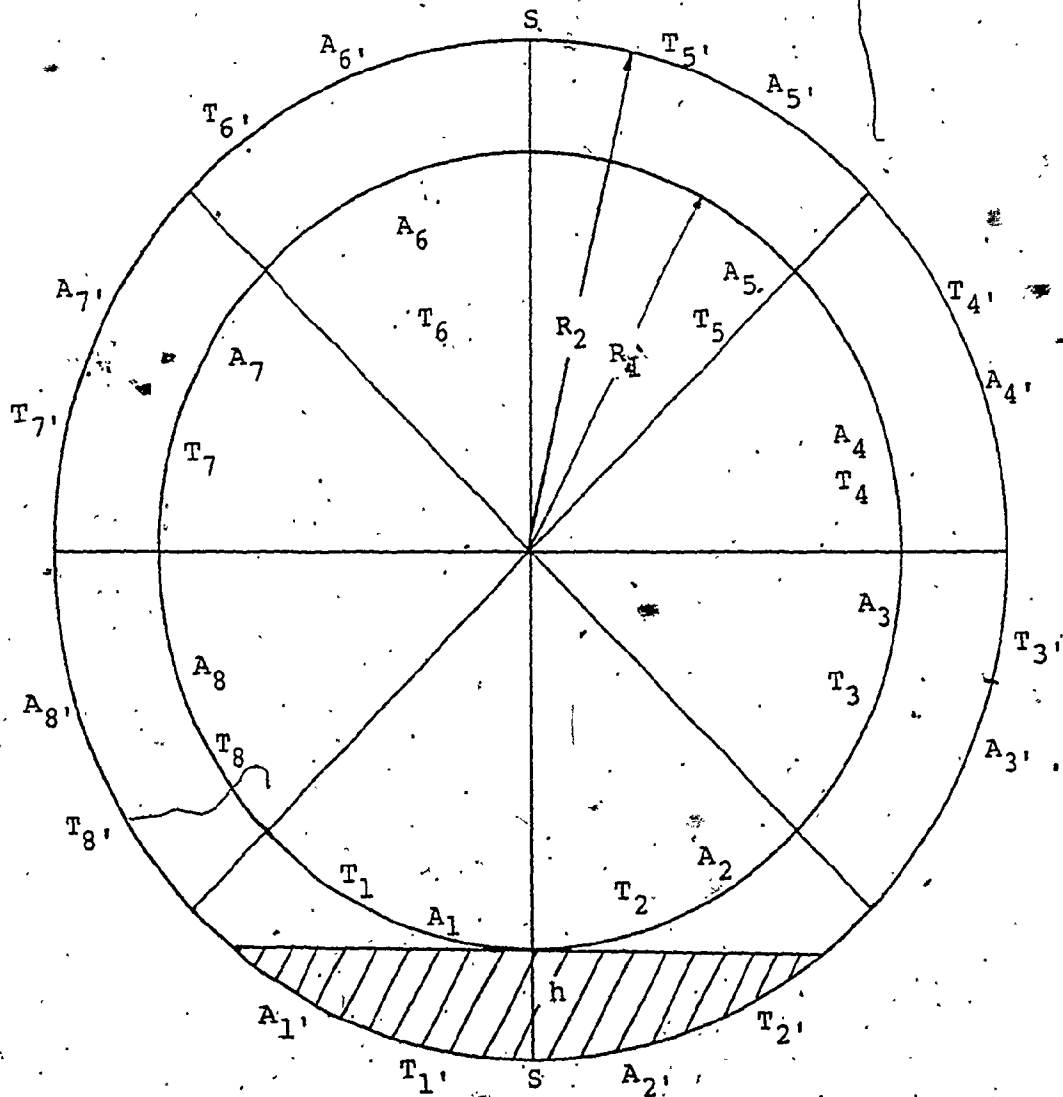
S-S is the axis of temperature
symmetry

FIGURE 8.2   Theoretical calculations of heat leak

surfaces. Therefore, both the calorimeter and adiabatic
shield surfaces are divided into eight equal subareas each,
i.e. $A_1$, $A_2$,...,$A_8$ for the calorimeter and $A_1'$, $A_2'$,...,$A_8'$ for
the adiabatic shield. It should be stressed that Figure 8.2
is just drawn for the purpose of illustration, and does not
represent the exact cross section of the sphere with the
mentioned way for dividing the sphere. It should also be
noted that the angles are not equal, and what is important
in this analysis is that the surface areas are equal.

The net effective rate of heat transfer by radiation for
a black body between an element or area i and surrounding
elements of areas j' is given in reference (60) by

$$\frac{Q_i}{A_i} = \sum_{j'=1}^{N} \sigma(T_i^4 - T_{j'}^4) F_{A_i-A_{j'}} \tag{8.3}$$

where

    $\sigma$ is the Stefan Boltzman constant.

    N is the total number of subareas (8 in this case)

    $F_{A_i-A_{j'}}$ is the shape factor for heat transfer from
        the area element $A_i$ to the area element $A_{j'}$.

Considering the heat transfer from element 1, in other
words taking i = 1 in the above equation, we obtain the
following relations with reference to Figure 8.2:

$$F_{A_1-A_{3'}} = F_{A_1-A_{4'}} = F_{A_1-A_{5'}} = F_{A_1-A_{6'}} = F_{A_1-A_{7'}} = 0$$

Consequently, for $i = 1$ in equation 8.3, the only contribution to the heat transfer comes from

$$F_{A_1-A_{1'}}, \quad F_{A_1-A_{2'}} \quad \text{and} \quad F_{A_1-A_{8'}}$$

Since the shape factor for heat transfer from element 1 to element $j'$ is given in reference (59) as:

$$F_{A_1-A_{j'}} = \frac{A_{j'}}{A_t} \qquad (8.4)$$

therefore areas $A_{j'}$ should be found first.

The subareas $A_{1'}, A_{2'}, A_{8'}$ are given by the following relations:

$$A_{1'} = \frac{1}{8}(4\pi R_2^2) = \frac{\pi}{2} \cdot R_2^2 \qquad (8.5)$$

$$A_{2'} = A_{8'} = \frac{1}{2}(2\pi R_2 h) = \pi R_2 (R_2 - R_1) \qquad (8.6)$$

where

   $A_{2'}$ and $A_{8'}$ are the effective areas for heat transfer between element of area 1 and each one of them respectively. Thus, each of $A_{2'}$ and $A_{8'}$ is equal to half the area of a cap of height h,

   $A_{1'}$ is equal to $\frac{1}{8}$th the total adiabatic shield surface area,

   $R_1$ and $R_2$ are the radii of the calorimeter and adiabatic shield respectively, and

   h is equal to $R_2 - R_1$

Therefore, the total area ($A_t$) contributing to heat exchange with element 1 is

$$A_t = A_{1'} + A_{2'} + A_{8'}$$

$$= \pi R_2 (\frac{5}{2} R_2 - 2R_1) \tag{8.7}$$

Using equations 8.5, 8.6 and 8.7 and substituting in equation 8.4 yields the following shape factors for the heat transfer between subarea $A_1$ and the different subareas $A_{1'}$, $A_{2'}$ and $A_{8'}$:

$$F_{A_1-A_{1'}} = \frac{A_{1'}}{A_t} = \frac{R_2}{5R_2 - 4R_1} \tag{8.8}$$

$$F_{A_1-A_{2'}} = \frac{A_{2'}}{A_t} = \frac{2(R_2-R_1)}{5R_2 - 4R_1} \tag{8.9}$$

$$F_{A_1-A_{8'}} = \frac{A_{8'}}{A_t} = \frac{2(R_2-R_1)}{5R_2 - 4R_1} \tag{8.10}$$

Since the radiant energy leaving any surface i in an enclosure must impinge on the various surfaces of the enclosure, none can be lost (Energy Conservation Principle). From this, it follows that

$$\sum_{j'=1}^{N} F_{A_i-A_{j'}} = 1 \tag{8.11}$$

where N denotes the number of surfaces in the enclosure.

Applying this principle to the results of equations 8.8, 8.9 and 8.10, we observe that

$$F_{A_1-A_1'} + F_{A_1-A_2'} + F_{A_1-A_8'} = 1$$

which satisfies the above principle.

In order to account for the heat transferred from area $A_1$, equation 8.3 is written in the following form:

$$\frac{\dot{Q}_1}{A_1} = \sigma(T_1^4 - T_1'^4)F_{A_1-A_1'} + \sigma(T_1^4 - T_2'^4)F_{A_1-A_2'} + \sigma(T_1^4 - T_8'^4)F_{A_1-A_8'} \quad (8.12)$$

Substituting for the shape factors from equations 8.8, 8.9 and 8.10 and rearranging, the following equation is obtained:

$$Q_1 = \sigma A_1 \left[ \frac{R_2(T_1^4 - T_1'^4)}{5R_2 - 4R_1} + \frac{2(R_2 - R_1)}{5R_2 - 4R_1}(2T_1^4 - T_2'^4 - T_8'^4) \right] \quad (8.13)$$

The total heat leak is obtained as the sum of all heat leaks from all regions. The general equation for the total heat leak is thus

$$Q = \sum_{K=1}^{N} \sigma A_K \left[ \frac{R_2(T_K^4 - T_K'^4)}{5R_2 - 4R_1} + \frac{2(R_2 - R_1)}{5R_2 - 4R_1}(2T_K^4 - T_{(K+1)'}^4 - T_{(K-1)'}^4) \right] \quad (8.14)$$

where

$$T_{0'} = T_{8'} \; ; \; T_{9'} = T_{1'}$$

8.4 APPLICATION OF THE HEAT LEAK EQUATION TO THE U.W.O.
APPARATUS

Since both the calorimeter and adiabatic shield surfaces tend to become black bodies only after the temperature is raised to high values and after the apparatus is used for

more experiments in which the temperature was repeatedly
raised and dropped, it is necessary to find the general equation for the non-black body case. In this case, the emissivity values for calorimeter and adiabatic shield surfaces are
less than unity. Consequently, equation 8.3 should be written in a different way to include the emissivities of the two
surfaces as follows (60):

$$\frac{Q_i}{A_i} = \sum_{j'=1}^{N} \sigma(\varepsilon_i T_i^4 - \varepsilon_{j'} T_{j'}^4) F_{A_i - A_{j'}} \tag{8.15}$$

Following the same procedure as above, the general
equation for the heat transfer between the calorimeter and
the adiabatic shield may be written as

$$Q = \sum_{K=1}^{N} \frac{\sigma A_K}{5R_2 - 4R_1} [R_2(\varepsilon_K T_K^4 - \varepsilon_{K'} T_{K'}^4)$$

$$+ 2(R_2 - R_1)(2\varepsilon_K T_K^4 - \varepsilon_{K'} T_{(K+1)'}^4 - \varepsilon_{K'} T_{(K-1)'}^4)] \tag{8.16}$$

## 8.5 ANALYSIS OF PREVIOUS U.W.O. WORK

In this research, equation 8.14 was used for heat leak
calculations using the temperature values at different regions
from the data obtained by Chan (7). Here, the different
temperature values were found from the temperature variations
on the calorimeter surface as well as on the adiabatic shield
surface as indicated by the differential thermocouples on
those surfaces. Figures 8-3, 8-4 and 8-5 give the temperature

FIGURE 8-3  Temperature variations on the calorimeter and
           adiabatic shield surfaces for calorimeter
           contents of 664.3845 grams.


LEGEND:  (7-12) ≡ control thermocouple

$T_{RC}$ =                         199.82°C

$T_{RA}$ =                         199.88°C

$T_4$  = $T_{RC}$ + 4.6 μv  = 199.9°C

$T_{11}$ = $T_{RA}$ + 10.8 μv = 200.07°C

$T_7$  = $T_{RC}$ + 10.3 μv = 200°C

$T_{12}$ = $T_{RA}$ + 8.0 μv  = 200.02°C

$T_8$  = $T_{RC}$ + 11.4 μv = 200.02°C

$T_{15}$ = $T_{RA}$ + 8.3 μv  = 200.025°C

$T_{16}$ = $T_{RA}$ + 9.1 μv  = 200.04°C
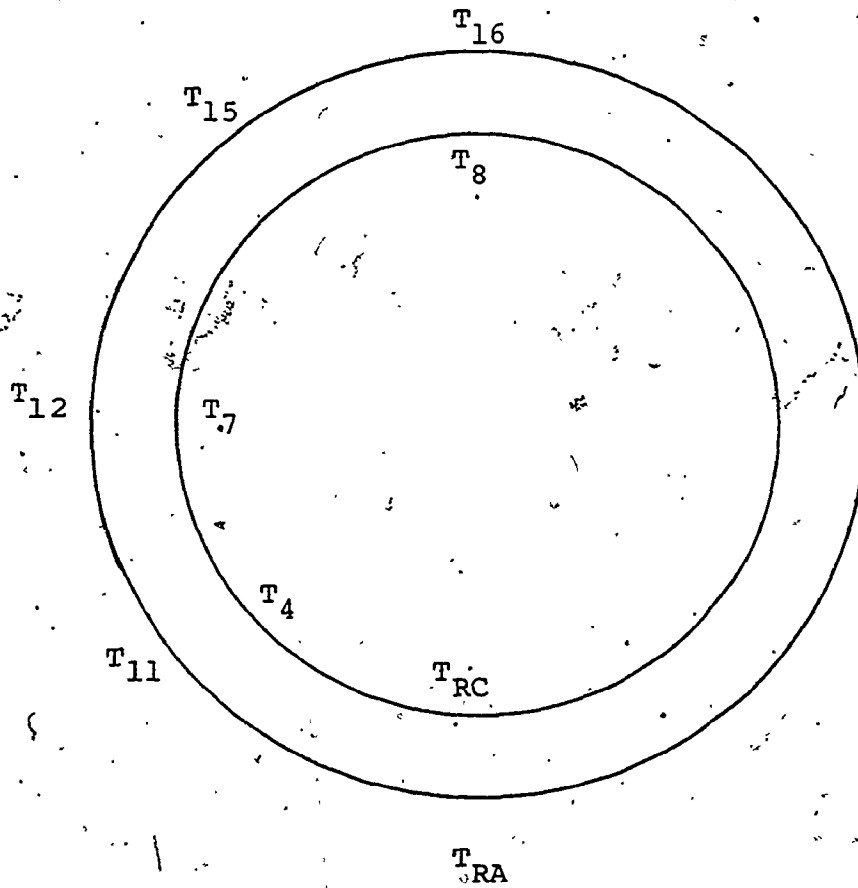
FIGURE 8.3 Temperature variations on the calorimeter
and adiabatic shield surfaces for calorimeter
contents of 664.3845 grams

FIGURE 8-4   Temperature variations on the calorimeter and
adiabatic shield surfaces for calorimeter
contents of 211.6122 grams


LEGEND:   (7-12) $\equiv$ Control thermocouple

$$T_{RC} \equiv \qquad\qquad 199.772°C$$

$$T_{RA} \equiv \qquad\qquad 199.732°C$$

$$T_4 = T_{RC} + 6.5 \ \mu v = 199.886°C$$

$$T_{11} = T_{RA} + 9.86 \ \mu v = 199.905°C$$

$$T_7 = T_{RC} + 13 \ \mu v = 200°C$$

$$T_{12} = T_{RA} + 14.7 \ \mu v = 199.99°C$$

$$T_8 = T_{RC} + 13.9 \ \mu v = 200.016°C$$

$$T_{15} = T_{RA} + 15.5 \ \mu v = 200.004°C$$

$$T_{16} = T_{RA} + 15.3 \ \mu v = 200°C$$
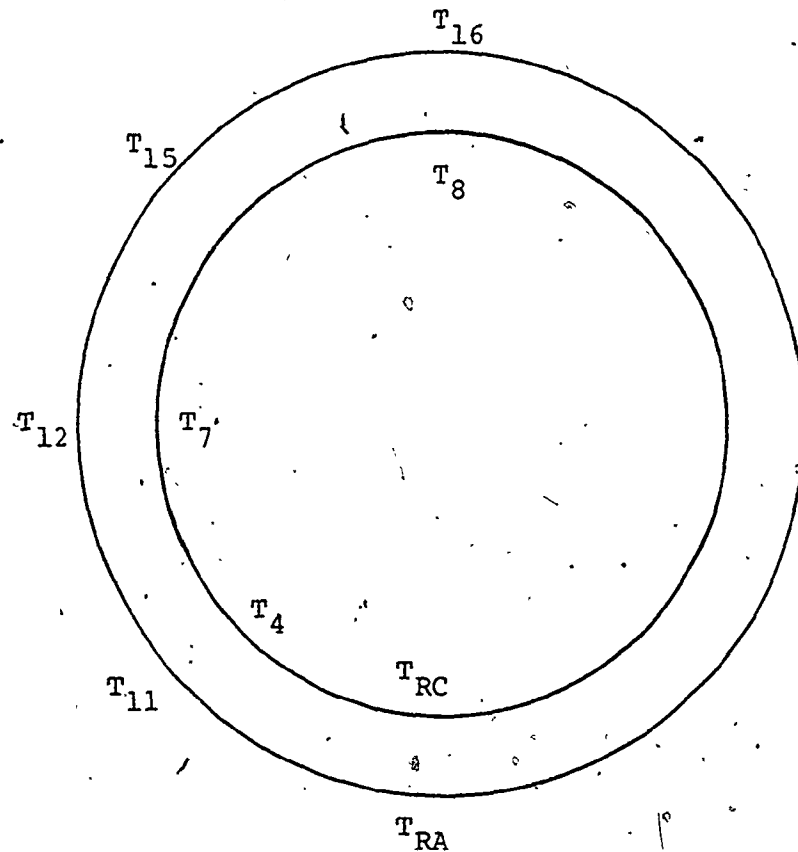
FIGURE 8.4   Temperature variations on the calorimeter
and adiabatic shield surfaces for
calorimeter contents of 211.6122 grams

FIGURE 8.5  Temperature variations on the calorimeter and
adiabatic shield surfaces for empty calorimeter

LEGEND:  (7-12) ≡ Control thermocouple

$$T_{RC} = \qquad\qquad 200.434°C$$

$$T_{RA} = \qquad\qquad 200.247°C$$

$$T_4 = T_{RC} - 26.2 \ \mu v = 199.975°C$$

$$T_{11} = T_{RA} - 13.7 \ \mu v = 200.006°C$$

$$T_7 = T_{RC} - 24.2 \ \mu v = 200.01°C$$

$$T_{12} = T_{RA} - 14.1 \ \mu v = 200°C$$

$$T_8 = T_{RC} - 24.5 \ \mu v = 200.004°C$$

$$T_{15} = T_{RA} - 14.8 \ \mu v = 199.987°C$$

$$T_{16} = T_{RA} - 16.6 \ \mu v = 199.955°C$$
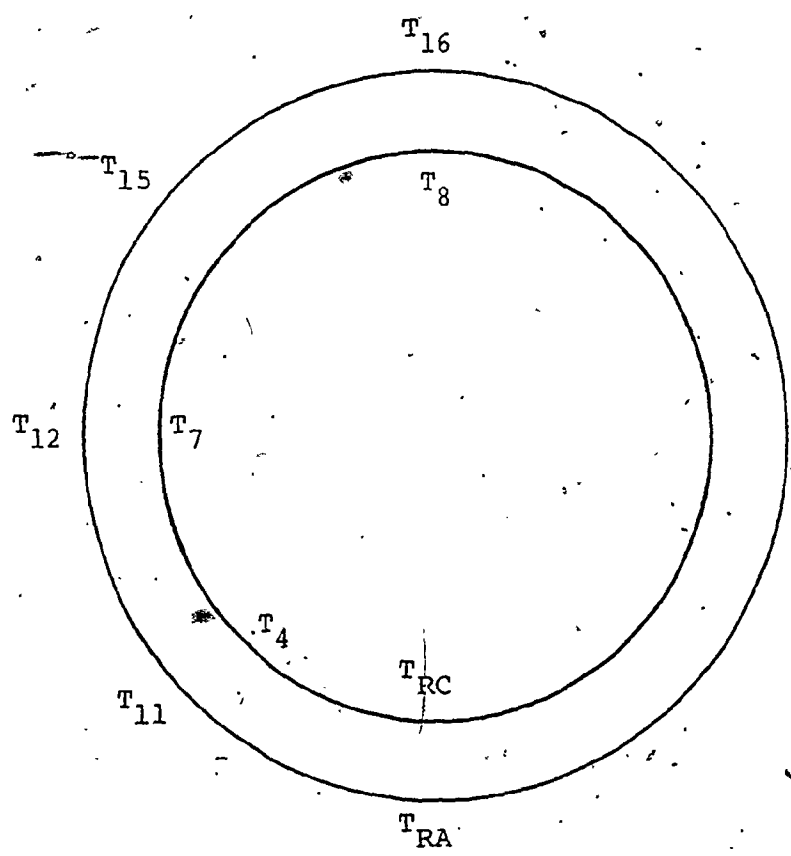
FIGURE 8.5  Temperature variations on the calorimeter
and adiabatic shield surfaces for empty
calorimeter

variations obtained for different cases of high and low fillings as well as for the empty calorimeter. Table 8.1 is obtained for the heat leak values at different absolute temperatures and for a temperature interval of 50°C. Calculations of the values in Table 8.1 are based on the substitution of temperature differences from Figures 8-3, 8-4 and 8-5 into equation 8.14.

The results of Table 8.1 indicate that the magnitude of radiative heat leak not only increases with temperature but it is strongly influenced by the mass of the fluid contents contained in the calorimeter. Moreover, the direction of the heat leak is influenced by the mass of the fluid contents. Thus, in taking the difference in the electrical energy added to the calorimeter system under conditions of high and low fillings, the heat leaks associated with these fillings are added together instead of cancelling each other out.

Knowledge hereby gained about the direction of the radiative heat leak and its magnitude can be systematically utilized to correct the earlier results obtained by Chan (7) for the empty calorimeter system. Chan's uncorrected results are shown in Table 8.2. The table shows that heat capacity for the empty calorimeter system is different when found from two different methods. The difference amounts to 2.6% at 300°C.

## TABLE 8.1

### HEAT LEAK VALUES CALCULATED ANALYTICALLY

### FOR DIFFERENT FILLINGS

| Temperature Interval (°C) | | Heat Leak For High Filling (Joules) | Heat Leak For Low Filling (Joules) | Heat Leak For Empty Calorimeter (Joules) |
|---|---|---|---|---|
| From | To | | | |
| 100 | 150 | 303.7 | -85.5 | -169.2 |
| 150 | 200 | 595.3 | -223.2 | -241.4 |
| 200 | 250 | 842.0 | -430.1 | -331.0 |
| 250 | 300 | 1201.6 | -643.9 | -441.6 |

## TABLE 8.2

COMPARISONS BETWEEN THE OBSERVED VALUES AND THE

ACTUAL VALUES OF THE HEAT CAPACITY OF THE EMPTY CALORIMETER

| Temperature Interval (°C) | | Measured Value Obtained Under Vacuum Conditions (Joules) | Actual Value Inferred From Constant Mass Measurements (Joules) | Deviation From Actual Value % |
|---|---|---|---|---|
| From | To | | | |
| 50 | 100 | 80502.0 | 80114.5 | +0.5 |
| 100 | 150 | 82771.8 | 82383.5 | +0.5 |
| 150 | 200 | 84990.9 | 84166.4 | +1.0 |
| 200 | 250 | 87190.0 | 85754.7 | +1.7 |
| 250 | 300 | 89332.2 | 87096.6 | +2.6 |

The corrected results of Chan (utilizing the radiative heat leak values of Table 8.1) are given in Table 8.3. The table indicates that results are significantly improved on taking radiative heat leak into consideration. The maximum deviation from the actual value is 1.17% at 300°C.

It must be mentioned that if the conduction heat transfer through the different metallic and non-metallic paths and the convective heat transfer through the system are taken into consideration, the results in Table 8.3 may be significantly improved.

It should also be emphasized that in deriving the equation for radiative heat leak, reflections between the surfaces were neglected. However, using the Bevon-Dunkle (72) method may take into account these reflection effects and consequently improve the results for radiative zero heat leak. Further research may therefore be necessary for the evaluation of the radiative zero heat leak by this method using a set of equations as follows and with reference to Figure 8.2.

$$q_{net_1} = \sum_{K=2}^{16} (J_K - J_1) F_{1K} A_1 \qquad (8.17)$$

$$q_{net_2} = \sum_{\substack{K=1 \\ K \neq 2}}^{16} (J_K - J_1) F_{2K} A_2 \qquad (8.18)$$

## TABLE 8.3

### COMPARISON BETWEEN THE OBSERVED VALUES

### AND THE ACTUAL VALUES OF THE HEAT CAPACITY

### OF THE EMPTY CALORIMETER WITH CORRECTION APPLIED

| Temperature Interval (°C) | | Measured Value Obtained Under Vacuum Conditions (Joules) | Actual Value From Constant Mass Measurements (Joules) | Deviation From Actual Value % |
|---|---|---|---|---|
| From | To | | | |
| 100 | 150 | 82771.8 | 82687.2 | 0.102 |
| 150 | 200 | 84990.9 | 84761.7 | 0.27 |
| 200 | 250 | 87190.0 | 86596.7 | 0.685 |
| 250 | 300 | 89332.2 | 88298.2 | 1.17 |

$$q_{net_8} = \sum_{\substack{K=1 \\ K \neq 8}}^{16} (J_K - J_8) F_{8K} A_8 \qquad (8.19)$$

This also might be clear from a comparison between the heat leak values for the empty calorimeter calculated analytically and shown in Table 8.1 as compared with Chan's measured values as given in Table 2.1. The two tables show that the magnitude of the measured values is much larger than the calculated ones. This may be attributed to the neglect of conduction and convection heat transfers as mentioned above.

## CHAPTER 9

## EXPERIMENTAL DETERMINATION OF INCREMENTAL HEAT LEAK

### 9.1 INTRODUCTION

It is necessary to study and understand the effect of heat leak on calorimetric determinations of thermodynamic properties of fluids. For this purpose, experiments were performed using the existing U.W.O. apparatus. However, this apparatus is not perfect, but rather deteriorated and after being used for a long time under high temperature and high pressure conditions, oxidation took place and caused the deterioration of the apparatus. The incremental heat leak experiments were conducted to systematically study the effect of

(i) the mass of fluid contents in the calorimeter,

(ii) the heating rate employed,

(iii) the temperature difference offset between the calorimeter and adiabatic shield.

### 9.2 METHOD OF INCREMENTAL HEAT LEAK DETERMINATION

The incremental heat leak values are found as the difference between the total energy added in two similar experiments where the calorimeter is filled with the same amount of fluid. In the first experiment, a certain

temperature difference is kept between the calorimeter and adiabatic shield, while in the second, there is no measured temperature difference.

Therefore, the incremental heat leak is found from the following two equations:

$$q_{\delta T} + q_{\delta T=0} = W_{e_{\delta T}} + M[h_f - Tv_f \frac{dP}{dT}]_1^2 = (V\ T\ \frac{dP}{dT} - PV)_1^2$$

$$+ M_c c_{p_c} \Delta T + W_S + W_{S.E.} \qquad (9.1)$$

$$q_{\delta T=0} = W_{e_{\delta T=0}} + M[h_f - Tv_f \frac{dP}{dT}]_1^2 + (V\ T\ \frac{dP}{dT} - PV)_1^2$$

$$+ M_c c_{p_c} \Delta T + W_S + W_{S.E.} \qquad (9.2)$$

where

$q_{\delta t}$    is the heat leak for the case when there is a temperature difference ($\delta T$) between the calorimeter and adiabatic shield (incremental heat leak).

$q_{\delta T=0}$    is the heat leak when there is no temperature difference (zero heat leak)

$W_{e_{\delta T}}$    is the electrical energy added to the system for the case of a temperature difference $\delta T$

$W_{e_{\delta T=0}}$    is the electrical energy added to the system for a zero temperature difference.

Since $W_S$ and $W_{S.E.}$ are very small as indicated in Chapters 5 and 6, then the last three terms of the Right Hand Side of equations 9.1 and 9.2 are equal. Therefore the incremental heat leak value is found from

$$q_{\delta T} = W_{e_{\delta T}} - W_{e_{\delta T=0}} \tag{9.3}$$

The heat transfer coefficient is also found from the heat leak.

The following equation is used to calculate the incremental heat transfer coefficient

$$Q_L = h \, A \, \delta T \tag{9.4}$$

where

$Q_L = q_{\delta T}$ heat leak (Joules)

$\delta T$ is the average temperature difference between calorimeter and adiabatic shield, and

A is the overall surface area of the calorimeter.

Two sets of experiments were performed for heat leak studies. The first is a set of heat leak experiments in which the calorimeter was filled with approximately 302 grams of light water. The second is a set of experiments in which the calorimeter was filled with approximately 678 grams.

Information on the heat leak when the temperature difference effect between the calorimeter and adiabatic shield

was varied from 0.26 to 1.01°C per hour is obtained.

## 9.3 EXPERIMENTAL RESULTS

Tables 9.1 to 9.5 contain incremental heat leak results with the calorimeter charged with about 302 grams of light water at a nominal fluid temperature of 300°C. For each of the five cases whose results are given in the tables, the heating rate was changed from 1 to 10°C/hr while the temperature difference between the calorimeter and adiabatic shield was kept at a nearly constant value which is different for each case.

Heat transfer coefficients are also given in the sixth column of Tables 9.1 to 9.5.

The incremental heat leak results for the same calorimeter charge as above and for a temperature difference of 0.6°C between the calorimeter and adiabatic shield and two different values of 100, 200°C for the absolute temperature are given in Tables 9.6 and 9.7. Again, the heat transfer coefficient is given in column 6 of the two tables.

With the calorimeter charged with about 678 grams, heat leak experiments were conducted for a temperature difference of 0.6°C between the calorimeter and adiabatic shield and with the heating rate varied from 1 to 10°C per hour. Tables 9.8, 9.9 and 9.10 summarize the incremental heat leak results

TABLE 9.1

HEAT LEAK FOR A TEMPERATURE DIFFERENCE OF 0.26°C BETWEEN CALORIMETER AND ADIABATIC SHIELD (Charge = 302.546 grams)

| Initial Temperature (°C) | Final Temperature (°C) | Temperature Difference Between Calorimeter and Adiabatic Shield (°C) | Heating Rate (°C/hr) | Heat Leak for 1°C Temperature Rise (Joules) | Heat Transfer Coefficient (watts/°C - overall area)* |
|---|---|---|---|---|---|
| 300.542 | 302.388 | 0.259 | 1.231 | 739.2746 | 0.976 |
| 304.841 | 306.3825 | 0.288 | 1.540 | 564.2864 | 0.838 |
| 302.943 | 305.572 | 0.263 | 1.972 | 423.8550 | 0.883 |
| 304.9685 | 309.741 | 0.262 | 3.182 | 247.828 | 0.836 |
| 301.933 | 306.464 | 0.257 | 4.270 | 144.3839 | 0.666 |
| 304.3475 | 310.9455 | 0.264 | 4.877 | 128.7498 | 0.661 |
| 303.929 | 312.536 | 0.264 | 6.197 | 103.9733 | 0.679 |
| 304.921 | 313.603 | 0.258 | 6.539 | 100.5874 | 0.708 |
| 306.646 | 314.688 | 0.262 | 7.825 | 97.4195 | 0.808 |
| 304.670 | 316.971 | 0.260 | 9.540 | 73.7032 | 0.751 |
| 306.748 | 320.094 | 0.272 | 9.810 | 92.7143 | 0.929 |

*Overall area used in this thesis is given by

overall area = $4\pi R^2$, R = 6.35 cms

## TABLE 9.2

### HEAT LEAK FOR A TEMPERATURE DIFFERENCE OF 0.38°C BETWEEN CALORIMETER AND ADIABATIC SHIELD (Charge = 302.546 grams)

| Initial Temperature (°C) | Final Temperature (°C) | Temperature Difference Between Calori- meter and Adia- batic Shield(°C) | Heating Rate (°C/hr) | Heat Leak for 1°C Temperature Rise (Joules) | Heat Transfer Coefficient (watts/°C - overall area) |
|---|---|---|---|---|---|
| 303.8905 | 306.3055 | 0.375 | 1.256 | 1092.9253 | 1.017 |
| 305.956 | 308.938 | 0.388 | 2.147 | 681.544 | 1.048 |
| 305.400 | 311.117 | 0.391 | 4.200 | 296.052 | 0.883 |
| 305.824 | 313.877 | 0.377 | 6.040 | 198.64 | 0.884 |
| 305.753 | 317.186 | 0.371 | 8.365 | 132.152 | 0.928 |
| 305.651 | 319.676 | 0.379 | 9.980 | 103.892 | 0.960 |

TABLE 9.3

HEAT LEAK FOR A TEMPERATURE DIFFERENCE OF 0.6°C BETWEEN CALORIMETER
AND ADIABATIC SHIELD (Charge = 302.546 grams)

| Initial Temperature (°C) | Final Temperature (°C) | Temperature Difference Between Calorimeter and Adiabatic Shield (°C) | Heating Rate (°C/hr) | Heat Leak for 1°C Temperature Rise (Joules) | Heat Transfer Coefficient (watts/°C - overall area) |
|---|---|---|---|---|---|
| 306.630 | 309.5205 | 0.591 | 2.262 | 1111.3865 | 1.182 |
| 304.3425 | 308.804 | 0.594 | 3.374 | 667.1149 | 1.053 |
| 305.817 | 310.8855 | 0.589 | 4.240 | 508.8108 | 1.018 |
| 305.178 | 311.220 | 0.609 | 4.517 | 504.3050 | 1.039 |
| 304.856 | 311.632 | 0.604 | 4.86 | 431.4720 | 0.964 |
| 304.683 | 312.897 | 0.595 | 6.160 | 330.4172 | 0.950 |
| 302.8405 | 312.380 | 0.604 | 7.338 | 263.605 | 0.890 |
| 305.438 | 315.645 | 0.592 | 7.953 | 272.7816 | 1.018 |
| 304.938 | 316.2275 | 0.582 | 8.467 | 257.6686 | 1.041 |
| 303.4735 | 313.591 | 0.591 | 8.510 | 237.4742 | 0.950 |
| 304.5453 | 315.886 | 0.592 | 8.510 | 235.1025 | 0.938 |
| 306.802 | 319.042 | 0.586 | 9.415 | 262.1646 | 1.17 |

TABLE 9.4.

HEAT LEAK FOR A TEMPERATURE DIFFERENCE OF 0.83°C BETWEEN CALORIMETER AND ADIABATIC SHIELD (Charge = 302.546 grams)

| Initial Temperature (°C) | Final Temperature (°C) | Temperature Difference Between Calorimeter and Adiabatic Shield (°C) | Heating Rate (°C/hr) | Heat Leak for 1°C Temperature Rise (Joules) | Heat Transfer Coefficient (watts/°C - overall area) |
|---|---|---|---|---|---|
| 304.2845 | 309.0735 | 0.816 | 3.394 | 1011.5064 | 1.169 |
| 304.931 | 311.201 | 0.819 | 4.802 | 702.3682 | 1.144 |
| 306.028 | 315.2435 | 0.843 | 6.505 | 525.9863 | 1.127 |
| 304.835 | 316.850 | 0.838 | 7.836 | 415.2587 | 1.079 |
| 305.904 | 317.680 | 0.825 | 8.869 | 361.3434 | 1.079 |
| 306.741 | 320.505 | 0.829 | 10.112 | 357.9872 | 1.213 |

## TABLE 9.5

HEAT LEAK FOR A TEMPERATURE DIFFERENCE OF 1.0°C BETWEEN CALORIMETER AND ADIABATIC SHIELD (Charge = 302.546 grams)

| Initial Temperature (°C) | Final Temperature (°C) | Temperature Difference Between Calorimeter and Adiabatic Shield (°C) | Heating Rate (°C/hr) | Heat Leak for 1°C Temperature Rise (Joules) | Heat Transfer Coefficient (watts/°C - overall area) |
|---|---|---|---|---|---|
| 304.821 | 310.713 | 0.979 | 3.708 | 1059.34 | 1.115 |
| 305.378 | 312.327 | 1.014 | 4.867 | 807.69 | 1.077 |
| 306.660 | 314.662 | 1.007 | 5.808 | 701.24 | 1.123 |
| 306.506 | 315.638 | 1.012 | 6.849 | 606.09 | 1.139 |
| 305.819 | 315.862 | 1.0006 | 7.725 | 514.00 | 1.102 |
| 304.334 | 316.852 | 1.028 | 9.235 | 417.02 | 1.041 |

TABLE 9.6

HEAT LEAK FOR A TEMPERATURE DIFFERENCE OF 0.6°C BETWEEN CALORIMETER
AND ADIABATIC SHIELD (Charge = 302.546 grams)

| Initial Temperature (°C) | Final Temperature (°C) | Temperature Difference Between Calorimeter and Adiabatic Shield (°C) | Heating Rate (°C/hr) | Heat Leak for 1°C Temperature Rise (Joules) | Heat Transfer Coefficient (watts/°C - overall area) |
|---|---|---|---|---|---|
| 102.658 | 104.931 | 0.572 | 1.705 | 535.6736 | 0.443 |
| 101.6725 | 105.5075 | 0.588 | 2.847 | 288.8849 | 0.388 |
| 102.891 | 108.1155 | 0.599 | 4.478 | 174.8383 | 0.363 |
| 101.589 | 109.715 | 0.581 | 6.649 | 95.8117 | 0.305 |
| 100.810 | 109.8675 | 0.597 | 7.548 | 79.9406 | 0.281 |
| 102.156 | 112.601 | 0.604 | 9.741 | 55.7432 | 0.250 |

TABLE 9.7

HEAT LEAK FOR A TEMPERATURE-DIFFERENCE OF 0.6°C BETWEEN CALORIMETER
AND ADIABATIC SHIELD (Charge = 302.546 grams)

| Initial Temperature (°C) | Final Temperature (°C) | Temperature Difference Between Calori-meter and Adia-batic Shield(°C) | Heating Rate (°C/hr) | Heat Leak for 1°C Temperature Rise (Joules) | Heat Transfer Coefficient (watts/°C - overall area) |
|---|---|---|---|---|---|
| 201.7375 | 204.427 | 0.572 | 1.841 | 792.066 | 0.708 |
| 201.012 | 204.676 | 0.568 | 3.039 | 485.6172 | 0.722 |
| 202.4175 | 209.117 | 0.591 | 5.025 | 296.4516 | 0.700 |
| 202.427 | 212.2325 | 0.603 | 7.175 | 219.8817 | 0.727 |
| 203.193 | 215.165 | 0.599 | 8.979 | 182.4243 | 0.760 |
| 202.1445 | 214.208 | 0.610 | 10.390 | 161.5382 | 0.764 |

TABLE 9.8

HEAT LEAK FOR A TEMPERATURE DIFFERENCE OF 0.6°C BETWEEN CALORIMETER
AND ADIABATIC SHIELD (Charge = 678.5554 grams)

| Initial Temperature (°C) | Final Temperature (°C) | Temperature Difference Between Calorimeter and Adiabatic Shield (°C) | Heating Rate (°C/hr) | Heat Leak for 1°C Temperature Rise (Joules) | Heat Transfer Coefficient (watts/°C - overall area) |
|---|---|---|---|---|---|
| 102.308 | 106.215 | 0.607 | 2.824 | 305.0266 | 0.394 |
| 103.178 | 107.961 | 0.608 | 3.311 | 262.3212 | 0.397 |
| 102.976 | 108.839 | 0.614 | 4.238 | 188.929 | 0.362 |
| 102.678 | 109.691 | 0.602 | 5.152 | 123.3959 | 0.293 |
| 102.3885 | 111.812 | 0.623 | 6.524 | 103.3073 | 0.300 |
| 105.187 | 116.925 | 0.619 | 8.485 | 76.3485 | 0.291 |

TABLE 9.9

HEAT LEAK FOR A TEMPERATURE DIFFERENCE OF 0.6°C BETWEEN CALORIMETER AND ADIABATIC SHIELD (Charge = 678.5554 grams)

| Initial Temperature (°C) | Final Temperature (°C) | Temperature Difference Between Calorimeter and Adiabatic Shield(°C) | Heating Rate (°C/hr) | Heat Leak for 1°C Temperature Rise (Joules) | Heat Transfer Coefficient (watts/°C.- overall area) |
|---|---|---|---|---|---|
| 199.583 | 203.059 | 0.579 | 2.406 | 598.4281 | 0.691 |
| 199.934 | 204.806 | 0.6165 | 3.654 | 427.1504 | 0.703 |
| 198.784 | 205.887 | 0.627 | 5.440 | 266.8746 | 0.643 |
| 200.818 | 208.549 | 0.618 | 6.627 | 219.8716 | 0.655 |
| 201.007 | 208.972 | 0.635 | 8.193 | 185.9602 | 0.666 |

TABLE 9.10

**HEAT LEAK FOR A TEMPERATURE DIFFERENCE OF 0..6°C BETWEEN CALORIMETER AND ADIABATIC SHIELD (Charge = 678.5554 grams)**

| Initial Temperature (°C) | Final Temperature (°C) | Temperature Difference Between Calorimeter and Adiabatic Shield (°C) | Heating Rate (°C/hr) | Heat Leak for 1°C Temperature Rise (Joules) | Heat Transfer Coefficient (watts/°C -overall area) |
|---|---|---|---|---|---|
| 302.795 | 306.429 | 0.558 | 2.145 | 1442.6406 | 1.677 |
| 302.543 | 305.864 | 0.585 | 2.491 | 1418.2935 | 1.540 |
| 304.477 | 309.198 | 0.605 | 3.332 | 824.8214 | 1.262 |
| 303.888 | 309.629 | 0.612 | 4.306 | 606.6278 | 1.179 |
| 304.746 | 310.788 | 0.611 | 4.35 | 534.8746 | 1.058 |
| 303.7915 | 312.748 | 0.630 | 6.45 | 370.7645 | 0.976 |
| 303.565 | 314.404 | 0.621 | 7.95 | 305.8932 | 0.945 |

for nominal temperatures of 100, 200 and 300°C respectively. Results of the heat transfer coefficient are given in the last column of each table.

## 9.4  ANALYSIS OF THE RESULTS

Figure 9-1 is a summary of the results given in Tables 9.1 to 9.5.  It gives the relation between incremental heat leak and heating rate for a nominal absolute temperature of 300°C with the temperature difference between the calorimeter and adiabatic shield varied from 0.26 to 1.01°C and the heating rate varied from 1 to 10°C/hr.  The curves are combined in one figure for the purpose of comparison between absolute heat leak values for different cases of temperature differences between calorimeter and adiabatic shield.

From the figure, we may conclude that:

(i)    the incremental heat leak values decrease with increasing the heating rate.

(ii)   the rate of change of incremental heat leak is small at high heating rates.

(iii)  the difference between incremental heat leak values for different temperature differences is small at high heating rates and increases with decreasing heating rate.

(iv)   Also, we may conclude that the scatter in the heat
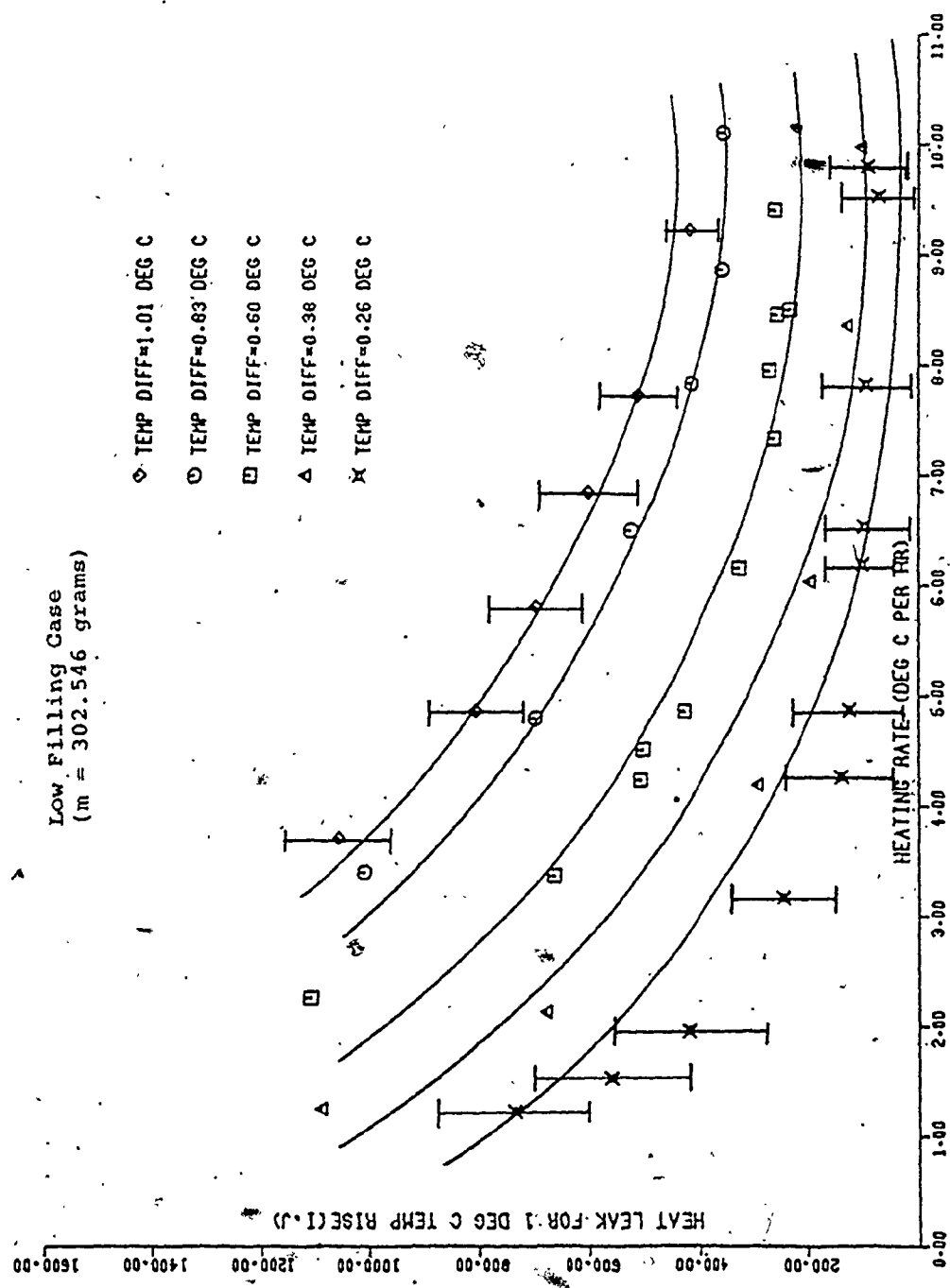
FIGURE 9.1 HEAT LEAK (I-J-) AT 300 DEG C VS HEATING RATE (DEG C PER HR)

leak values for small temperature differences is larger than for large temperature differences. An example of the scatter and error limits is illustrated on both the 0.26°C and 1.01°C temperature difference curves. The error limits for other temperature differences lie between the values on the two curves. The error limits are calculated from the percentage errors in measuring different values. For example, the percentage error in the mass measurements is $\pm$ 0.0001% (7), that of the energy measurements $\pm$ 0.03% (7) and of the $\alpha$ measurements $\pm$ 0.07% (7). Therefore, the percentage error for incremental heat leak is calculated from the above errors as applied to equations 9.1 and 9.2.

Also, the relationship between the heat transfer coefficient (h) and heating rate at a nominal temperature of 300°C and the aforementioned temperature differences for a calorimeter charge of about 302 grams is illustrated by Figure 9-2. This figure indicates that the heat transfer coefficient has a minimum value in the middle region of each curve. The curves were drawn in this manner so as to give a more reliable agreement with the theoretical model explained in Chapter 10. The figure also indicates that the heat transfer coefficient increases with increasing temperature difference at all heating rates.

FIGURE 9.2 HEAT TRANSFER COEFF (WATTS PER DEG C-OVERALL AREA)

VS HEATING RATE (DEG C PER HR)

Figure 9-3 gives the relationship between incremental heat leak and heating rate for nominal temperatures of 100, 200 and 300°C and a temperature difference of 0.6°C between the calorimeter and adiabatic shield when the calorimeter is charged with a fluid sample of about 302 grams.

The following conclusions may be drawn from Figure 9-3:

(i)    the incremental heat leak values increase with increasing absolute temperature.

(ii)   for all absolute temperatures, incremental heat leak decreases with increasing heat rate and has a minimum value at about 8°C per hour.

(iii)  the rate of change of incremental heat leak with absolute temperature is small at high heating rates and increases with a decrease in heating rate.

Table 9.11 gives the results of the incremental heat leak for different temperature differences between the calorimeter and adiabatic shield, different heating rates and a nominal absolute temperature of 300°C. The table is constructed from Figure 9-1 and Tables 9.1 to 9.5. These results are also summarized in Figure 9-4 from which the following conclusions may be drawn:

(i)    as expected, heat leak increases with the temperature difference between the calorimeter and adiabatic shield.

(ii)   for large heating rates and large temperature difference,

Low Filling Case
(m = 302.546 grams)

◇ T=100 DEG C.

⊙ T=200 DEG C

⊡ T=300 DEG C
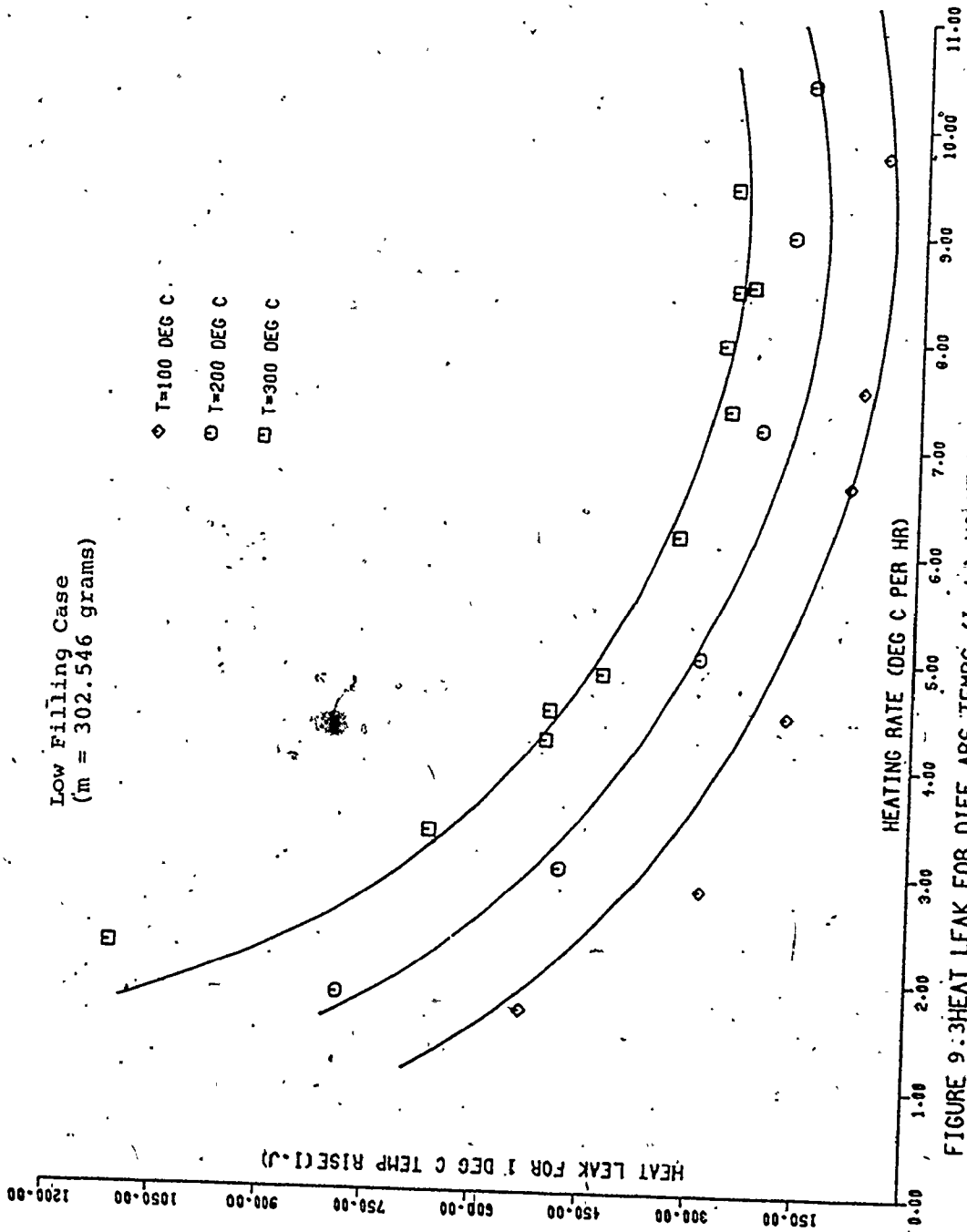
FIGURE 9:3 HEAT LEAK FOR DIFF ABS TEMPS (I.J.) VS HEATING RATE (DEG C PER HR)

HEATING RATE (DEG C PER HR)

HEAT LEAK FOR I DEG C TEMP RISE (I.J.)

## TABLE 9.11

### HEAT LEAK FOR DIFFERENT TEMPERATURE DIFFERENCES, DIFFERENT HEATING RATES AND A CONSTANT TEMPERATURE OF 300°C

(Charge = 302.546 grams)

| Heating Rate °C/hr | Heat Leak (Joules) | | | | |
|---|---|---|---|---|---|
| Temperature Difference Between Calorimeter and Adiabatic Shield(°C) | 0.26 | 0.38 | 0.6 | 0.83 | 1.01 |
| 2 | 438.2 | 673.6 | – | – | – |
| 3 | 275.2 | 451.8 | 762.6 | – | – |
| 4 | 188.6 | 327.8 | 560.2 | 850.6 | 991.3 |
| 5 | 134.7 | 252.5 | 429.3 | 674.1 | 807.8 |
| 6 | 104.8 | 200.2 | 338 | 551.8 | 678.2 |
| 7 | 88.0 | 158 | 282 | 467 | 577.5 |
| 8 | 75.3 | 130.1 | 249.5 | 407.3 | 492.5 |
| 9 | 74.8 | 108.4 | 245.6 | 368.2 | 430 |
| 10 | 75.1 | 95.5 | 273 | 357.5 | 385.3 |

123
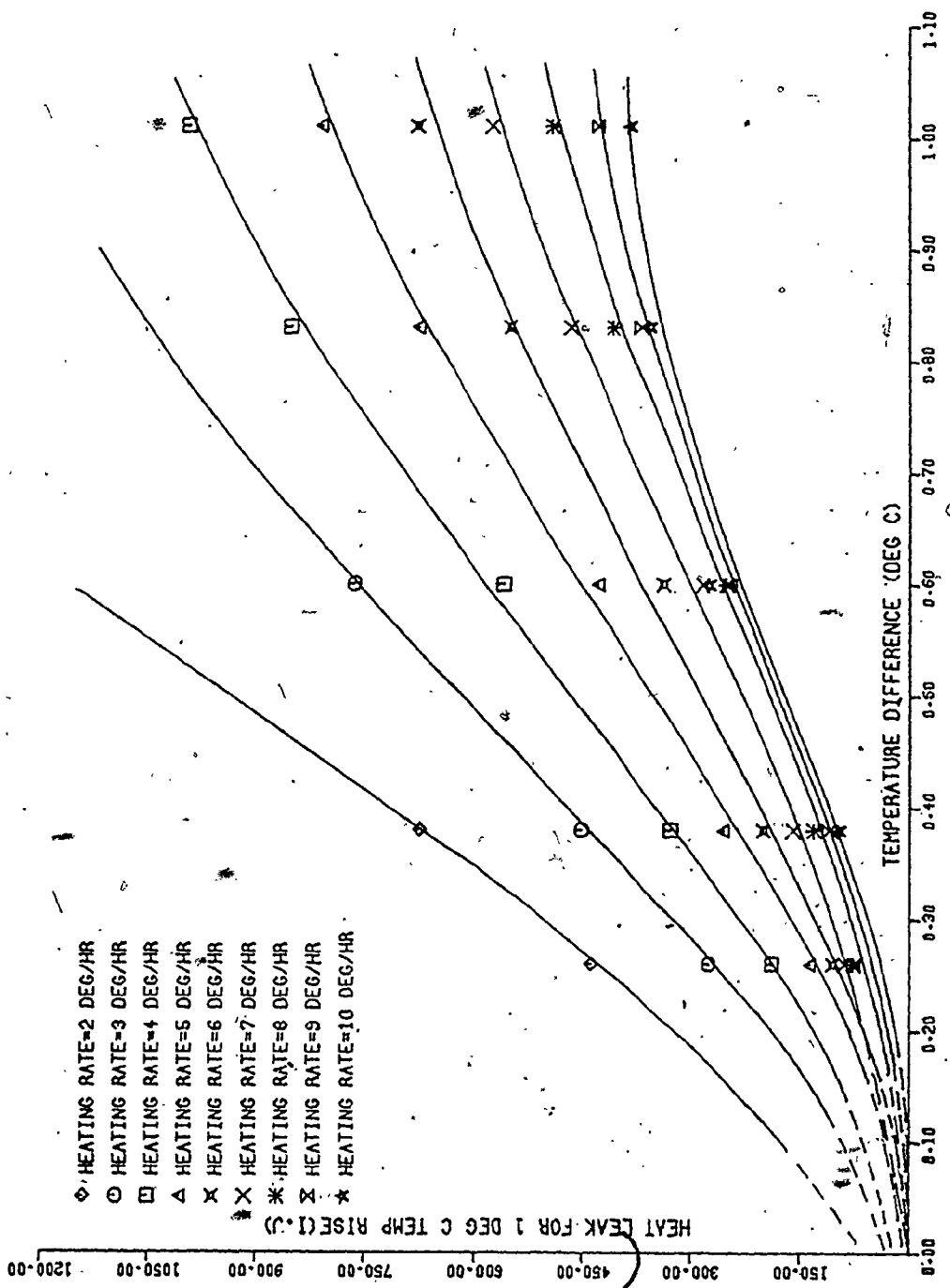


Figure 9.4    HEAT LEAK (JJ.J.) AT 300 DEG C VS TEMPERATURE DIFFERENCE (DEG C)

.the rate of increase of heat leak becomes very small.

(iii) the rate of increase of heat leak is large for small heating rate and decreases with increasing heating rate.

(iv) at small temperature differences, heat leak decreases for small heating rates while it is nearly constant for large heating rates.

(v) the intersection of the curves with the ordinate gives the change in the zero heat leak for a given heating rate when the temperature difference offsets changes from $0^0C$ to approximately $0:5^0C$.

The relationship between incremental heat leak and heating rate for a calorimeter charge of about 678 grams with a temperature difference of $0.6^0C$ and nominal absolute temperatures of 100, 200 and $300^0C$ is given in Figure 9-5. The conclusions drawn before from Figure 9-3 for a charge of 302 grams apply again for this case with a filling of 678 grams.

Tables 9.12, 9.13 and 9.14 summarize the results of incremental heat leak for different heating rates with different calorimeter charges and a temperature difference of $0.6^0C$ between the calorimeter and adiabatic shield. The results of these tables are obtained from previous tables for different fillings at nominal temperatures of 100, 200 and $300^0C$ respectively.

High Filling Case
($\bar{m}$ = 678.5554 grams)

◇ T=100 DEG C

⊖ T=200 DEG C

⊡ T=300 DEG C

HEATING RATE (DEG C PER HR)

HEAT LEAK FOR 1 DEG C TEMP RISE(I.J)
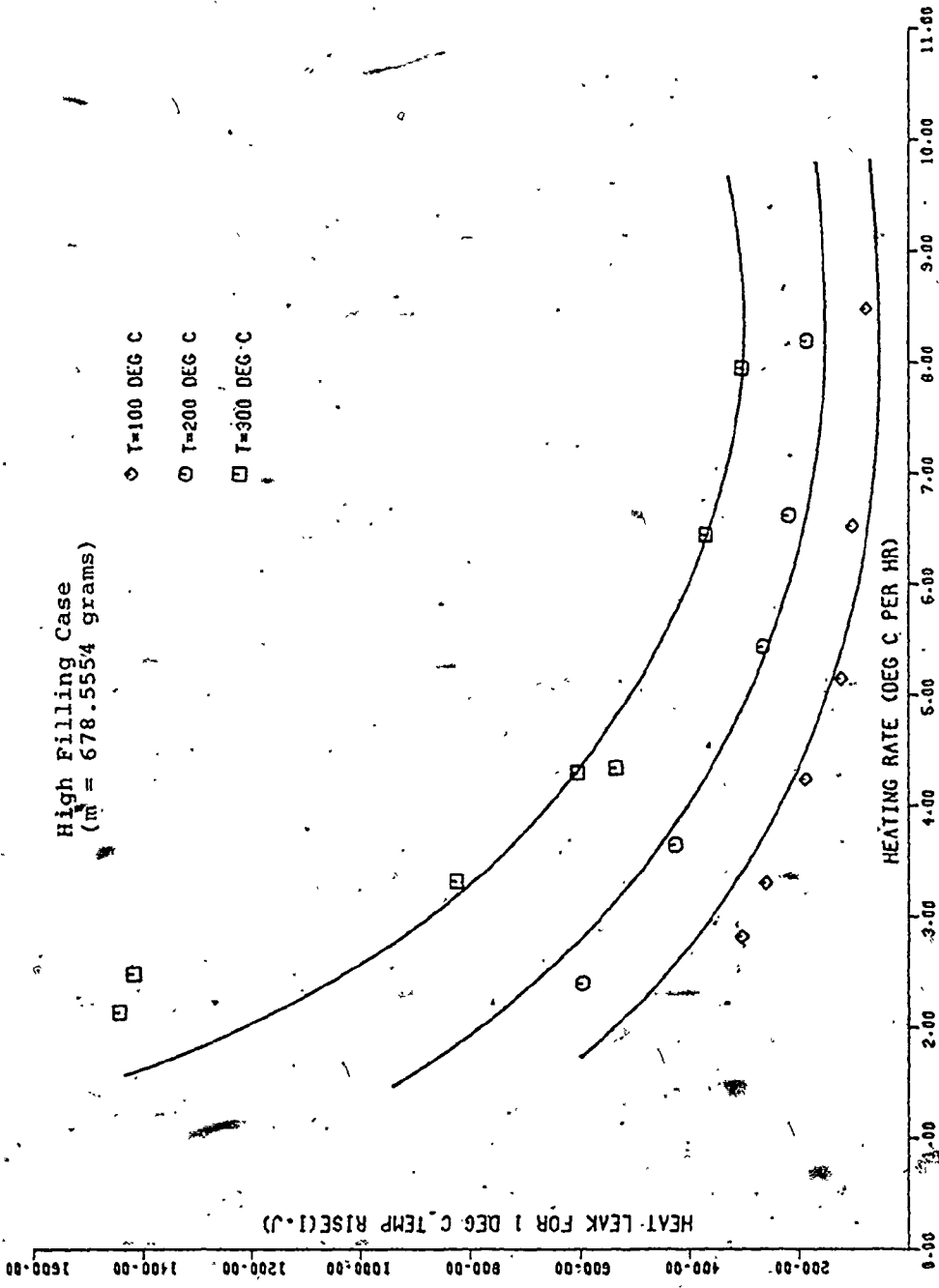
FIGURE 9.5 HEAT LEAK FOR DIFF ABS TEMPS (I.J.) VS HEATING RATE (DEG C PER HR)

## TABLE 9.12

HEAT LEAK FOR A CONSTANT TEMPERATURE DIFFERENCE
OF 0.6°C AND A CONSTANT ABSOLUTE TEMPERATURE OF
100°C WITH DIFFERENT MASSES

| Heating Rate | Heat Leak (Joules) mass (grams) | |
|---|---|---|
| °C/hr | $m_1 = 302.546$ | $m_2 = 678.5554$ |
| 2 | 446.3 | 446.8 |
| 3 | 287.7 | 191.6 |
| 4 | 200.6 | 200.4 |
| 5 | 142.5 | 146.6 |
| 6 | 108 | 104.7 |
| 7 | 81.9 | 77.9 |
| 8 | 67.4 | 68.4 |
| 9 | 58.1 | 76.7 |
| 10 | 55.2 | 110.2 |

## TABLE 9.13

### HEAT LEAK FOR A CONSTANT TEMPERATURE DIFFERENCE OF 0:6°C AND CONSTANT ABSOLUTE TEMPERATURE OF 200°C WITH DIFFERENT MASSES

| Heating Rate | Heat Leak (Joules) | |
| --- | --- | --- |
| | mass (grams) | |
| °C/hr | $m_1 = 302.546$ | $m_2 = 678.5554$ |
| 2 | 726.9 | 688.7 |
| 3 | 506.8 | 507.6 |
| 4 | 381.7 | 380.9 |
| 5 | 303.5 | 291.7 |
| 6 | 249.8 | 233.6 |
| 7 | 217.5 | 198.4 |
| 8 | 194.8 | 178.9 |
| 9 | 175.6 | 189.8 |
| 10 | 163.4 | 239.6 |

## TABLE 9.14

HEAT LEAK FOR A CONSTANT TEMPERATURE DIFFERENCE
OF 0.6°C AND CONSTANT ABSOLUTE TEMPERATURE OF
300°C WITH DIFFERENT MASSES

| Heating Rate °C/hr | Heat Leak (Joules) mass (grams) | |
|---|---|---|
| | $m_1 = 302.546$ | $m_2 = 678.5554$ |
| 2 | — | — |
| 3 | 762.6 | 1023.8 |
| 4 | 560.2 | 652.3 |
| 5 | 429.3 | 476.8 |
| 6 | 338 | 386.4 |
| 7 | 282 | 338.2 |
| 8 | 249.5 | 318.9 |
| 9 | 245.6 | 329.8 |
| 10 | 273 | 385.6 |

From Tables 9.12, 9.13 and 9.14, we notice that the difference between incremental heat leak values for the two different calorimeter charges increases with temperature for all heating rates. From this, we may conclude that considering the heat leak to be the same for both high and low fillings could cause serious errors in the final results of the calorimetric measurements on the thermodynamic properties of fluids.

From the previous analysis, we may conclude that heat leak is a function of absolute temperature, temperature variations on the calorimeter and adiabatic shield surfaces, temperature difference between the calorimeter and adiabatic shield, the amount of liquid contained in the calorimeter and the heating rate.

# CHAPTER 10

## MATHEMATICAL MODEL FOR THE CALORIMETER PERFORMANCE

### 10.1 GENERAL

The heat leak experiments performed on a calorimeter charged with water under conditions of coexisting liquid and vapour phases indicate that the relationship between the heat transfer coefficient (h) and the heating rate ($dT/d\tau$) takes the general form shown in Figure 10-1. The heat transfer coefficient was shown to have a minimum value at some intermediate value of heating rate. It is postulated here that this relationship applies for any system under conditions of coexisting liquid and vapour phases.

Applying the First Law of Thermodynamics,

$$\delta Q = \delta U + \delta W \tag{10.1}$$

the general equation for the different energy transfers to and from the "charged calorimeter" may be written as

$$(q_{\delta T})_M + (q_{\delta T=0})_M - (W_e)_M = (\Delta U_S)_M \tag{10.2}$$

where

$(W_e)_M$ is the electrical energy added to the system*

---

*If work energy is added to a system then it is designated as a negative energy addition process.
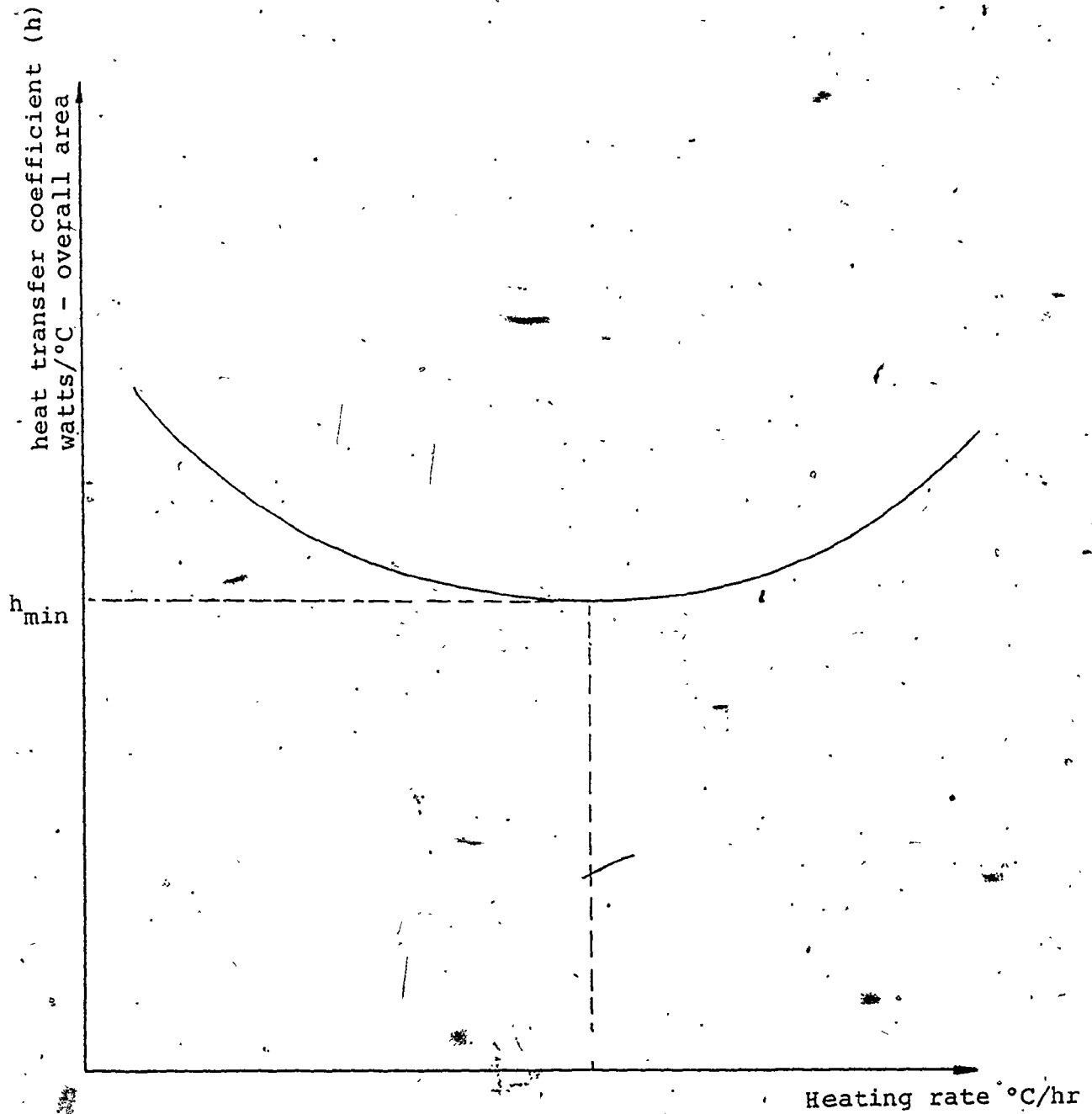
FIGURE 10.1   General form for heat transfer coefficient
(watts/°C-overall area) vs heating rate (°C/hr)

$$(W_e)_M = -I^2 R_e d\tau \tag{10.3}$$

$(q_{\delta T})_M$ is the incremental heat leak,

$$(q_{\delta T})_M = hA(\Delta T')d\tau \tag{10.4}$$

$\Delta T'$ is the integrated temperature difference between the calorimeter and adiabatic shield

$d\tau$ is the experimental time for temperature rise of $(T_f - T_i)$

$T_f$ is the final saturation temperature

$T_i$ is the initial saturation temperature

$\Delta U_S$ is the change in internal energy of the calorimeter system

$$(\Delta U_S)_M = m_f c_{s_f} dT + m_g c_{s_g} dT + m_{fg} h_{fg} + M_c c_{p_c} dT \tag{10.5}$$

$dT$ is the temperature rise

$c_{s_f}$ and $c_{s_g}$ are the specific heats of saturated liquid and vapour respectively.

Also, the first two terms in the Right Hand Side of equation 10.5 represent the sensible heating of the liquid and vapour phases respectively while the third term represents the energy needed to bring the two phases back into equilibrium.

Upon substitution of $W_e$ and $(q_{\delta T})_M$ into equation 10.2, and rearranging, the following equation results:

$$(I^2 R_e + hA\Delta T')d\tau + (q_{\delta T=0})_M = (m_f c_{s_f} + m_g c_{s_g} + M_c c_{p_c})dT$$

$$+ m_{fg} h_{fg} \tag{10.6}$$

It can be shown that the R.H.S. of equation 10.6 is given by

$$R.H.S. = M \, c_{s_f} dT + M_c c_{p_c} dT + m_g (c_{s_g} - c_{s_f}) dT$$

$$+ m_{fg} h_{fg} \qquad\qquad (10.7)$$

Even for the worst case of low filling and at extreme temperatures between 250 and 300°C, $m_g$ was less than 10% of the total mass loading, i.e. about an order of magnitude less. An examination of the magnitude of the term $m_g(c_{s_g} - c_{s_f}) dT$ indicates that its effect is only five percent of the dominant fluid term $M \, c_{s_f} dT$. Therefore, the R.H.S. of equation 10.6 may be written in the following form

$$R.H.S. \cong (M_c c_{p_c} + M \, c_{s_f}) dT + m_{fg} h_{fg}$$

The above approximation becomes even better for high filling and for both high and low fillings at more moderate levels of temperatures. Equation 10.6 now reads

$$(I^2 R_e + hA\Delta T') d\tau \cong (M_c c_{p_c} + M \, c_{s_f}) dT + m_{fg} h_{fg} - (q_{\delta T=0})_M \qquad (10.8)$$

Dividing by $d\tau$ and denoting $\frac{dT}{d\tau} \equiv \dot{T}$, we obtain

$$I^2 R_e + hA\Delta T' = M_c c_{p_c} \dot{T} + M \, c_{s_f} \dot{T} + \frac{m_{fg} h_{fg}}{d\tau} - \frac{1}{d\tau} (q_{\delta T=0})_M \qquad (10.9)$$

In order to find the heating rate for a minimum h value, equation 10.9 is differentiated with respect to the heating

rate $(dT/d\tau)$. The following condition exists for a minimum heat transfer coefficient:

$$\frac{dh}{d(\frac{dT}{d\tau})} = 0 \tag{10.10}$$

since $M_c c_{p_c}$, $M c_{s_f}$ and $m_{fg} h_{fg}$ are properties independent of the external heating rate. Therefore, the following equation is obtained:

$$\frac{dI}{d\dot{T}} = \frac{M_c c_{p_c} + M c_{s_f}}{2IR_e} - \frac{m_{fg} h_{fg}}{2IR_e (d\tau)^2} \frac{d\tau}{d\dot{T}} \tag{10.11}$$

where $M_c c_{p_c}$ is a parameter associated with the empty calorimeter system

$M c_{s_f}$ is a parameter associated with the fluid contents inside of the calorimeter.

The value of I and the corresponding value of the heating rate $\dot{T}$ which satisfy equation 10.11 may then be found. This value of the heating rate is the value at which the heat transfer coefficient (h) is a minimum.

## 10.2. APPLICATION OF THE MATHEMATICAL MODEL TO THE U.W.O. CALORIMETER

A specific case is considered in this calculation in which the temperature difference between the calorimeter and adiabatic shield is 0.83°C. (The temperature difference in the constant mass experiments is much smaller, but this value

is used since it is one of the five temperature differences which were used in the experiments.) Also, the relationship between heat leak and heating rate was the same for all temperature differences and only one of them is to be used in the calculations. Substituting numerical values for all the constants in equation 10.11 at 300°C and for a temperature rise of 25°C, the following general equation for the current change with the heating rate for a calorimeter charge of 281.2213 grams results in,

$$\frac{dI}{dT} = \frac{1}{I}[12.607 - \frac{75.857}{(d\tau)^2} \frac{d\tau}{dT}] \qquad (10.12)$$

From the results given in Table 10.1 and the graph in Figure 10.2 relating average current and heating rate, as well as the relation in Figure 10.3 between time for a 25°C temperature rise and heating rate, the value of I which satisfies equation 10.12 may be obtained. In this specific case, the value of I is found to be 0.2639 amperes. The corresponding heating rate is thus 7.5°C/hr approximately. For this specific case also, the experimental curve for the heat transfer coefficient against the heating rate is shown in Figure 10.4. From the curve, it may be seen that the heat transfer coefficient is minimum at a heating rate of 7.9°C/hr approximately, which indicates a good agreement between analytical and experimental results.

In analyzing the reasons behind having this form for the relationship between the heat transfer coefficient and the heating rate instead of the expected curve which is

## TABLE 10.1

AVERAGE CURRENT WITH HEATING RATE FOR A TEMPERATURE DIFFERENCE
OF 0.83°C BETWEEN CALORIMETER AND ADIABATIC SHIELD

| Heating Rate °C/hr | 3.394 | 4.802 | 6.505 | 7.836 | 8.869 | 10.112 |
|---|---|---|---|---|---|---|
| Average Current Amp. | 0.189287 | 0.217515 | 0.247925 | 0.268447 | 0.28367 | 0.3027 |
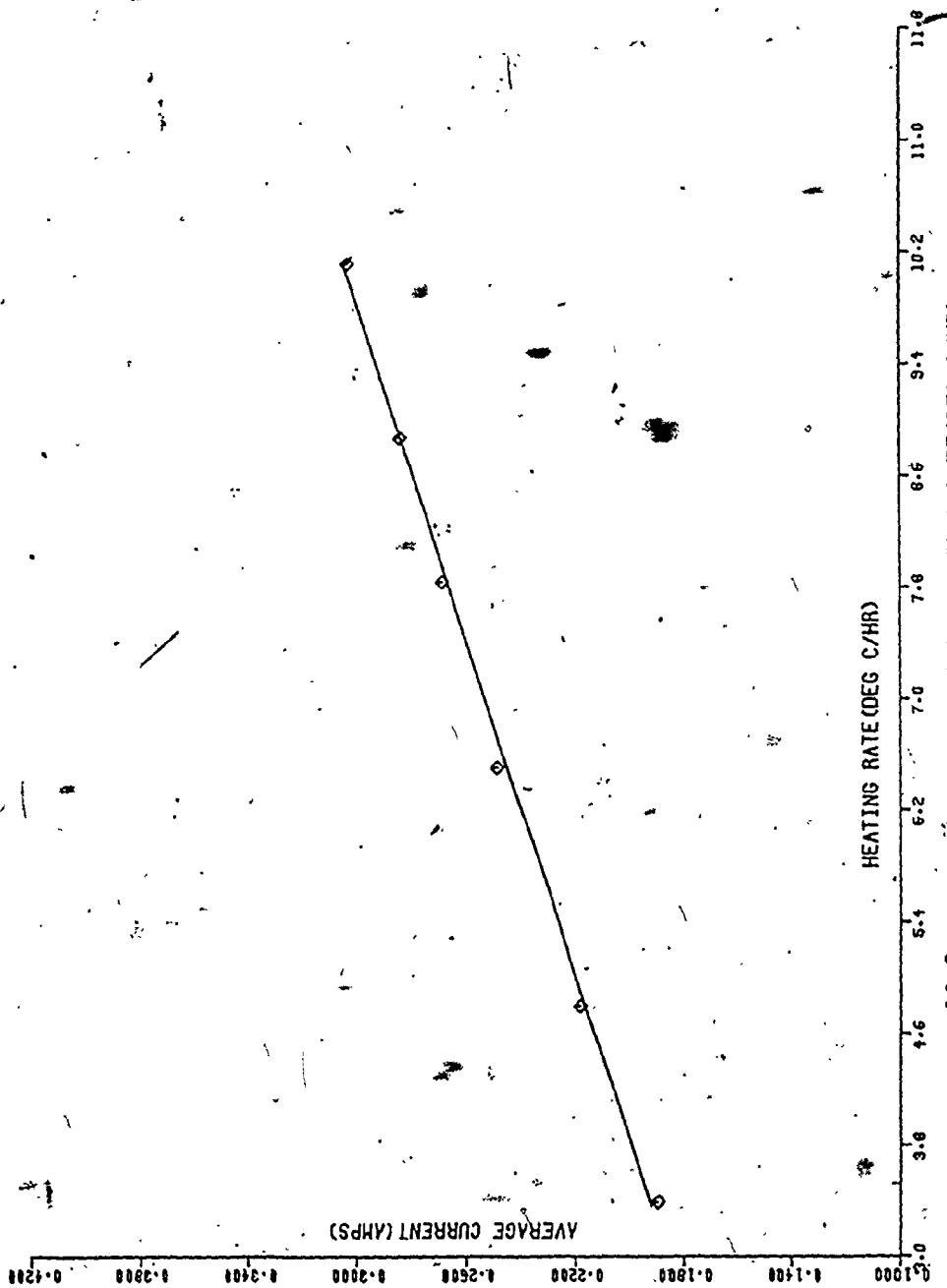
FIGURE10.2AVERAGE CURRENT(AMPS) VS HEATING RATE(DEG C/HR)

HEATING RATE(DEG C/HR)
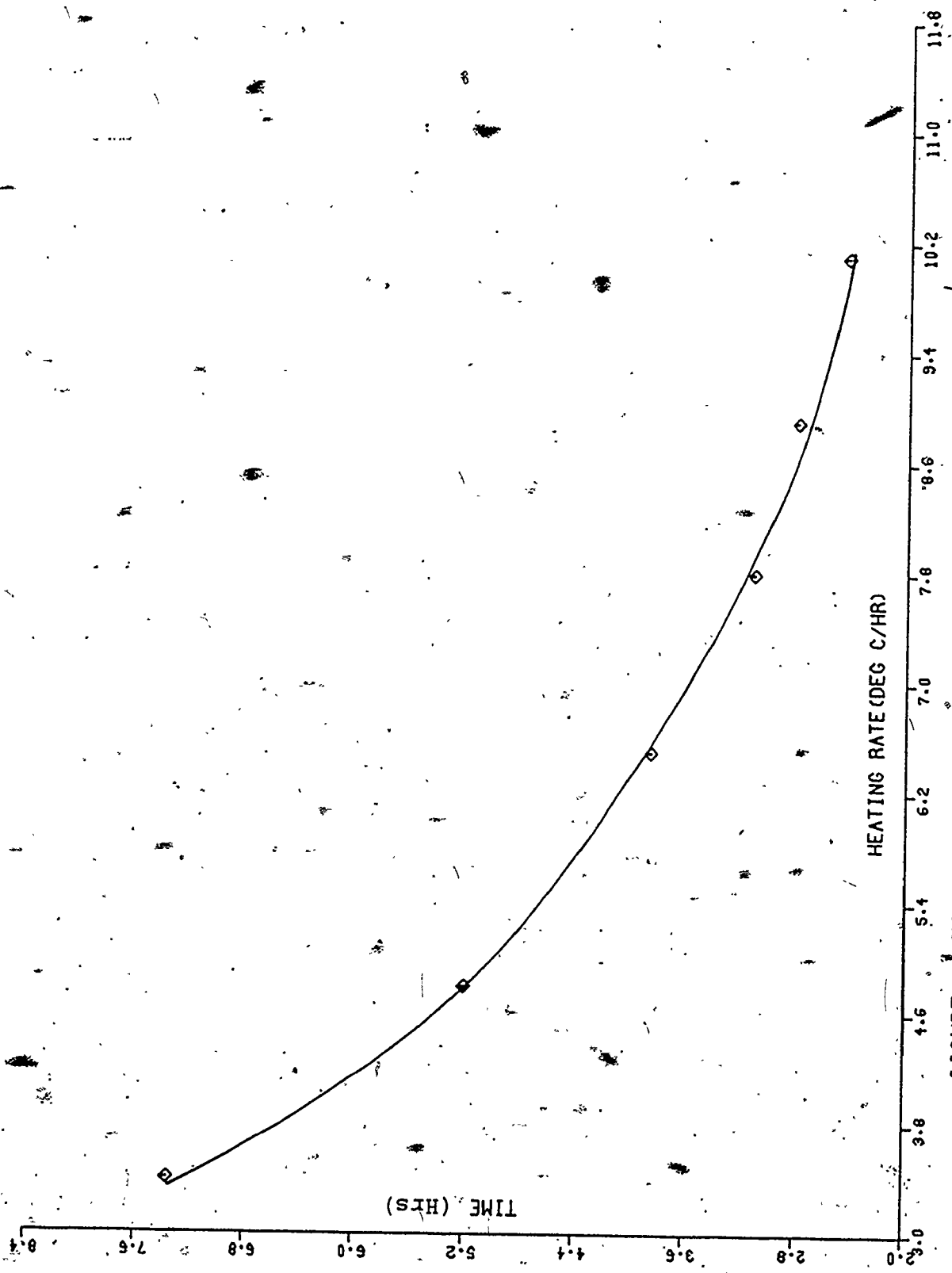
FIGURE 10.3 TIME (HRS) VS HEATING RATE (DEG. C/HR)
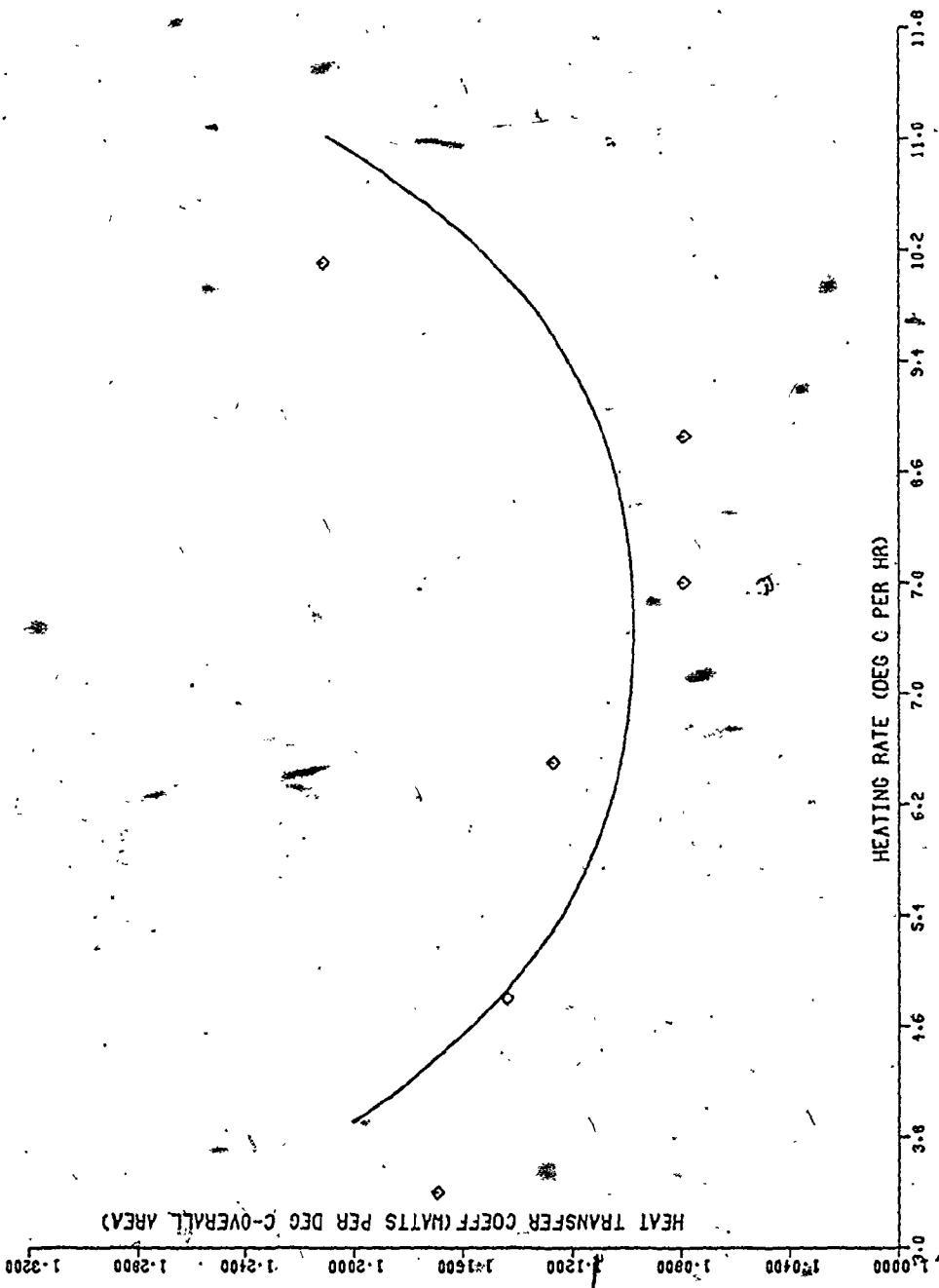
FIGURE10.4 HEAT TRANSFER COEFF (WATTS PER DEG C-OVERALL AREA)
VS HEATING RATE (DEG C PER HR)

similar to the heat leak curve, it was thought that tempera-
ture variation over the calorimeter and adiabatic shield
surfaces was the reason.  However, from Table 10.2 and Figure
10-5, it may be noticed that the temperature variation on the
calorimeter surface is linearly changing with the heating
rate.  Therefore, the temperature variation is excluded as
being the reason behind such a relation.  A suitable explana-
tion is perhaps that while the heat leak is a point function,
thus the heat leak is calculated for certain temperature
rise, the heat transfer coefficient is an integrated value.
Therefore, the heat transfer coefficient has different values
at different heating rates and different temperatures, while
the values shown in the curves are the average values of h,
over the whole temperature range of each experiment.

From the foregoing discussion, we may thus conclude
that the heat transfer coefficient has its minimum value at
a heating rate of approximately 8°C/hr in all cases.

## TABLE 10.2

TEMPERATURE VARIATION ON THE CALORIMETER SURFACE WITH HEATING
RATE FOR A TEMPERATURE DIFFERENCE OF 0.83°C BETWEEN CALORIMETER
AND ADIABATIC SHIELD

| Heating Rate °C/hr | 3.394 | 4.802 | 6.505 | 7.836 | 8.869 | 10.112 |
|---|---|---|---|---|---|---|
| Temp. Variation °C | 0.085 | 0.142 | 0.189 | 0.236 | 0.274 | 0.321 |
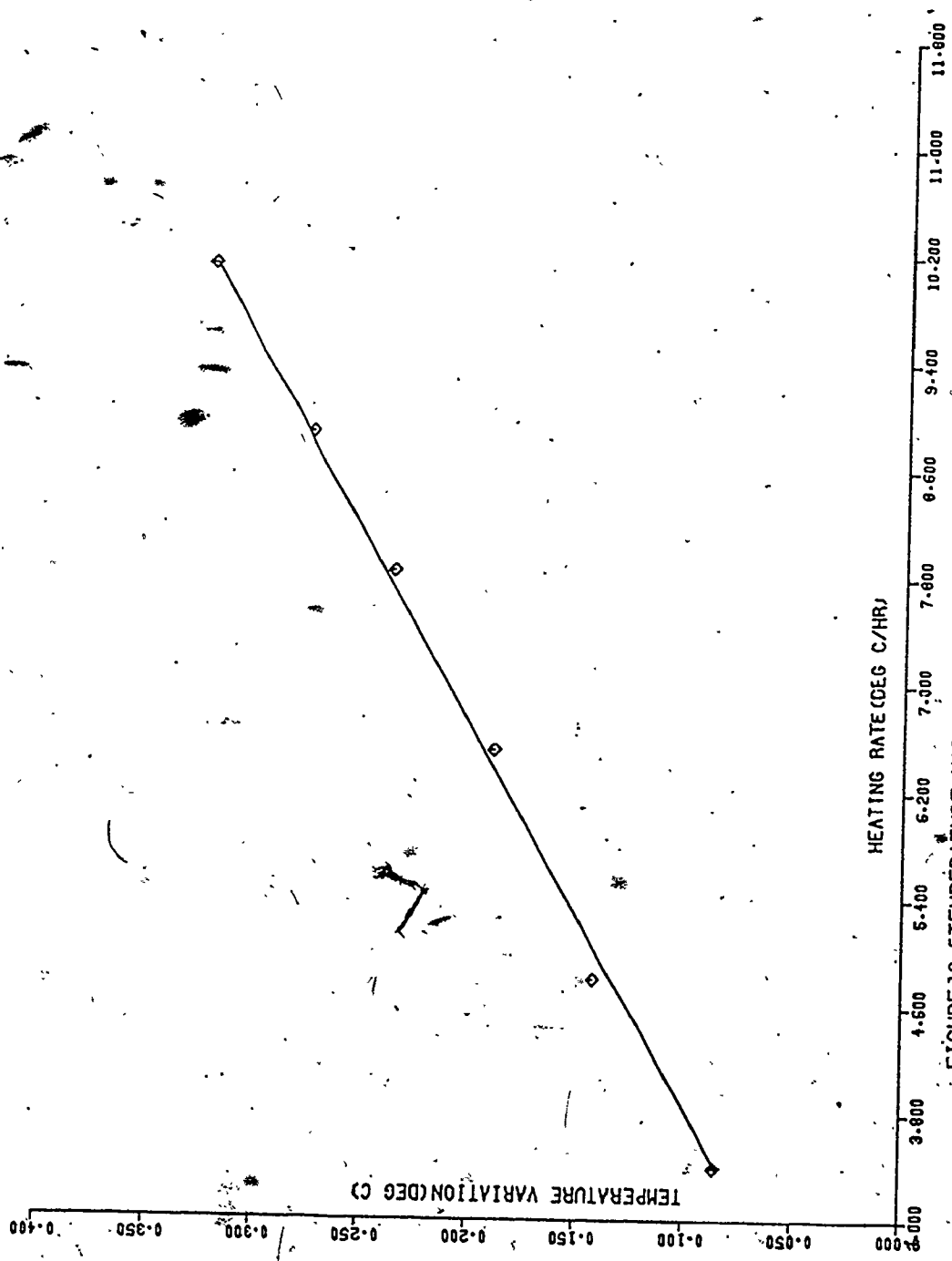
FIGURE 10.5 TEMPERATURE VARIATION ON CALORIMETER SURFACE (DEG C)
VS HEATING RATE (DEG C/HR)

# CHAPTER 11

## EXPERIMENTAL RESULTS ON LIGHT WATER

### 11.1 GENERAL

Subsequent to the above-mentioned heat leak experiments on light water, from which it was seen that the heat leak has large values in comparison to the total energy added, it was necessary to conduct some experiments for enthalpy determination. The large values of heat leak were concluded to result since the calorimeter was badly oxidized and totally deteriorated, as mentioned in Chapter 10. The enthalpy determination measurements were necessary in order to find the exact effect of heat leak on the results. Details of the constant mass experiments and their corresponding heat leak experiments are described separately below.

### 11.2 CONSTANT MASS EXPERIMENTS

Three sets of constant mass experiments were performed on light water from 100 to 300°C. The first two sets of constant mass experiments were conducted on the calorimeter when it was filled with 281.2213 grams of light water, whereas the third set of experiments was conducted on the calorimeter when it was filled with 678.554 grams. Upon

successive completion of measurements, the samples were collected and weighed a second time. The final mass values in those two types of experiments were found to be 281.1792 and 678.5031 grams. The uncertainty in the difference between the filling is evidently less than 0.1 grams. The initial mass values were therefore used to evaluate the $\alpha$ quantities.

As described previously in Chapter 2, the general equation for a constant mass experiment might be derived as follows:

$$(-W_e)_M = M(h_f - Tv_f \frac{dP}{dT})_1^2 + (V \ T \ \frac{dP}{dT} - PV)_1^2$$

$$+ M_c c_{p_c} \Delta T - (q_{\delta T})_M - (q_{\delta T=0})_M + W_S + W_{S.E.} \tag{11.1}$$

where $M_c$ is the mass of the calorimeter shell

$c_{p_c}$ is the heat capacity per unit mass of the calorimeter.

## 11.3 HEAT LEAK EXPERIMENTS

Three sets of heat leak experiments were conducted, and their results were used for the computation of the corrected $\alpha$ values. Two sets of these experiments were conducted on the calorimeter when it was filled with 281.2213 grams of light water whereas the third set was conducted on the calorimeter when it was filled with 678.5554 grams. In these heat leak experiments, the temperature difference between

the calorimeter and adiabatic shield was maintained at a constant value of $0.1°C$ during the experiment.

In order to show the effect of the incremental heat leak on the calorimetric measurements, two tables were constructed. In the first table, heat leak was not taken into consideration. In the second, incremental heat leak corrections were applied.

Firstly, neglecting the effect of heat leak on the results, the last six terms in the Right Hand Side of equation 11.1 are then independent of the mass of the fluid sample contained in the calorimeter. Therefore, equation 11.1 can be written in the following form:

$$(-W_e)_M = M\Delta\alpha + z \qquad (11.2)$$

where

$$\Delta\alpha = (h_f - Tv_f \frac{dP}{dT})_1^2$$

$$z = (T V \frac{dP}{dT} - PV)_1^2 + M_c c_{p_c} \Delta T - (q_{\delta T})_M - (q_{\delta T=0})_M + W_S + W_{S.E.}$$

The values of $W_e$ and M of each group of experiments for a single temperature interval were fitted to equation 11.2 by means of a least squares technique. The reduction yielded mean values for $\alpha$ and z. Using the mean value of z, the individual values of $\alpha$ for each experiment were computed and compared with the mean value of $\alpha$ for each group. The results are given in Table 11.1.

## TABLE 11.1

### UNCORRECTED CONSTANT MASS EXPERIMENTS ON LIGHT WATER

| Test No. | Mass (gram) | Initial Temp. (°C) | Final Temp. (°C) | Total Energy Added (Joules) | Energy Added for 50°C Interval | $\Delta\alpha$ (Joules/gram) | Deviation From Mean Value (%) |
|---|---|---|---|---|---|---|---|
| 1 | 678.5554 | 101.403 | 149.69 | 209159.0 | 216579.0 | 214.25 | +0.26 |
| 9 | 281.2213 | 99.9295 | 150.024 | 131697.8 | 131449.4 | 213.70 | 0.00 |
| 17 | 281.2213 | 100.960 | 151.148 | 132382.2 | 131886.3 | 213.15 | -0.26 |
| For temperature interval from 100 to 150°C | | | | | $z_m$=71570.3 Joules | $\alpha_m$=213.70 Joules/gram | |
| 2 | 678.5554 | 149.4545 | 200.395 | 228032.7 | 223822.5 | 215.25 | +0.39 |
| 10 | 281.2213 | 149.556 | 199.749 | 138828.2 | 138294.4 | 214.41 | 0.0 |
| 18 | 281.2213 | 151.0365 | 200.918 | 138633.1 | 138962.4 | 213.57 | -0.39 |
| For temperature interval from 150 to 200°C | | | | | $z_m$=78330.6 Joules | $\alpha_m$=214.41 Joules/gram | |
| 3 | 678.5554 | 200.579 | 249.849 | 231206.2 | 234631.8 | 213.61 | +0.12 |
| 11 | 281.2213 | 200.8865 | 249.767 | 145425.1 | 148755.7 | 213.36 | 0.00 |
| 19 | 281.2213 | 199.221 | 250.616 | 153109.8 | 148954.0 | 213.11 | -0.12 |
| For temperature interval from 200 to 250°C | | | | | $z_m$=88852.2 Joules | $\alpha_m$=213.36 Joules/gram | |
| 4 | 678.5554 | 250.713 | 300.177 | 245523.5 | 248184.0 | 214.41 | +0.25 |
| 12 | 281.2213 | 250.363 | 299.941 | 162044.2 | 163423.4 | 213.87 | 0.00 |
| 20 | 281.2213 | 249.319 | 299.898 | 164880.4 | 162992.9 | 213.32 | -0.26 |
| For temperature interval from 250 to 300°C | | | | | $z_m$=103064.8 Joules | $\alpha_m$=213.87 Joules/gram | |

Secondly, by taking incremental heat leak into consideration, equation 11.1 may be written as

$$-W_{e_{corrected}} = M\Delta\alpha + Z' \qquad\qquad (11.3)$$

where $W_{e_{corrected}} = W_e - (q_{\delta T})_M$

$$Z' = (T \cdot V \frac{dP}{dT} - PV)_1^2 + M_c c_{p_c} \Delta T + W_S + W_{S.E.} - (q_{\delta T=0})_M$$

The values of $W_{e_{corrected}}$ and M of each group of experiments for a single temperature interval were also fitted to equation 11.3 by means of the least squares technique. Again, this reduction yielded mean values for the corrected $\alpha$ and $Z'$. The individual values of $\alpha$ for each experiment were then computed using the mean value of $Z'$. The results are summarized in Table 11.2. Comparison between the mean value and the individual values of $\alpha$ is shown in the last column of the table.

## TABLE 11.2

### CONSTANT MASS EXPERIMENTS ON LIGHT WATER WITH HEAT LEAK CORRECTIONS APPLIED*

| Test No. | Mass (gram) | Initial Temp. (°C) | Final Temp. (°C) | Energy Added for 50°C Interval (Joules) | Heat Leak (Joules) | Corrected Values of Energy Added (Joules) | $\Delta\alpha$ (Joules/gram) | Deviation From Mean Value % |
|---|---|---|---|---|---|---|---|---|
| 5 | 678.5554 | 101.403 | 149.69 | 216579.0 | -877.7 | 215701.3 | 207.94 | 0.00 |
| 13 | 281.2213 | 99.9295 | 150.024 | 131449.4 | -1632.2 | 133081.6 | 207.94 | 0.00 |
| 21 | 281.2213 | 100.960 | 151.148 | 131886.3 | -1195.3 | 133081.6 | 207.94 | 0.00 |
| For temperature interval from 100 to 150°C. $Z_m$=74606.1 Joules $\alpha_m$=207.94 Joules/gram | | | | | | | | |
| 6 | 678.5554 | 149.4545 | 200.395 | 223822.5 | -1037.0 | 222785.5 | 207.68 | 0.00 |
| 14 | 281.2213 | 149.556 | 199.749 | 138294.4 | -1973.3 | 140267.7 | 207.68 | 0.00 |
| 22 | 281.2213 | 151.0365 | 200.918 | 138962.4 | -1305.2 | 140267.6 | 207.68 | 0.00 |
| For temperature interval from 150 to 200°C $Z_m$=81864.1 Joules $\alpha_m$=207.68 Joules/gram | | | | | | | | |
| 7 | 678.5554 | 200.579 | 249.849 | 234631.8 | -1507.7 | 233124.1 | 207.34 | 0.00 |
| 15 | 281.2213 | 200.8865 | 249.767 | 148755.7 | -1985.0 | 150740.7 | 207.34 | 0.00 |
| 23 | 281.2213 | 199.221 | 250.616 | 148954.0 | -1786.8 | 150740.8 | 207.34 | 0.00 |
| For temperature interval from 200 to 250°C $Z_m$=92432.3 Joules $\alpha_m$=207.34 Joules/gram | | | | | | | | |
| 8 | 678.5554 | 250.713 | 300.177 | 248184.0 | -1998.7 | 246185.3 | 206.99 | 0.00 |
| 16 | 281.2213 | 250.363 | 299.941 | 163423.4 | -6513.4 | 169936.8 | 206.99 | 0.00 |
| 24 | 281.2213 | 249.319 | 299.898 | 162992.9 | -6943.9 | 169936.8 | 206.99 | 0.00 |
| For temperature interval from 250 to 300°C $\alpha_m$=206.99 Joules/gram; $Z_m$=111725.5 Joules | | | | | | | | |

*The calorimeter was maintained at temperatures where levels were always 0.1°C above the adiabatic shield.

The effect of incremental heat leak on the final results of α is given in Table 11.3. From the table, it may be concluded that the heat leak effect on the α results is as large as 3.3% which indicates that heat leak is very large in the apparatus. This might be expected since the apparatus has deteriorated because of the oxidation effects.

It is interesting to note that when incremental heat leak corrections were applied, values of the total energy added for 50°C in the two low filling series were exactly the same. Therefore, the individual values of α were equal and were exactly the same as the mean value of α. Thus, the deviations between the individual and the mean values of α were zero in all cases as may be seen in Table 11.2.

## 11.4  COMPARISONS AND DISCUSSION

.Comparison of the α quantities for saturated light water among Osborne et al., Chan and this work is given in Table 11.4. The results are also illustrated by Figure 11.1. From the table, it may be seen that there is a deviation between the results obtained in this research and those obtained by Osborne and also by Chan. Also, we may notice that the difference is in the negative side for low temperatures, then changes to the positive side and increases for high temperatures. The maximum deviation between this work and Osborne's

## TABLE 11.3

### EFFECT OF INCREMENTAL HEAT LEAK ON THE $\alpha$ RESULTS

| Temperature Interval °C | | $\Delta\alpha$ (Joules/gram) | $\Delta'\alpha_h$ With Heat Leak Corrections (Joules/gram) | $\dfrac{\Delta\alpha - \Delta\alpha_h}{\Delta\alpha}$ % |
|------|------|--------|--------|------|
| From | To | | | |
| 100 | 150 | 213.70 | 207.94 | 2.77 |
| 150 | 200 | 214.41 | 207.68 | 3.24 |
| 200 | 250 | 213.36 | 207.34 | 2.82 |
| 250 | 300 | 213.87 | 206.99 | 3.32 |

## TABLE 11.4

### COMPARISON OF α VALUES OF LIGHT WATER
### BETWEEN OBSERVATIONS OF THIS WORK AND OTHERS

| Temperature Interval °C | | This Work | Osborne | Chan | α difference (Joules/gram) $\frac{\text{This Work} - \text{Osborne}}{\text{This Work}}$ % | $\frac{\text{This Work} - \text{Chan}}{\text{This Work}}$ % |
|---|---|---|---|---|---|---|
| From | To | | | | | |
| 100 | 150 | 207.94 | 208.45 | 208.39 | -0.25 | -0.22 |
| 150 | 200 | 207.68 | 208.42 | 208.11 | -0.36 | -0.21 |
| 200 | 250 | 207.34 | 206.78 | 207.38 | +0.27 | -0.02 |
| 250 | 300 | 206.99 | 205.61 | 206.14 | +0.67 | +0.41 |
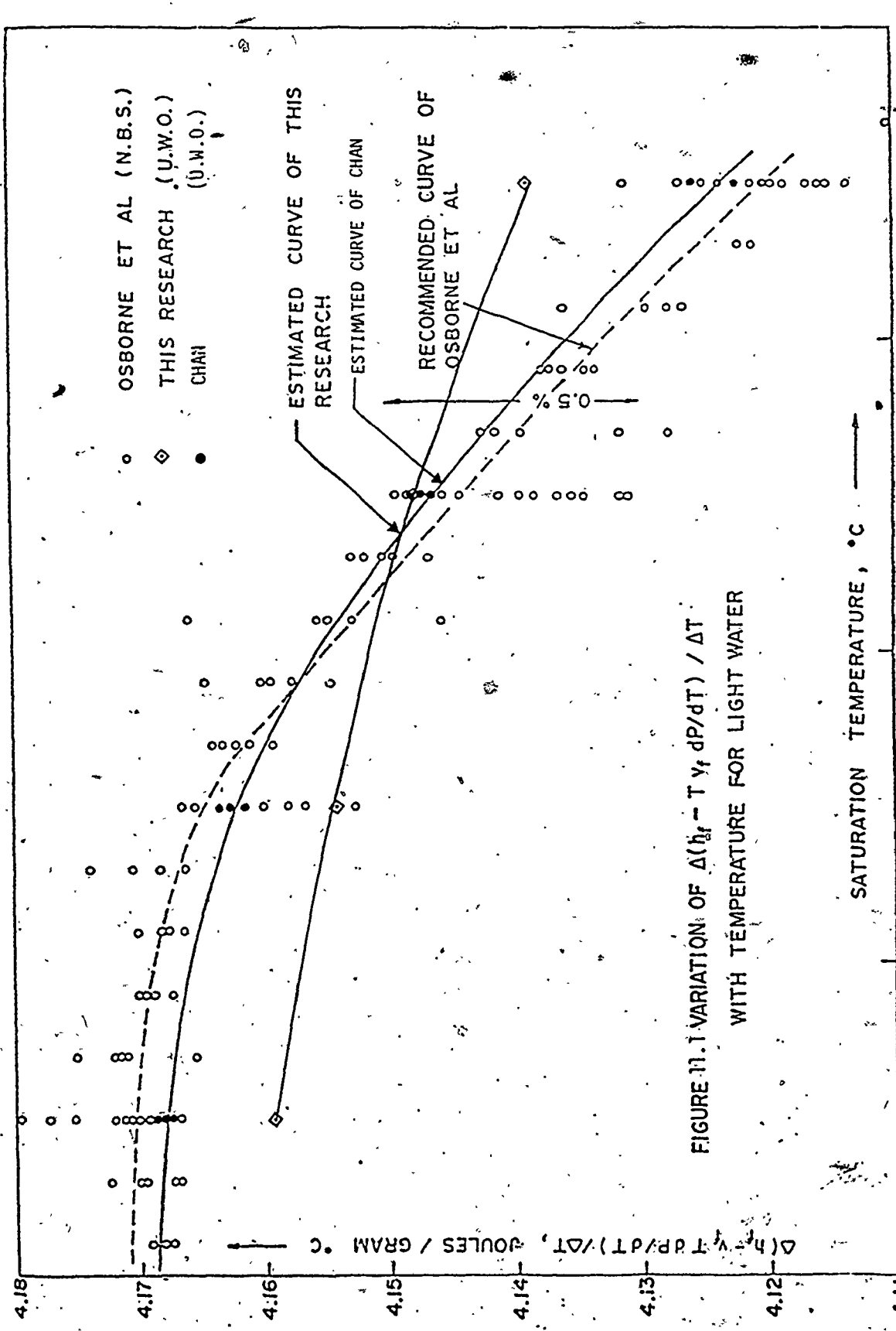
FIGURE 11.1 VARIATION OF $\Delta(h_{af} - T v_f dP/dT)/\Delta T$
WITH TEMPERATURE FOR LIGHT WATER

is 0.67% on the high side, while the difference between this work and Chan's is reduced to 0.41% on the high side. We may also notice that the difference increases suddenly for temperatures in the range from 250 to 300°C.

The reason for these deviations may be due to the fact that the present calorimeter is not perfect but rather deteriorated and therefore has large values for heat leak as compared to that of Osborne and also of Chan's apparatus.

The condition of the calorimeter used in this research no doubt adversely affected its thermal performance. Its badly oxidized surfaces in all likelihood increased the zero heat leak beyond the one per cent level that existed in Chan's investigation. Therefore, the lack of agreement between the data of this thesis and the Osborne and Chan experimental data is considered to be entirely due to the impact of the much larger zero heat leak values of this thesis research.

# CHAPTER 12

## THE HEAT CAPACITY OF THE EMPTY CALORIMETER

The heat capacity of the empty calorimeter may be derived from the results of the constant mass experiments. It is described in Chapter 11 how values for the constants $Z_{uncorrected}$ and $Z_{corrected}$ for a single temperature interval are obtained and then utilized in computing uncorrected and corrected mean values respectively for the term $\alpha$, i.e. $\Delta\alpha_{mean_{uncorrected}}$ and $\Delta\alpha_{mean_{corrected}}$.

From the constant mass experiments, applying the First Law of Thermodynamics, we have

$$(-W_e)_M = M(h_f - Tv_f \frac{dP}{dT})^2_1 + (T V \frac{dP}{dT} - PV)^2_1$$

$$+ M_c c_{p_c} \Delta T - (q_{\delta T})_M - (q_{\delta T=0})_M + W_S + W_{S.E.} \qquad (12.1)$$

The above equation may be written in the following form:

$$(-W_e)_M = M\Delta\alpha_{uncorrected} + Z_{uncorrected} \qquad (12.2)$$

where

$$Z_{uncorrected} = (T V \frac{dP}{dT} - PV)^2_1$$

$$+ M_c c_{p_c} \Delta T - (q_{\delta T})_M - (q_{\delta T=0})_M + W_S + W_{S.E.} \qquad (12.3)$$

As mentioned before, the values of $W_S$ and $W_{S.E.}$ were found to be negligible. Therefore, neglecting $W_S$ and $W_{S.E.}$,

equation 12.3 may be rewritten in the following form:

$$Z = (T \ V \ \frac{dP}{dT} - PV)_1^2 + M_c c_{p_c} \Delta T - (q_{\delta T})_M - (q_{\delta T=0})_M \quad (12.4)$$

In the heat capacity determinations of this thesis, values for the term $(T \ V \ \frac{dP}{dT} - PV)_1^2$ were obtained from the steam tables. Furthermore, the heat leak values obtained from special heat leak experiments for a temperature difference offset of 0.1°C between the calorimeter and adiabatic shield (as described in Chapter 11) were used to evaluate the heat leak term $(q_{\delta T})_M$. Upon utilizing the numerical values for the above-mentioned terms and also utilizing the uncorrected values for $Z_{uncorrected}$, heat capacity values for the empty calorimeter were obtained. The results are summarized in Table 12.1. It should be mentioned that there is an uncertainty in the values of the last column of Table 12.1 due to the zero heat leak which occurs when the observed temperature difference between the calorimeter and adiabatic shield is zero.

In order to compare the measured heat capacity of the empty calorimeter and the value inferred from the constant mass experiments, two sets of tare energy measurements were conducted under vacuum conditions from 100 to 300°C. The first set was conducted with no observed temperature difference between the calorimeter and the adiabatic shield, while

## TABLE 12.1

### HEAT CAPACITY OF THE EMPTY CALORIMETER
### INFERRED FROM CONSTANT MASS EXPERIMENTS

| Temperature Interval | | $Z_{uncorrected}$ | $(TV\frac{dP}{dT} - PV)^2_1$ | Incremental Heat Leak $(W_{e_{\delta T}} - W_{e_{\delta T=0}})$ | Heat Capacity of The Empty Calorimeter |
|------|------|------|------|------|------|
| (°C) | | (Joules) | (Joules) | (Joules) | (Joules) |
| From | To | | | | |
| 100 | 150 | 71570.3 | 341.5 | −807.7 | 70421.1 |
| 150 | 200 | 78330.6 | 2390.7 | −1037.0 | 74902.9 |
| 200 | 250 | 88852.2 | 7162.7 | −1507.7 | 80181.8 |
| 250 | 300 | 103064.8 | 16543.1 | −1998.7 | 84523.0 |

the second one was a heat leak experiment in which the temperature difference between the calorimeter and adiabatic shield was maintained at a constant offset of 0.1°C.

Table 12.2 gives the results of measurements on the empty system under two sets of vacuum conditions. The second column gives the effect of both incremental heat leak and the zero heat leak while the third column gives the effect of the zero heat leak only. The difference in the second and third columns gives the magnitude of the incremental heat leak. Thus, the uncertainty in the results of the heat capacity given in Table 12.2 is due to the zero heat leak for the case of the empty calorimeter.

Also, comparison between the results of the heat capacity of the empty calorimeter obtained from the two different methods is given in Table 12.3. It may be seen from Table 12.3 that the measured values deviate from the actual values by 0.91% on the high side. This deviation may be attributed to uncertainty in measured heat leak values which was found to have large values in the present apparatus and also because of the zero heat leak which may have different values for different cases of empty and charged calorimeter.

## TABLE 12.2

### HEAT CAPACITY MEASUREMENTS ON EMPTY CALORIMETER UNDER VACUUM CONDITIONS

| Temperature Interval (°C) | | Energy Added to Calorimeter System With 0.1°C Temperature Difference Offset (Joules) | Energy Added to Calorimeter System With 0°C Temperature Difference Offset (Joules) |
|------|------|------|------|
| From | To | | |
| 100 | 150 | 71374.2 | 70271.8 |
| 150 | 200 | 75679.4 | 74583.1 |
| 200 | 250 | 81610.7 | 79602.6 |
| 250 | 300 | 85904.4 | 83757.5 |

## TABLE 12.3

### COMPARISON BETWEEN THE OBSERVED VALUES AND THE ACTUAL VALUES OF THE HEAT CAPACITY OF THE EMPTY CALORIMETER

| Temperature Interval (°C) | | Measured Value Obtained Under Vacuum Conditions | Actual Values Calculated From Constant Mass Measurements | Deviation From Actual Value |
|------|------|------|------|------|
| From | To | (Joules) | (Joules) | % |
| 100 | 150 | 70271.8 | 70421.1 | -0.21 |
| 150 | 200 | 74583.1 | 74902.9 | -0.43 |
| 200 | 250 | 79602.6 | 80181.8 | -0.72 |
| 250 | 300 | 83757.5 | 84523.0 | -0.91 |

# CHAPTER 13

## CONCLUSIONS AND RECOMMENDATIONS

### 13.1 CONCLUSIONS

The general working equation for the theory of calorimetric measurements derived by Osborne and Chan, has been derived here using a similar approach. The effect of heat leak, surface energy, strain energy and temperature scale was systematically studied in this thesis.

The equation derived for radiative zero heat leak produced large numerical values. Therefore, the neglect of the heat leak term may result in serious errors in enthalpy and other thermodynamic properties, especially if the surface conditions of the calorimeter become tarnished (errors in the order of 1% at 300°C may result).

Experimental studies conducted on heat leak showed that its numerical values are large in the present apparatus as compared to the total energy added to the system (heat leak amounted to 3.7% of the total energy added at 300°C for tare energy measurements and 4.1% at 300°C for constant mass measurements). This might be related to the fact that the calorimeter is badly tarnished and deteriorated.

Experiments revealed that heat leak is a strong function of the absolute temperature, overall temperature difference

between the calorimeter and adiabatic shield, the heating rate, the liquid mass contained in the calorimeter and most importantly, the temperature variations on the calorimeter and adiabatic shield surfaces.

On optimizing the working conditions of the calorimeter based on the experimental results, it was found that minimum heat leak values were obtained at a heating rate of approximately 8°C/hr. The equation derived here for the optimum working conditions of the calorimeter may be used to find the optimum working conditions for any two-phase system.

The numerical values obtained from the strain energy equation showed that the absolute values of strain energy are small in comparison to the total energy added to the system. More specifically, the ratio of the strain energy to the total energy added amounted to 0.02% at 300°C for the low filling case and 0.01% at 300°C for the high filling case.

Basing the calculations and the Platinum Resistance Thermometer calibrations on the IPTS-68 rather than the IPTS-48 has no effect on the calorimetric measurements. This is because, on one hand, the differences are very small and on the other hand, they are exactly the same for all calorimeter fillings.

Numerical values for surface energy were obtained from

the general equation derived for it. Calculations indicated that the effect of surface energy on the calorimetric determination of thermodynamic properties is negligible.

## 13.2. RECOMMENDATIONS

In view of the fact that heat transfer increases with time and temperature which indicates that the calorimeter and adiabatic shield surfaces tarnish because of the poor vacuum inside the system, it is recommended that design studies be conducted in order to increase vacuum and therefore reduce heat leak by eliminating oxidation conditions.

Although an extremely difficult design problem, internal heaters are recommended to be used in the calorimeter to improve temperature uniformity on the calorimeter surface.

For any apparatus, the emissivities and absorptivities of the calorimeter and adiabatic shield may be obtained from heat leak experiments which need to be performed only once. These values can then be used in conjunction with the theoretical heat leak equation derived in this thesis to determine the actual heat leak values at any time.

An automatic control system should be used in conjunction with the computer in order to automatically control the power to different heaters from all power supplies. Thus

temperature differences could be maintained within the required limits. Although manual control by a skilled operator is feasible and often employed, the full advantage of the adiabatic method can be conveniently realized only with automatic control so that a true equilibrium state may be reached.

A sufficient number of differential thermocouples should be installed on both the calorimeter and adiabatic shield surfaces for surveying and determining the temperature variations on the surfaces. This allows for determination of the unavoidable zero heat leak.

## APPENDIX A

## DERIVATION OF THE EXPERIMENTAL ENERGY EQUATIONS

### A.1 CONSTANT MASS EXPERIMENT

According to the First Law of Thermodynamics, the energy balance for the constant volume heat addition process may be written as follows:

$$-W_e + m_{f_1} u_{f_1} + m_{g_1} u_{g_1} = m_{f_2} u_{f_2} + m_{g_2} u_{g_2} + M_c c_{p_c} \Delta \tilde{T} - q_E + W_S + W_{S.E.} \quad (A.1)^*$$

Two cases are to be considered:

(a) Case 1 — When we have liquid evaporation (i.e. low filling case) take dm as +ve quantity

$$m_{f_2} = m_{f_1} - dm$$

$$m_{g_2} = m_{g_1} + dm$$

In terms of $m_{f_2}$ and $m_{g_2}$, equation A.1 may be rearranged as follows:

$$-W_{e_L} = m_{f_2}(u_{f_2} - u_{f_1}) + m_{g_2}(u_{g_2} - u_{g_1}) - dm(u_{f_1} - u_{g_1}) + M_c c_{p_c} \Delta T - q_{E_L} + W_{S_L} + W_{S.E._L}$$

$$(A.2)$$

but $m_{f_2} = M - m_{g_2}$

$$-W_{e_L} = m_{f_2}(u_{f_2} - u_{f_1}) + (M - m_{f_2})(u_{g_2} - u_{g_1}) + dm(u_{g_1} - u_{f_1})$$

$$+ M_c c_{p_c} \Delta T - q_{E_L} + W_{S_L} + W_{S.E._L}$$

---

* $q_E \equiv q_{\delta T} + q_{\delta T = 0}$ = the sum of the zero heat leak and the incremental heat leak.

i.e.

$$-W_{e_L} = m_{f_2}[(u_{f_2}-u_{g_2})-(u_{f_1}-u_{g_1})]+M(u_{g_2}-u_{g_1})+dm(u_{g_1}-u_{f_1})$$

$$+ M_c c_{p_c}\Delta T - q_{E_L}+W_{S_L}+W_{S.E._L} \qquad (A.3)$$

By utilizing the definition of enthalpy, i.e. $h_f = u_f + Pv_f$ and $h_g = u_g + Pv_g$, equation A.3 may be written as follows:

$$-W_{e_L} = m_{f_2}[(h_{f_2}-h_{f_1})-(h_{g_2}-h_{g_1})-P_2 v_{f_2}+P_1 v_{f_1}+P_2 v_{g_2}-P_1 v_{g_1}]$$

$$+ M[(h_{g_2}-h_{g_1})-P_2 v_{g_2}+P_1 v_{g_1}]+dm[(h_{g_1}-h_{f_1})-P_1(v_{g_1}-v_{f_1})]$$

$$+ M_c c_{p_c}\Delta T - q_{E_L}+W_{S_L}+W_{S.E._L} \qquad (A.4)$$

Using the definition of the enthalpy of saturated vapour

$$h_g = h_f + h_{fg}$$

we get, after substitution in equation A.4,

$$-W_{e_L} = m_{f_2}[(h_{fg_1}-h_{fg_2})+P_2(v_{g_2}-v_{f_2})-P_1(v_{g_1}-v_{f_1})]$$

$$+ dm[h_{fg_1}-P_1(v_{g_1}-v_{f_1})] + M[(h_{fg_2}-h_{fg_1})+(h_{f_2}-h_{f_1})$$

$$- P_2 v_{g_2}+P_1 v_{g_1}] + M_c c_{p_c}\Delta T - q_{E_L}+W_{S_L}+W_{S.E._L}$$

Substituting for $m_{f_2}$ in the first term as

$$m_{f_2} = M - dm - m_{g_1}$$

the above equation reduces to:

$$-W_{e_L} = (dm)h_{fg_2} - m_{g_1}(h_{fg_1} - h_{fg_2}) + m_{f_2}P_2(v_{g_2} - v_{f_2}) - m_{f_2}P_1(v_{g_1} - v_{f_1})$$

$$+ M(h_{f_2} - h_{f_1}) + MP_1 v_{g_1} - MP_2 v_{g_2} - (dm)P_1(v_{g_1} - v_{f_1})$$

$$+ M_c c_{p_c} \Delta T - q_{E_L} + W_{S_L} + W_{S.E._L}$$

Using the same relation as above, we change $M-dm$ to $m_{g_1} + m_{f_2}$
for the term

$$P_1 v_{g_1}(M-dm)$$

i.e.

$$(M-dm)P_1 v_{g_1} = (m_{g_1} + m_{f_2})P_1 v_{g_1}$$

and we have:

$$-W_{e_L} = (dm)h_{fg_2} - m_{g_1}(h_{fg_1} - h_{fg_2}) + m_{f_2}P_2(v_{g_2} - v_{f_2}) - m_{f_2}P_1(v_{g_1} - v_{f_1})$$

$$+ M(h_{f_2} - h_{f_1}) - MP_2 v_{g_2} + (dm)P_1 v_{f_1} + m_{g_1}P_1 v_{g_1} + m_{f_2}P_1 v_{g_1}$$

$$+ M_c c_{p_c} \Delta T - q_{E_L} + W_{S_L} + W_{S.E._L} \qquad (A.5)$$

but $\quad m_{f_2} = m_{f_1} - dm$

i.e.

$$m_{f_2}P_1 v_{f_1} = m_{f_1}P_1 v_{f_1} - (dm)P_1 v_{f_1}$$

and so:

$$m_{f_2}P_1 v_{f_1} + (dm)P_1 v_{f_1} + m_{g_1}P_1 v_{g_1} = m_{f_1}P_1 v_{f_1} + m_{g_1}P_1 v_{g_1}$$

i.e.

$$m_{f_2} P_1 v_{f_1} + (dm) P_1 v_{f_1} + m_{g_1} P_1 v_{g_1} = P_1 V$$

Consequently, equation A.5 reduces to:

$$-W_{e_L} = (dm) h_{fg_2} + M(h_{f_2} - h_{f_1}) - m_{g_1}(h_{fg_1} - h_{fg_2}) + m_{f_2} P_2 (v_{g_2} - v_{f_2})$$

$$-MP_2 v_{g_2} + P_1 V + M_c c_{p_c} \Delta T - q_{E_L} + W_{S_L} + W_{S.E._L} \tag{A.6}$$

Again, substituting for M from the relation

$$M = m_{f_2} + m_{g_2}$$

the two terms $m_{f_2} P_2 (v_{g_2} - v_{f_2}) - MP_2 v_{g_2}$ reduce to $-P_2 V$.

Thus, equation A.6 tends to be:

$$-W_{e_L} = (dm) h_{fg_2} + M(h_{f_2} - h_{f_1}) - m_{g_1}(h_{fg_1} - h_{fg_2}) + (P_1 - P_2) V$$

$$-q_{E_L} + M_c c_{p_c} \Delta T + W_{S_L} + W_{S.E._L} \tag{A.7}$$

Using the Clausius Clapeyron equation $h_{fg} = (v_g - v_f) T \frac{dP}{dT}$ to substitute for $h_{fg}$, the third term in the Right Hand Side becomes:

$$m_{g_1}(h_{fg_1} - h_{fg_2}) = m_{g_1} [(v_{g_1} - v_{f_1})(T \frac{dP}{dT})_1 - (v_{g_2} - v_{f_2})(T \frac{dP}{dT})_2]$$

and substituting in this equation for $m_{g_2}$ and M by

$$m_{g_2} = m_{g_1} + dm$$

and

$$M = m_{f_1} + m_{g_1}$$

and rearranging, the above equation reduces to:

$$m_{g_1}(h_{fg_1} - h_{fg_2}) = (m_{f_1}v_{f_1} + m_{g_1}v_{g_1})(T\frac{dP}{dT})_1 - (m_{f_2}v_{f_2} + m_{g_2}v_{g_2})(T\frac{dP}{dT})_2$$

$$+ M[v_{f_2}(T\frac{dP}{dT})_2 - v_{f_1}(T\frac{dP}{dT})_1] + (dm)(T\frac{dP}{dT})_2(v_{g_2} - v_{f_2})$$

Substituting for the total volume from the relation

$$V = m_f v_f + m_g v_g$$

we get the following equation:

$$m_{g_1}(h_{fg_1} - h_{fg_2}) = V[(T\frac{dP}{dT})_1 - (T\frac{dP}{dT})_2] + M[v_{f_2}(T\frac{dP}{dT})_2 - v_{f_1}(T\frac{dP}{dT})_1]$$

$$+ (dm)(v_{g_2} - v_{f_2})(T\frac{dP}{dT})_2$$

Therefore, equation A.7 reduces to:

$$-W_{e_L} = (dm)h_{fg_2} + M_L(h_{f_2} - h_{f_1}) - V[(T\frac{dP}{dT})_1 - (T\frac{dP}{dT})_2] - (dm)(v_{g_2} - v_{f_2})(T\frac{dP}{dT})_2$$

$$-M_L[v_{f_2}(T\frac{dP}{dT})_2 - v_{f_1}(T\frac{dP}{dT})_1] + (P_1 - P_2)V + M_c c_{p_c}\Delta T - q_{E_L} + W_{S_L} + W_{S.E._L}$$

Rearranging, the following equation is obtained:

$$-W_{e_L} = (dm)h_{fg_2} + M_L[(h_{f_2} - h_{f_1}) - v_{f_2}(T\frac{dP}{dT})_2 + v_{f_1}(T\frac{dP}{dT})_1] - (dm)(v_{g_2} - v_{f_2})$$

$$(T\frac{dP}{dT})_2 + V[(P_1 - P_2) - (T\frac{dP}{dT})_1 + (T\frac{dP}{dT})_2] + M_c c_{p_c}\Delta T - q_{E_L} + W_{S_L} + W_{S.E._L} \qquad (A.8)$$

Since Clausius Clapeyron equation states that

$$h_{fg} = (v_g - v_f)(T\frac{dP}{dT})$$

therefore, the first and third terms in the Right Hand Side of equation A.8 are equal. Consequently, they cancel each other. The final equation for the constant mass experiment in the case of liquid evaporation thus becomes:

$$-W_{e_L} = M_L [\hat{h}_f - Tv_f \frac{dP}{dT}]_1^2 + [TV\frac{dP}{dT} - PV]_1^2$$

$$+ M_c c_{p_c} \Delta T - q_{E_L} + W_{S_L} + W_{S.E._L} \tag{A.9}$$

(b)  Case 2 - Case of Vapour Condensation (High Filling)

From the First Law of Thermodynamics, the general energy equation may be written as follows:

$$-W_e + m_{f_1} u_{f_1} + m_{g_1} u_{g_1} = m_{f_2} u_{f_2} + m_{g_2} u_{g_2} + M_c c_{p_c} \Delta T - q_E + W_S + W_{S.E.} \tag{A.1}$$

Considering dm as a positive quantity, we may write,

$$m_{f_2} = m_{f_1} + dm$$

$$m_{g_2} = m_{g_1} - dm$$

In terms of $m_{f_2}$ and $m_{g_2}$, equation A.1 may be written as follows:

$$-W_e = m_{f_2}(u_{f_2} - u_{f_1}) + m_{g_2}(u_{g_2} - u_{g_1}) + dm(u_{f_1} - u_{g_1})$$

$$+ M_c c_{p_c} \Delta T - q_E + W_S + W_{S.E.}$$

Following the same procedure as in Case 1 and substituting for $m_{f_2}$ and u from

$$m_{f_2} = M - m_{g_2} \,,$$

$$h = u + Pv$$

we obtain;

$$-W_e = m_{f_2}[(h_{fg_1} - h_{fg_2}) + P_2(v_{g_2} - v_{f_2}) - P_1(v_{g_1} - v_{f_1})] - (dm)[h_{fg_1} - P_1(v_{g_1} - v_{f_1})]$$

$$+ M[(h_{fg_2} - h_{fg_1}) + (h_{f_2} - h_{f_1}) - P_2 v_{g_2} + P_1 v_{g_1}] + M_c c_{p_c} \Delta T - q_E + W_S + W_{S.E.}$$

Substituting for $m_{f_2}$ in the first term from

$$m_{f_2} = M + dm - m_{g_1}$$

and using the relations for the total volume and the total mass, i.e.

$$V = m_{f_1} v_{f_1} + m_{g_1} v_{g_1}$$

$$M = m_{f_2} + m_{g_2}.$$

Also using the Clausius Clapeyron equation, the following equation is obtained for the case of vapour condensation:

$$-W_{e_H} = M_H [h_f - Tv\frac{dP}{fdT}]_1^2 + [Tv\frac{dP}{dT} - Pv]_1^2 + M_c c_{p_c} \Delta T - q_{E_H} + W_{S_H} + W_{S.E._H} \quad (A.10)$$

Subtracting equation A.9 from equation A.10 yields the following general equation for the enthalpy determination:

$$-\frac{W_{e_H} - W_{e_L}}{M_H - M_L} = \Delta(h_f - Tv_f \frac{dP}{dT}) - \frac{q_{E_H} - q_{E_L}}{M_H - M_L} + \frac{W_{S_H} - W_{S_L}}{M_H - M_L} + \frac{W_{S.E._H} - W_{S.E._L}}{M_H - M_L}$$

Assuming that $W_{S_H}$ and $W_{S_L}$ are equal, and also assuming that $W_{S.E._H}$ and $W_{S.E._L}$ are equal, the final equation is written as follows:

$$-\frac{W_{e_H} - W_{e_L}}{M_H - M_L} = \Delta(h_f - Tv_f \frac{dP}{dT}) - \frac{q_{E_H} - q_{E_L}}{M_H - M_L} \tag{A.11}$$

## THEORETICAL SCANNER LAYOUT

INITIAL CONSTANTS AND EQUATIONS

RESISTANCE-TEMPERATURE CONVERSION EQUATION

$$R_t/R_o = 1 + AT + BT^2$$

$$A = 3.983854 \times 10^{-3}$$

$$B = -5.816369 \times 10^{-7}$$

$$R_o = 25.55995$$

VOLTAGE-TEMPERATURE CONVERSION EQUATION (FOR COPPER-CONSTANTAN THERMOCOUPLE)

$$T = a_o + a_1 x + a_2 x^2 + a_3 x^3 + a_4 x^4 + a_5 x^5 + a_6 x^6 + a_7 x^7$$

x in volts

T in $^o$C

$a_o = 0.10086091$  $a_1 = 25727.94369$

$a_2 = -767345.8296$  $a_3 = 78025595.81$

$a_4 = -9247486589$  $a_5 = 6.97688E+11$

$a_6 = -2.66192E+11$  $a_7 = 3.94078E+14$

STANDARD RESISTANCES USED WITH HEATERS FOR POWER DETERMINATION

$R_{S_1} \equiv$ Value of Shunt Resistance #1 = $.1\Omega$

$R_{S_2} \equiv$ Value of Shunt Resistance #2 = $1\Omega$

$R_{S_3} \equiv$ Value of Shunt Resistance #3 (with capsule heater) = $0.1\Omega$

$R_{S_4}, R_{S_5} \equiv$ Values of Shunt Resistances #4 & #5 (for ad. shield) = $0.1\Omega$ each

$R_{S_6}, R_{S_7} \equiv$ Values of Shunt Resistances #6 & #7 (for outerguard) = $0.1\Omega$ each

$R_{S_8} \rightarrow R_{S_{12}} \equiv$ Values of Shunt Resistances #'s 8, 9, 10, 11, 12 (for tube heaters) = $0.1\Omega$ each

VOLTAGE-PRESSURE CONVERSION EQUATION

$$P = b_o + b_1 V + b_2 V^2$$

$b_o, b_1, b_2$ Constants to be determined

V in volts

P in P.S.I.

*Values in brackets in the range column in the following table denote maximum values needed.

FIGURE B.1 Flow chart for constant mass experiment (1 hour exp.)

IF $(t-t_i)=N$

YES

READ $t$
$t_f = t$

TURN CALORIMETER HEATER OFF

READ $R, T_A, T_{D_M}, E_T, E_O, P$

IF $R, P, T_A$ CONSTANT; $T_{D_M} = 0$ FOR 10 MIN.

YES

NO

PRINT $R, T_A, T_{D_M}, E_T, E_O, P$

READ $R, P$
$R_F = R$, $P_f = P$

CALL SUBROUTINE DATA DEDUCTION

NO

$N = 60$
(OR 120, 240, 480)

READ $N$

READ $R, T_A, T_{D_M}, P, t$
5-MINUTE PERIOD

IF $R, T_A, P =$ CONSTANT; $T_{D_M} = 0$ FOR 60 MIN.

YES

NO

STAND BY (HOLD-UP)

READ $E_T, E_O, t, R$
$t_i = t$

TURN CALORIMETER HEATER ON

READ $R, T_A, T_{D_M}, E_C, E_T, E_A, E_O, P, t, R_S$

PRINT $R, T_{D_M}, P$

STORE $R, T_A, T_{D_M}, E_C, E_T, E_A, E_O, P, t$

FIGURE B.2 Flow chart for vapor withdrawal test (10 min. exp.)

N=10 OR (20, 30, 60)

READ N

READ $R, T_A, T_M, P, t$ 5-MINUTE PERIOD

IF $R, P, T_A$ = CONSTANT; $T_{D_M} = 0$ FOR 30 MIN.

NO → STANDBY (HOLD-UP)

YES → READ $E_T, E_O, t$; $t_i = t$

TURN CALORIMETER HEATER ON

READ $T_A, T_{D_{1-5}}, T_{D_{6-10}}, T_{D_{18,19}}, T_{D_{22}}, E_c$

PRINT $T_A, T_{D_{1-5}}, T_{D_{6-10}}, T_{D_{16}}, T_{D_{18,19}}, T_{D_{22}}, P, E_c$

STORE $T_A, T_{D_{1-5}}, T_{D_{6-10}}, T_{D_{16}}, T_{D_{18,19}}, T_{D_{22}}, P, E_c$

IF $(t-t_i) = N$

NO (loop back)

YES → READ $t$; $t_f = t$

TURN CALORIMETER HEATER OFF

READ $R, T_A, T_{D_{1-5}}, T_{D_{6-10}}, T_{D_{16}}, T_{D_{18,19}}, T_{D_{22}}$

IF $R, T, P$ = CONSTANT; $T_{D_M} = 0$ FOR 10 MIN.

NO → PRINT $R, T_A, T_{D_M}, P$

YES → READ $R, P$; $R_f = R$, $P_f = P$

CALL SUBROUTINE DATA REDUCTION

# 3

# 3

ARC-374

| SCANNER CHANNEL | TYPE OF READING | FUNCTION | RANGE | PRESENT PERIOD OF READING | REQUIRED PERIOD OF READING | STORAGE | PRINT |
|---|---|---|---|---|---|---|---|
| 00 | Read short circuit (or zero reading) | mV<br>V<br>V<br>V<br>Ω<br>A | 0-100mV<br>0-1.0V<br>0-10V<br>0-100V<br>0-10Ω<br>0-1.0Amp | | | | |
| 01 | Read voltage across calorimeter heater #1 $V_{H_1}(\tau)$ | V | 0-100V (0-60V) | 5 min | 1 sec | Store voltage as a function of time | Print voltage as a function of time |
| 02 | Read voltage across shunt #1 $V_{S_1}(\tau)$ | V | 0-1V | 5 min | 1 sec | Store voltage as a function of time<br>Store $P_{H_1}(t)$ | Print voltage as a function of time<br>Print $P_{H_1}(t)$ * |
| 03 | Read voltage across calorimeter heater #2 $V_{H_2}(\tau)$ | V | 0-100V (0-60V) | 5 min | 1 sec | Store voltage as a function of time | Print voltage as a function of time |
| 04 | Read voltage across shunt #2 $V_{S_2}(\tau)$ | V | 0-1V | 5 min | 1 sec | Store voltage as a function of time<br>Store $P_{H_2}(\tau)$ | Print voltage as a function of time<br>Print $P_{H_2}(\tau)$ |
| 05 | Read voltage across capsule heater $V_{CH}(\tau)$ | V | 0-100V (0-30V) | 5 min | 1 sec | Store voltage as a function of time<br>Store $P_{CH}(t)$ | Print voltage as a function of time<br>Print $P_{CH}(t)$ |
| 06 | Read voltage across shunt #3 $V_{S_3}(\tau)$ | V | 0-1V | 5 min | 1 sec | Store voltage as a function of time<br>Store $P_{H}(t)$ | Print voltage as a function of time<br>Print $P_{H}(\tau)$ |
| 07 | Read voltage across adiabatic shield heater #1 $V_{A_1}(\tau)$ | V | 0-100V (0-30V) | 5 min | 1 sec | Store voltage as a function of time | Print voltage as a function of time |

* Whenever there is a ____, it means a step in the computation part for the variable that appears in the next line.

| # | | | | | | Store | Print |
|---|---|---|---|---|---|---|---|
| 08 | Read voltage across shunt #4 $V_{S_4}(\tau)$ | v | 0-1v | 5 min | 1 sec | Store voltage as a function of time — Store $P_{A_1}(\tau)$ | Print voltage as a function of time — Print $P_{A_1}(\tau)$ |
| 09 | Read voltage across adiabatic shield heater #2 $V_{A_2}(\tau)$ | v | 0-100v (0-30v) | 5 min | 1 sec | Store voltage as a function of time — Store $P_{A_2}(\tau)$ | Print voltage as a function of time — Print $P_{A_2}(\tau)$ |
| 10 | Read voltage across shunt #5 $V_{S_5}(\tau)$ | v | 0-1v | 5 min | 1 sec | Store voltage as a function of time — Store $P_{A_2}(\tau)$ | Print voltage as a function of time — Print $P_A(\tau)$ |
| 11 | Read voltage across outerguard heater #1 $V_{O_1}(\tau)$ | v | 0-100v (0-60v) | 5 min | 1 sec | Store voltage as a function of time — Store $P_O(\tau)$ | Print voltage as a function of time |
| 12 | Read voltage across shunt #6 $V_{S_6}(\tau)$ | v | 0-1v | 5 min | 1 sec | Store voltage as a function of time — Store $P_{O_1}(\tau)$ | Print voltage as a function of time — Print $P_{O_1}(\tau)$ |
| 13 | Read voltage across outerguard heater #2 $V_{O_2}(\tau)$ | v | 0-100v (0-60v) | 5 min | 1 sec | Store voltage as a function of time — Store $P_{O_2}(\tau)$ | Print voltage as a function of time |
| 14 | Read voltage across shunt #7 $V_{S_7}(\tau)$ | v | 0-1v | 5 min | 1 sec | Store voltage as a function of time — Store $P_{O_2}(\tau)$ | Print voltage as a function of time — Print $P_{O_2}(\tau)$ |
| 15 | Read voltage across tube heater #1 $V_{T_1}(\tau)$ | v | 0-100v (0-30v) | 5 min | 1 sec | Store voltage as a function of time — Store $P_O(\tau)$ | Print voltage as a function of time — Print $P_O(\tau)$ |

| | | | | | | Store voltage as a function of time | Print voltage as a function of time |
|---|---|---|---|---|---|---|---|
| 16 | Read voltage across shunt #8 $V_{S_8}(\tau)$ | V | 0-1v | 5 min | 1 sec | Store voltage as a function of time | Print voltage as a function of time  Print $P_{T_1}(\tau)$ |
| 17 | Read voltage across tube heater #2 $V_{T_2}(\tau)$ | V | 0-100v (0-30v) | 5 min | 1 sec | Store $P_{T_1}(\tau)$ | Print voltage as a function of time |
| 18 | Read voltage across shunt #9 $V_{S_9}(\tau)$ | V | 0-1v | 5 min | 1 sec | Store voltage as a function of time | Print voltage as a function of time  Print $P_{T_2}(\tau)$ |
| 19 | Read voltage across tube heater #3 $V_{T_3}(\tau)$ | V | 0-100v (0-30v) | 5 min | 1 sec | Store $P_{T_2}(\tau)$ | Print voltage as a function of time  Print $P_{T_3}(\tau)$ |
| 20 | Read voltage across shunt #10 $V_{S_{10}}(\tau)$ | V | 0-1v | 5 min | 1 sec | Store voltage as a function of time | Print voltage as a function of time |
| 21 | Read voltage across tube heater #4 $V_{T_4}(\tau)$ | V | 0-100v (0-30v) | 5 min | 1 sec | Store $P_{T_3}(\tau)$ | Print voltage as a function of time  Print $P_{T_4}(\tau)$ |
| 22 | Read voltage across shunt #11 $V_{S_{11}}(\tau)$ | V | 0-1v | 5 min | 1 sec | Store voltage as a function of time | Print voltage as a function of time |
| 23 | Read voltage across tube heater #5 $V_{T_5}(\tau)$ | V | 0-100v (0-30v) | 5 min | 1 sec | Store $P_{T_4}(\tau)$ | Print voltage as a function of time  Print $P_{T_5}(\tau)$ |
| 24 | Read voltage across shunt #12 $V_{S_{12}}(\tau)$ | V | 0-1v | 5 min | 1 sec | Store voltage as a function of time  Store $P_{T_5}(\tau)$ | Print voltage as a function of time |

| # | Operation | Range | Unit | | | Store | Print |
|---|---|---|---|---|---|---|---|
| | Go to Channel 00 Read Short Circuit | 0-10Ω | Ω | | | | Print S.C. Reading |
| 25,26 | Read RTD | 0-10Ω (25-75Ω) | Ω | 5 min | 1 sec | Store resistance as a function of time | Print resistance as a function of time |
| | | | | | | Store $T_{68}$ as a function of time | Print $T_{68}$ as a function of time |
| | Go to Channel 00 Read Short Circuit | 0-100mV | mV | | | | Print S.C. Reading |
| 27 | Read absolute thermocouple $T_A$ | 0-100mV (0-25mV) | mV | 0.5 min | 1 sec | Store voltage as a function of time | Print voltage as a function of time |
| | | | | | | Store $T_{68}$ as a function of time | Print $T_{68}$ as a function of time |
| | Go to Channel 00 Read Short Circuit | | μV | | | | Print S.C. Reading |
| 28 | Read differential thermocouple between calorimeter and adiabatic shield $T_{D_{16}}$ | 0-100mV (0-200μV) | μV | 0.5 min | 1 sec | Store voltage as a function of time | Print voltage as a function of time |
| | | | | | | Store $\Delta T_{68}$ as a function of time | Print $\Delta T_{68}$ as a function of time |
| 29 | Read differential thermocouple between adiabatic shield and outerguard $T_{D_{17}}$ | 0-100mV (0-200μV) | μV | 0.5 min | 1 sec | Store voltage as a function of time | Print voltage as a function of time |
| | | | | | | Store $\Delta T_{68}$ as a function of time | Print $\Delta T_{68}$ as a function of time |
| 30 | Read differential thermocouple controlling power to tube heater #1 $T_{D_{18}}$ | 0-100mV (0-200μV) | μV | 0.5 min | 1 sec | Store voltage as a function of time | Print voltage as a function of time |
| | | | | | | Store $\Delta T_{68}$ as a function of time | Print $\Delta T_{68}$ as a function of time |

| | | | | | | Store | Print |
|---|---|---|---|---|---|---|---|
| 31 | Read differential thermocouple controlling power to tube heater #2 $T_{D_{19}}$ | μV | 0-100mV (0-200μV) | 0.5 min | 1 sec | Store voltage as a function of time<br>Store $\overline{\Delta T_{68}}$ as a function of time | Print voltage as a function of time<br>Print $\Delta T_{68}$ as a function of time |
| 32 | Read differential thermocouple controlling power to tube heater #3 $T_{D_{20}}$ | μV | 0-100mV (0-200μV) | 0.5 min | 1 sec | Store voltage as a function of time<br>Store $\overline{\Delta T_{68}}$ as a function of time | Print voltage as a function of time<br>Print $\Delta T_{68}$ as a function of time |
| 33 | Read differential thermocouple controlling power to tube heater #4 $T_{D_{21}}$ | μV | 0-100mV (0-200μV) | 0.5 min | 1 sec | Store voltage as a function of time<br>Store $\Delta T_{68}$ as a function of time | Print voltage as a function of time<br>Print $\Delta T_{68}$ as a function of time |
| 34 | Read differential thermocouple on vapor withdrawal tube $T_{D_{22}}$ | μV | 0-100mV (0-200μV) | 0.5 min | 1 sec | Store voltage as a function of time<br>Store $\overline{\Delta T_{68}}$ as a function of time | Print voltage as a function of time<br>Print $\Delta T_{68}$ as a function of time |
| 35 | Read differential thermocouple #1 for temperature variation on calorimeter surface $T_{D_1}$ | μV | 0-100mV (0-200μV) | 2 min | 1 sec | Store voltage as a function of time<br>Store $\overline{\Delta T_{68}}$ as a function of time | Print voltage as a function of time<br>Print $\Delta T_{68}$ as a function of time |
| 36 | Read differential thermocouple #2 for temperature variation on calorimeter surface $T_{D_2}$ | μV | 0-100mV (0-200μV) | 2 min | 1 sec | Store voltage as a function of time<br>Store $\Delta T_{68}$ as a function of time | Print voltage as a function of time<br>Print $\Delta T_{68}$ as a function of time |

| | | | | | | |
|---|---|---|---|---|---|---|
| 37 | Read differential thermocouple #3 for temperature variation on calorimeter surface $T_{D_3}$ | μV | 0-100mV (0-200 μV) | 2 min | 1 sec | Store voltage as a function of time / Store $\Delta T_{68}$ as a function of time | Print voltage as a function of time / Print $\Delta T_{68}$ as a function of time |
| 38 | Read differential thermocouple #4 for temperature variation on calorimeter surface $T_{D_4}$ | μV | 0-100mV (0-200μV) | 2 min | 1 sec | Store voltage as a function of time / Store $\Delta T_{68}$ as a function of time | Print voltage as a function of time / Print $\Delta T_{68}$ as a function of time |
| 39 | Read differential thermocouple #5 for temperature variation on calorimeter surface $T_{D_5}$ | μV | 0-100mV (0-200μV) | 2 min | 1 sec | Store voltage as a function of time / Store $\Delta T_{68}$ as a function of time | Print voltage as a function of time / Print $\Delta T_{68}$ as a function of time |
| 40 | Read differential thermocouple #1 for temperature variation on adiabatic shield surface $T_{D_6}$ | μV | 0-100mV (0-200μV) | 2 min | 1 sec | Store voltage as a function of time / Store $\Delta T_{68}$ as a function of time | Print voltage as a function of time / Print $\Delta T_{68}$ as a function of time |
| 41 | Read differential thermocouple #2 for temperature variation on adiabatic shield surface $T_{D_7}$ | μV | 0-100mV (0-200μV) | 2 min | 1 sec | Store voltage as a function of time / Store $\Delta T_{68}$ as a function of time | Print voltage as a function of time / Print $\Delta T_{68}$ as a function of time |
| 42 | Read differential thermocouple #3 for temperature variation on adiabatic shield surface $T_{D_8}$ | μV | 0-100mV (0-200μV) | 2 min | 1 sec | Store voltage as a function of time / Store $\Delta T_{68}$ as a function of time | Print voltage as a function of time / Print $\Delta T_{68}$ as a function of time |

| # | | | | | | | |
|---|---|---|---|---|---|---|---|
| 43 | Read differential thermocouple #4 for temperature variation on adiabatic shield surface $T_{D_9}$ | µV | 0-100mV (0-200µV) | 2 min | 1 sec | Store voltage as a function of time / Store $\Delta T_{68}$ as a function of time | Print voltage as a function of time / Print $\Delta T_{68}$ as a function of time |
| 44 | Read differential thermocouple #5 for temperature variation on adiabatic shield surface $T_{D_{10}}$ | µV | 0-100mV (0-200µV) | 2 min | 1 sec | Store voltage as a function of time / Store $\Delta T_{68}$ as a function of time | Print voltage as a function of time / Print $\Delta T_{68}$ as a function of time |
| 45 | Read differential thermocouple #1 for temperature variation on outerguard surface $T_{D_{11}}$ | µV | 0-100mV (0-200µV) | 2 min | 1 sec | Store voltage as a function of time / Store $\Delta T_{68}$ as a function of time | Print voltage as a function of time / Print $\Delta T_{68}$ as a function of time |
| 46 | Read differential thermocouple #2 for temperature variation on outerguard surface $T_{D_{12}}$ | µV | 0-100mV (0-200µV) | 2 min | 1 sec | Store voltage as a function of time / Store $\Delta T_{68}$ as a function of time | Print voltage as a function of time / Print $\Delta T_{68}$ as a function of time |
| 47 | Read differential thermocouple #3 for temperature variation on outerguard surface $T_{D_{13}}$ | µV | 0-100mV (0-200µV) | 2 min | 1 sec | Store voltage as a function of time / Store $\Delta T_{68}$ as a function of time | Print voltage as a function of time / Print $\Delta T_{68}$ as a function of time |
| 48 | Read differential thermocouple #4 for temperature variation on outerguard surface $T_{D_{14}}$ | µV | 0-100mV (0-200µV) | 2 min | 1 sec | Store voltage as a function of time / Store $\Delta T_{68}$ as a function of time | Print voltage as a function of time / Print $\Delta T_{68}$ as a function of time |

| # | Description | | Range | | | Store | Print |
|---|---|---|---|---|---|---|---|
| 49 | Read differential thermocouple #5 for temperature variation on outerguard surface $T_{D_{15}}$ | μV | 0-100mV (0-200μV) | 2 min | 1 sec | Store voltage as a function of time | Print voltage as a function of time |
| | | | | | | Store $\Delta T_{68}$ as a function of time | Print $\Delta T_{68}$ as a function of time |
| | Go to Channel -00 | V | 0-10V | | | | Print S.C. Reading |
| 50 | Read Pressure | V | 0-10V | 5 min | 1 sec | Store voltage as a function of time | Print voltage as a function of time |
| | | | | | | Store pressure as a function of time | Print pressure as a function of time |

# EXPERIMENTAL PROCEDURE AND CALCULATIONS

## CONSTANT MASS EXPERIMENT

1) Read Channels:
25,26,27,28,29,30,31,32,33,35,36,37
38,39,40,41,42,43,44,45,46,47,48,49,
50 (5 min. period)

2) Print Readings of These Channels

3) If Readings of Channels:25,26,27,
50 are $\doteq$ Constant
and
Readings of Channels: 28,29,30,31,
32,33,35,36,37,38,39,40,41,42,43,44,
45,46,47,48,49 are $\doteq$ 0 (0-2μV)
for 30 min.

Then:

4) Read Channels:
11,12,13,14,15,16,17,18,19,20,21,22,
23,24,25,26 and Time

Assign $\tau = \tau_i$

Assign $T = T_i$(Reading of Channels
25,26 Converted to Temperature)

Assign $P = P_i$(Reading of Channel 50
Converted to Pressure)

5) Give an Indication Monitor to
Turn Calorimeter Heaters On

6) Start the Experiment

## LIQUID WITHDRAWAL EXPERIMENT

1) Read Channels:
25,26,27,28,29,30,31,32,33,35,36,37,38,
39,40,41,42,43,44,45,46,47,48,49,50
(5 min. period)

2) Print Readings of These Channels

3) If Readings of Channels:25,26,27,50
are $\doteq$ Constant
and:
Readings of Channels: 28,29,30,31,32,33,
35,36,37,38,39,40,41,42,43,44,45,46,47,
48,49 are $\doteq$ 0 (0-2μV)
for 30 min.

Then:

4)Read Channels:
11,12,13,14,15,16,17,18,19,20,21,22,23,
24 and Time

Assign $\tau = \tau_i$

Assign $T = T_i$(Reading of Channels 25,
26 Converted to Temperature)

Assign $P = P_i$(Reading of Channel 50
Converted to Pressure)

5) Give an Indication Monitor to Turn
Calorimeter Heaters On

6) Start the Experiment

## VAPOR WITHDRAWAL EXPERIMENT

1) Read Channels:
25,26,27,28,29,30,31,32,33,35,36,
37,38,39,40,41,42,43,44,45,46,47,
48,49,50 (5 min. period)

2) Print Readings of These Channels

3) If Readings of Channels:25,26,
27,50 are $\doteq$ Constant
and:
Readings of Channels:
28,29,30,31,32,33,35,36,37,38,39,
40,41,42,43,44,45,46,47,48,49
are $\doteq$ 0(0-2μV) for 30 min.

Then:

4) Read Channels:
11,12,13,14,15,16,17,18,19,20,21,
22,23,24 and Time

Assign $\tau = \tau_i$

Assign $T = T_i$(Reading of Channels
25,26 Converted to Temperature)

Assign $P = P_i$(Reading of Channel
50 Converted to Pressure)

5) Give an Indication Monitor
to Turn Calorimeter Heaters On

6) Start the Experiment

| SCANNER CHANNEL | CONSTANT MASS EXPERIMENT | LIQUID WITHDRAWAL EXPERIMENT | VAPOR WITHDRAWAL EXPERIMENT |
|---|---|---|---|
| 02 | Compute $\dfrac{V_{H_1}(\tau) V_{S_1}(\tau)}{R_{S_1}} = P_{H_1}(\tau)$ | Compute $\dfrac{V_{S_1}(\tau) V_{H_1}(\tau)}{R_{S_1}} = P_{H_1}(\tau)$ | Compute $\dfrac{V_{H_1}(\tau) V_{S_1}(\tau)}{R_{S_1}} = P_{H_1}(\tau)$ |
| 04 | Compute $\dfrac{V_{H_2}(\tau) V_{S_2}(\tau)}{R_{S_2}} = P_{H_2}(\tau)$ | Compute $\dfrac{V_{H_2}(\tau) V_{S_2}(\tau)}{R_{S_2}} = P_{H_2}(\tau)$ | Compute $\dfrac{V_{H_2}(\tau) V_{S_2}(\tau)}{R_{S_2}} = P_{H_2}(\tau)$ |
| 06 | Compute $P_{H_1}(\tau) + P_{H_2}(\tau) = P_H(\tau)$ | Compute $\dfrac{V_{CH}(\tau) V_{S_3}(\tau)}{R_{S_3}} = P_{CH}(\tau)$ Compute $P_{H_1}(\tau) + P_{H_2}(\tau) + P_{CH}(\tau) = P_H(\tau)$ | Compute $\dfrac{V_{CH}(\tau) V_{S_3}(\tau)}{R_{S_3}} = P_{CH}(\tau)$ Compute $P_{H_1}(\tau) + P_{H_2}(\tau) + P_{CH}(\tau) = P_H(\tau)$ |
| 08 | Compute $\dfrac{V_{A_1}(\tau) V_{S_4}(\tau)}{R_{S_4}} = P_{A_1}(\tau)$ | Compute $\dfrac{V_{A_1}(\tau) V_{S_4}(\tau)}{R_{S_4}} = P_{A_1}(\tau)$ | Compute $\dfrac{V_{A_1}(\tau) V_{S_4}(\tau)}{R_{S_4}} = P_{A_1}(\tau)$ |
| 10 | Compute $\dfrac{V_{A_2}(\tau) V_{S_5}(\tau)}{R_{S_5}} = P_{A_2}(\tau)$ | Compute $\dfrac{V_{A_2}(\tau) V_{S_5}(\tau)}{R_{S_5}} = P_{A_2}(\tau)$ | Compute $\dfrac{V_{A_2}(\tau) V_{S_5}(\tau)}{R_{S_5}} = P_{A_2}(\tau)$ |
| 10 | Compute $P_{A_1}(\tau) + P_{A_2}(\tau) = P_A(\tau)$ (Needed for calculation of heat transfer coefficient only) | Compute $P_{A_1}(\tau) + P_{A_2}(\tau) = P_A(\tau)$ | Compute $P_{A_1}(\tau) + P_{A_2}(\tau) = P_A(\tau)$ |

| SCANNER CHANNEL | | | |
|---|---|---|---|
| 12 | Compute $\dfrac{V_{O_1}(\tau)V_{S_6}(\tau)}{R_{S_6}} = P_{O_1}(\tau)$ | Compute $\dfrac{V_{O_1}(\tau)V_{S_6}(\tau)}{R_{S_6}} = P_{O_1}(\tau)$ | Compute $\dfrac{V_{O_1}(\tau)V_{S_6}(\tau)}{R_{S_6}} = P_{O_1}(\tau)$ |
| 14 | Compute $\dfrac{V_{O_2}(\tau)V_{S_7}(\tau)}{R_{S_7}} = P_{O_2}(\tau)$ | Compute $\dfrac{V_{O_2}(\tau)V_{S_7}(\tau)}{R_{S_7}} = P_{O_2}(\tau)$ | Compute $\dfrac{V_{O_2}(\tau)V_{S_7}(\tau)}{R_{S_7}} = P_{O_2}(\tau)$ |
| 14 | Compute $P_{O_1}(\tau)+P_{O_2}(\tau)=P_O(\tau)$ | Compute $P_{O_1}(\tau)+P_{O_2}(\tau)=P_O(\tau)$ | Compute $P_{O_1}(\tau)+P_{O_2}(\tau)=P_O(\tau)$ |
| 16 | Compute $\dfrac{V_{T_1}(\tau)V_{S_8}(\tau)}{R_{S_8}} = P_{T_1}(\tau)$ | Compute $\dfrac{V_{T_1}(\tau)V_{S_8}(\tau)}{R_{S_8}} = P_{T_1}(\tau)$ | Compute $\dfrac{V_{T_1}(\tau)V_{S_8}(\tau)}{R_{S_8}} = P_{T_1}(\tau)$ |
| 18 | Compute $\dfrac{V_{T_2}(\tau)V_{S_9}(\tau)}{R_{S_9}} = P_{T_2}(\tau)$ | Compute $\dfrac{V_{T_2}(\tau)V_{S_9}(\tau)}{R_{S_9}} = P_{T_2}(\tau)$ | Compute $\dfrac{V_{T_2}(\tau)V_{S_9}(\tau)}{R_{S_9}} = P_{T_2}(\tau)$ |
| 20 | Compute $\dfrac{V_{T_3}(\tau)V_{S_{10}}(\tau)}{R_{S_{10}}} = P_{T_3}(\tau)$ | Compute $\dfrac{V_{T_3}(\tau)V_{S_{10}}(\tau)}{R_{S_{10}}} = P_{T_3}(\tau)$ | Compute $\dfrac{V_{T_3}(\tau)V_{S_{10}}(\tau)}{R_{S_{10}}} = P_{T_3}(\tau)$ |
| 22 | Compute $\dfrac{V_{T_4}(\tau)V_{S_{11}}(\tau)}{R_{S_{11}}} = P_{T_4}(\tau)$ | Compute $\dfrac{V_{T_4}(\tau)V_{S_{11}}(\tau)}{R_{S_{11}}} = P_{T_4}(\tau)$ | Compute $\dfrac{V_{T_4}(\tau)V_{S_{11}}(\tau)}{R_{S_{11}}} = P_{T_4}(\tau)$ |
| 24 | Compute $\dfrac{V_{T_5}(\tau)V_{S_{12}}(\tau)}{R_{S_{12}}} = P_{T_5}(\tau)$ | Compute $\dfrac{V_{T_5}(\tau)V_{S_{12}}(\tau)}{R_{S_{12}}} = P_{T_5}(\tau)$ | Compute $\dfrac{V_{T_5}(\tau)V_{S_{12}}(\tau)}{R_{S_{12}}} = P_{T_5}(\tau)$ |

| SCANNER CHANNEL | | | |
|---|---|---|---|
| 25 and 26 | Compute Temp. from the Equation:<br>$R_T = R_0(1+AT+BT^2)$<br>Compute $T_{68}$ from the Equation:<br>$t_{68}-t_{48}=f(t')$<br>$+\dfrac{t_{48}(t_{48}-100)(\delta_{68}-\delta_{48})}{\delta_{68}(100-2t_{48})+10^4}$<br>$+\dfrac{\delta_{68}[t_{68}-t_{48}-f(t')]^2}{\delta_{68}(100-2t_{48})+10^4}$ | Compute Temp. from the Equation:<br>$R_T=R_0(1+AT+BT^2)$<br>Compute $T_{68}$ from the Equation:<br>$t_{68}-t_{48}=f(t')$<br>$+\dfrac{t_{48}(t_{48}-100)(\delta_{68}-\delta_{48})}{\delta_{68}(100-2t_{48})+10^4}$<br>$+\dfrac{\delta_{68}[t_{68}-t_{48}-f(t')]^2}{\delta_{68}(100-2t_{48})+10^4}$ | Compute Temp. from the Equation:<br>$R_T=R_0(1+AT+BT^2)$<br>Compute $T_{68}$ from the Equation:<br>$t_{68}-t_{48}=f(t')$<br>$+\dfrac{t_{48}(t_{48}-100)(\delta_{68}-\delta_{48})}{\delta_{68}(100-2t_{48})+10^4}$<br>$+\dfrac{\delta_{68}[t_{68}-t_{48}-f(t'')]^2}{\delta_{68}(100-2t_{48})+10^4}$ |
| 27 | Compute Temp. from the Equation:<br>$T=a_0+a_1x+a_2x^2+a_3x^3+a_4x^4+a_5x^5$<br>$+a_6x^6+a_7x^7$ | Compute Temp. from the Equation:<br>$T=a_0+a_1x+a_2x^2+a_3x^3+a_4x^4+a_5x^5$<br>$+a_6x^6+a_7x^7$ | Compute Temp. from the Equation:<br>$T=a_0+a_1x+a_2x^2+a_3x^3+a_4x^4+a_5x^5$<br>$+a_6x^6+a_7x^7$ |
| 28 | Compute $\Delta T_{68}$ from: $1°C=Y\mu V$ | Compute $\Delta T_{68}$ from: $1°C=Y\mu V$ | Compute $\Delta T_{68}$ from: $1°C=Y\mu V$ |
| 29 | Compute $\Delta T_{68}$ from: $1°C=Y\mu V$ | Compute $\Delta T_{68}$ from: $1°C=Y\mu V$ | Compute $\Delta T_{68}$ from: $1°C=Y\mu V$ |
| 30 | Compute $\Delta T_{68}$ from: $1°C=Y\mu V$ | Compute $\Delta T_{68}$ from: $1°C=Y\mu V$ | Compute $\Delta T_{68}$ from: $1°C=Y\mu V$ |

| SCANNER CHANNEL | | | | |
|---|---|---|---|---|
| 31 | Compute $\Delta T_{68}$ from: $1°C=X$ μV | Compute $\Delta T_{68}$ from: $1°C=Y$ μV | Compute $\Delta T_{68}$ from: $1°C=Y$ μV | Compute $\Delta T_{68}$ from: $1°C=Y$ μV |
| 32 | Compute $\Delta T_{68}$ from: $1°C=Y$ μV | Compute $\Delta T_{68}$ from: $1°C=Y$ μV | Compute $\Delta T_{68}$ from: $1°C=Y$ μV | Compute $\Delta T_{68}$ from: $1°C=Y$ μV |
| 33 | Compute $\Delta T_{68}$ from: $1°C=Y$ μV | Compute $\Delta T_{68}$ from: $1°C=Y$ μV | Compute $\Delta T_{68}$ from: $1°C=Y$ μV | Compute $\Delta T_{68}$ from: $1°C=Y$ μV |
| 34 | Compute $\Delta T_{68}$ from: $1°C=Y$ μV | Compute $\Delta T_{68}$ from: $1°C=Y$ μV | Compute $\Delta T_{68}$ from: $1°C=Y$ μV | Compute $\Delta T_{68}$ from: $1°C=X$ μV |
| 35 | Compute $\Delta T_{68}$ from: $1°C=Y$ μV | Compute $\Delta T_{68}$ from: $1°C=Y$ μV | Compute $\Delta T_{68}$ from: $1°C=Y$ μV | Compute $\Delta T_{68}$ from: $1°C=Y$ μV |
| 36 | Compute $\Delta T_{68}$ from: $1°C=Y$ μV | Compute $\Delta T_{68}$ from: $1°C=Y$ μV | Compute $\Delta T_{68}$ from: $1°C=Y$ μV | Compute $\Delta T_{68}$ from: $1°C=Y$ μV |
| 37 | Compute $\Delta T_{68}$ from: $1°C=X$ μV | Compute $\Delta T_{68}$ from: $1°C=Y$ μV | Compute $\Delta T_{68}$ from: $1°C=Y$ μV | Compute $\Delta T_{68}$ from: $1°C=Y$ μV |
| 38 | Compute $\Delta T_{68}$ from: $1°C=Y$ μV | Compute $\Delta T_{68}$ from: $1°C=Y$ μV | Compute $\Delta T_{68}$ from: $1°C=Y$ μV | Compute $\Delta T_{68}$ from: $1°C=Y$ μV |
| 39 | Compute $\Delta T_{68}$ from: $1°C=Y$ μV | Compute $\Delta T_{68}$ from: $1°C=Y$ μV | Compute $\Delta T_{68}$ from: $1°C=Y$ μV | Compute $\Delta T_{68}$ from: $1°C=Y$ μV |
| 40 | Compute $\Delta T_{68}$ from: $1°C=Y$ μV | Compute $\Delta T_{68}$ from: $1°C=Y$ μV | Compute $\Delta T_{68}$ from: $1°C=Y$ μV | Compute $\Delta T_{68}$ from: $1°C=Y$ μV |
| 41 | Compute $\Delta T_{68}$ from: $1°C=Y$ μV | Compute $\Delta T_{68}$ from: $1°C=Y$ μV | Compute $\Delta T_{68}$ from: $1°C=Y$ μV | Compute $\Delta T_{68}$ from: $1°C=Y$ μV |
| 42 | Compute $\Delta T_{68}$ from: $1°C=Y$ μV | Compute $\Delta T_{68}$ from: $1°C=Y$ μV | Compute $\Delta T_{68}$ from: $1°C=Y$ μV | Compute $\Delta T_{68}$ from: $1°C=Y$ μV |
| 43 | Compute $\Delta T_{68}$ from: $1°C=Y$ μV | Compute $\Delta T_{68}$ from: $1°C=X$ μV | Compute $\Delta T_{68}$ from: $1°C=Y$ μV | Compute $\Delta T_{68}$ from: $1°C=Y$ μV |
| 44 | Compute $\Delta T_{68}$ from: $1°C=Y$ μV | Compute $\Delta T_{68}$ from: $1°C=Y$ μV | Compute $\Delta T_{68}$ from: $1°C=Y$ μV | Compute $\Delta T_{68}$ from: $1°C=Y$ μV |
| 45 | Compute $\Delta T_{68}$ from: $1°C=X$ μV | Compute $\Delta T_{68}$ from: $1°C=Y$ μV | Compute $\Delta T_{68}$ from: $1°C=Y$ μV | Compute $\Delta T_{68}$ from: $1°C=Y$ μV |
| 46 | Compute $\Delta T_{68}$ from: $1°C=X$ μV | Compute $\Delta T_{68}$ from: $1°C=Y$ μV | Compute $\Delta T_{68}$ from: $1°C=Y$ μV | Compute $\Delta T_{68}$ from: $1°C=Y$ μV |
| 47 | Compute $\Delta T_{68}$ from: $1°C=X$ μV | Compute $\Delta T_{68}$ from: $1°C=Y$ μV | Compute $\Delta T_{68}$ from: $1°C=Y$ μV | Compute $\Delta T_{68}$ from: $1°C=Y$ μV |
| 48 | Compute $\Delta T_{68}$ from: $1°C=Y$ μV | Compute $\Delta T_{68}$ from: $1°C=Y$ μV | Compute $\Delta T_{68}$ from: $1°C=Y$ μV | Compute $\Delta T_{68}$ from: $1°C=Y$ μV |

SCANNER
CHANNEL
49

Compute $\Delta T_{68}$ from: $1°C=Y$ μV

Compute Pressure from the Equation:

$$P=b_0 +b_1 v+b_2 v^2 +b_3 v^3$$

50

Compute $\Delta T_{68}$ from: $1°C=Y$ μV

Compute Pressure from the Equation:

$$P=b_0 +b_1 v+b_2 v^2 +b_3 v^3$$

Compute $\Delta T_{68}$ from: $1°C=Y$ μV

Compute Pressure from the Equation:

$$P=b_0 +b_1 v+b_2 v^2 +b_3 v^3$$

After the experiment is finished:
1) Read time: Assign $\tau = \tau_f$
2) Give an indication monitor to turn the calorimeter heaters off
3) Read channels: 25,26,27,28,30, 31,32,33,34,35,36,37,38,39,40,41, 42,43,44,50 (2 min. period)
4) If readings of channels: 25,26, 27,50 are $\doteq$ constant
And:
28,30,31,32,33,35,36,37,38,39,40, 41,42,43,44 are $\doteq$ 0(0-2µV) for,
10 min. then:
5) Read channels: 25,26,50
   Assign $T_{68}=T_f$
   Assign $P=P_f$
6) Compute $\Delta T=T_f-T_i$
7) Compute $\Delta P=P_f-P_i$
8) Plot pressure against temperature
9) Sum the total power($E_C$,$E_A$,$E_O$, $E_{T_1}$,$E_{T_2}$,$E_{T_3}$,$E_{T_4}$,$E_{T_5}$)by using subroutine 20.
10)Plot total calorimeter power $E_C$ against temperature.

After the experiment is finished:
1) Read time:Assign $\tau = \tau_f$
2) Give an indication monitor to turn the calorimeter heaters off
3) Read Channels: 25,26,27,28,29,30,31, 32,33,35,36,37,38,39,40,41,42,43,44,50 (2 min. period)
4) If readings of channels: 25,26,27, 50 are $\doteq$ constant
And:
28,30,31,32,33,35,36,37,38,39,40,41,42, 43,44 are $\doteq$ 0(0-2µV) for 10 min. then:
5) Read channels: 25,26,50
   Assign $T_{68}=T_f$
   Assign $P=P_f$
6) Compute $\Delta T=T_f-T_i$
7) Compute $\Delta P=P_f-P_i$
8) Plot pressure against temperature
9) Sum the total power ($E_C$,$E_A$,$E_O$, $E_{T_1}$,$E_{T_2}$,$E_{T_3}$,$E_{T_4}$,$E_{T_5}$) by using subroutine 20.
10)Plot total calorimeter power $E_C$ against temperature.

After the experiment is finished:
1) Read time:Assign $\tau = \tau_f$
2) Give an indication monitor to turn the calorimeter heaters off
3) Read channels: 25,26,27,28,29, 30,31,32,33,35,36,37,38,39,40,41, 42,43,44,45,46,47,48,49,11,12,13, 14,15,16,17,18,19,20,21,22,23,24, 50 (2 min. period)
4) If readings of channels:25,26, 50 are $\doteq$ constant
And:
28,29,30,31,32,33,35,36,37,38,39, 40,41,42,43,44,45,46,47,48,49 are $\doteq$ 0(0-2µV)
For 10 min.
Then:
5) Read channels: 25,26,50
   Assign $T_{68}=T_f$
   Assign $P = P_f$
6) Compute $\Delta T=T_f-T_i$
7) Compute $\Delta P=P_f-P_i$
8) Plot pressure against temperature
9) Sum the total power($E_C$,$E_A$,$E_O$, $E_{T_1}$,$E_{T_2}$,$E_{T_3}$,$E_{T_4}$,$E_{T_5}$)by using subroutine 20
10)Plot total calorimeter power $E$ against temperature
1f) Call subroutine 50 to calculate heat leak
12) Plot temperature against time
13) From the curve compute $dT/d\tau$.

190

PDVM Interface

CSR     764000
DBRII   764002
DBRL    764004
BR      5
VECTOR  170

| | 15 | 14 | 13 | 12 | 11 | 10 | 9 | 8 | 7 | 6 | 5 | 4 | 3 | 2 | 1 | 0 |
|---|---|---|---|---|---|---|---|---|---|---|---|---|---|---|---|---|

CSR

Auto Range ARX

Range AX

Range BX

Range CX

Function GX

Function FX

Function EX

A/D Done(Print)

Interrupt Enable

NO

Hold

Delay T

Set S1

Set S2

External Trigger
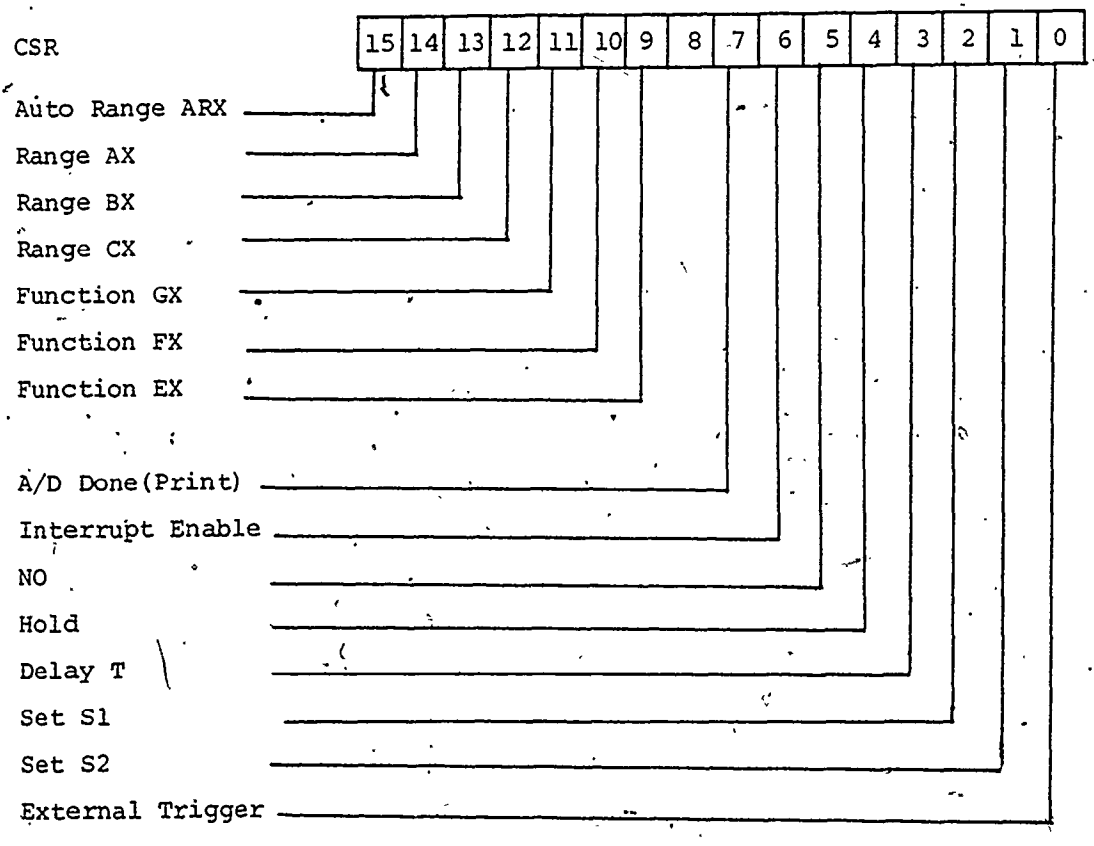
*NOTE:  Due to PDVM architecture it is mandatory that at least one
        digitize would have occurred after loading the CSR to allow
        accurate reading of status.  Bit 11 (GX) is transferred into
        the PDVM status register during a digitize cycle.

| CSR Bit | Description |
|---|---|

**15** — Auto Range, the PDVM will automatically switch range to accommodate the input. When this bit is set the instrument ignores the AX, BX and CX inputs.

**14, 13, 12** — Range data, hence,

| AX | BX | CX | Range |
|---|---|---|---|
| 0 | 0 | 0 | 1000 |
| 0 | 0 | 1 | 100 |
| 0 | 1 | 0 | 10 |
| 0 | 1 | 1 | 1 |
| 1 | 0 | 0 | 0.1 |
| 1 | 0 | 1 | 0.01 |

The remaining codes (110, 111) are invalid and if programmed the PDVM will range at 1000.

**11, 10, 9** — Function data, hence,

| GX | FX | EX | Function |
|---|---|---|---|
| 1 | 1 | 1 | VDC |
| 1 | 1 | 0 | VAC |
| 1 | 0 | 1 | KOHM |
| 1 | 0 | 0 | mADC |
| 0 | X | X | mAAC |

KOHM = OHMS X 1000, mA = AMPERE ÷ 1000.
(X = Don't care)

**8** — N/U

**7** — Conversion Done, a character is waiting to be read. Will interrupt the PDP-11 if bit 6 is also set. This bit is cleared when DBRH is read.

**6** — Interrupt Enable, when set allows bit 7 or bit 5 to interrupt the computer.
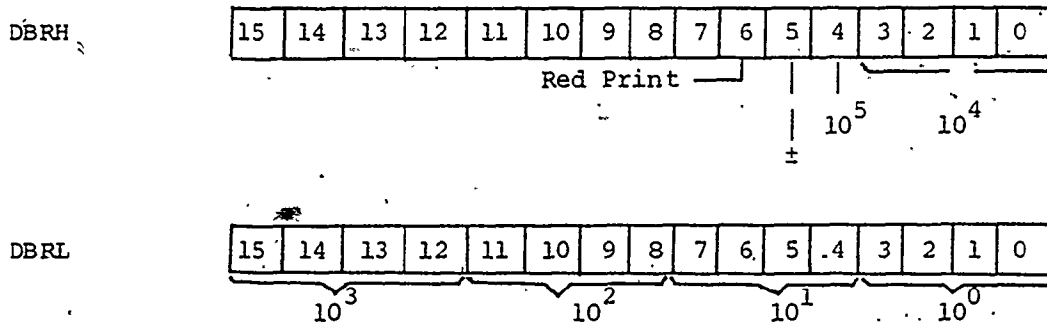
**5** — NG, when set indicates an error condition such as non-existent Function or Range. It interrupts the computer providing bit 6 is also set. The program must clear this bit by removing the illegal condition.

**4** — Hold, when reset will prevent the PDVM from making additional measurements. It will perform one digitization for every External Trigger.

| CSR Bit | Description |
|---------|-------------|
| 3 | Delay T, when set will delay the initiation of a measurement cycle by the External Trigger command by a time T.  T is determined by the setting of the front panel. |
| 2, 1 | Set S1, Set S2, set the PDVM into Step 1 or Step 2 respectively of the measuring cycle. |
| 0 | External Trigger, start pulse to the PDVM. |

All bits of the CSR except 0, 5 and 15 are Read/Write.  Bit 5 is Read Only while bit 0 and 15 are Write Only.  Bits 5 and 7 interrupt the computer via an Inclusive OR function and share the same vector locations.  Further information regarding bit meaning may be obtained from the Leeds & Northrup manuals.

DBRH

| 15 | 14 | 13 | 12 | 11 | 10 | 9 | 8 | 7 | 6 | 5 | 4 | 3 | 2 | 1 | 0 |
|----|----|----|----|----|----|---|---|---|---|---|---|---|---|---|---|

Red Print

$\pm$   $10^5$   $10^4$

DBRL

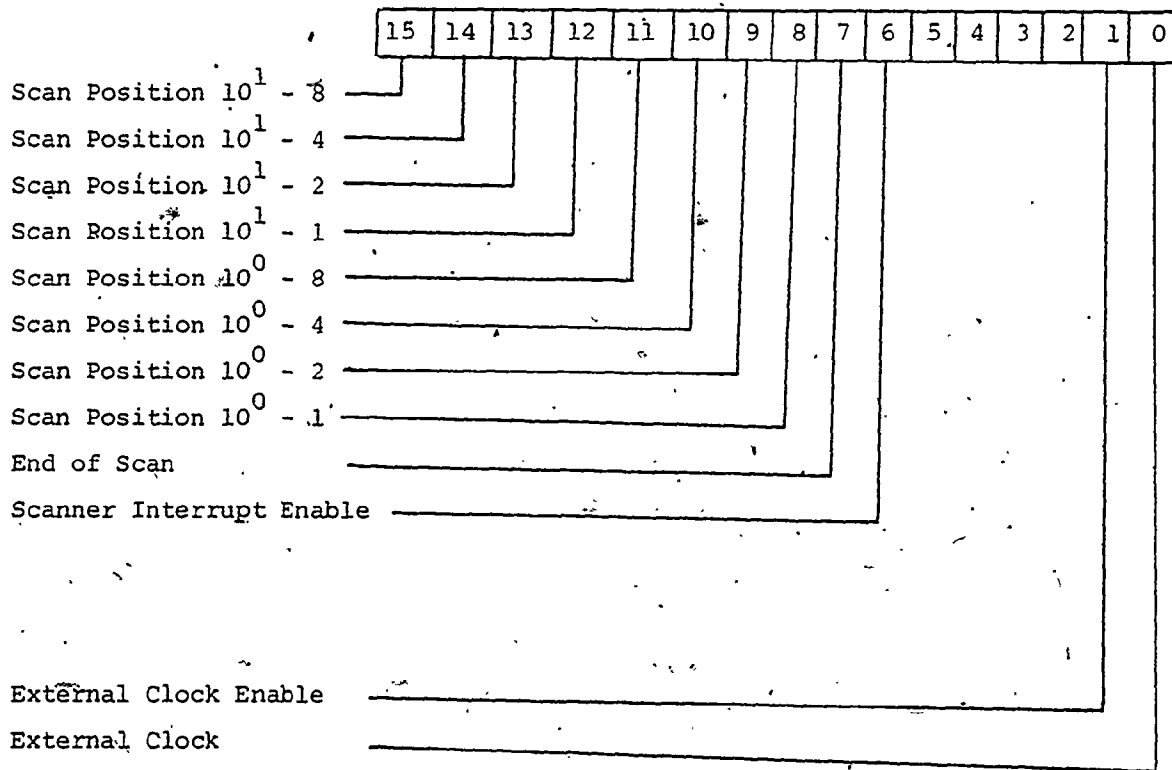| 15 | 14 | 13 | 12 | 11 | 10 | 9 | 8 | 7 | 6 | 5 | 4 | 3 | 2 | 1 | 0 |
|----|----|----|----|----|----|---|---|---|---|---|---|---|---|---|---|

$10^3$   $10^2$   $10^1$   $10^0$

The Data Buffer consists of two registers whose addresses are shown above.  The high register, DBRH, transfers the two most significant digits, the polarity (1 = +, 0 = -) and an error indicator called Red Print.  Red Print indicates an input overload condition into the PDVM, hence the digitized information is not valid.

DBRL transfers the least significant four digits of the PDVM output.  Both registers are read only.

## Scanner Interface

CSR      764006
BR       5
Vector   174

| 15 | 14 | 13 | 12 | 11 | 10 | 9 | 8 | 7 | 6 | 5 | 4 | 3 | 2 | 1 | 0 |
|----|----|----|----|----|----|---|---|---|---|---|---|---|---|---|---|

Scan Position $10^1$ - 8

Scan Position $10^1$ - 4

Scan Position $10^1$ - 2

Scan Position $10^1$ - 1

Scan Position $10^0$ - 8

Scan Position $10^0$ - 4

Scan Position $10^0$ - 2

Scan Position $10^0$ - 1

End of Scan

Scanner Interrupt Enable

External Clock Enable

External Clock

*NOTE:   End-of-Scan is generated as a result of writing bit 8-15 of the
         CSR.   Such action occurs on instructions such as MOV, BIS, BIC,
         etc.  To avoid unexpected interrupts it is advisable that Byte
         operations (MOVB, BISB, BICB, etc) be used when dealing with
         bits 0-7 of the Scanner CSR.

| CSR Bit | Description |
|---|---|
| 15 - 8 | Scanner Position, represents the line address in BCD format. |
| 7 | End of Scan, indicates that the Scanner has advanced to the next address, or a new address loaded in, and the lines are stable. Will interrupt the PDP-11 if bit 6 is set. |
| 6 | Scanner Interrupt Enable, allows bit 7 to interrupt the computer. |
| 5, 4, 3, 2 | N/U |
| 1 | External Clock Enable, when set will allow the Scanner to increment on each setting of bit 0. |
| 0 | External Clock, each setting will advance the Scanner providing bit 1 is reset. |

All CSR bits are Read/Write except bit 0, which is Write Only.

## PDVM Test Program

The purpose of the test program is to ensure proper operation of the PDVM, the Scanner, the Real-Time-Clock and the interfaces in between. It consists of three major tests, one per device.

The Real-Time-Clock is checked first to ensure that the flag gets set and that it interrupts the computer. The R.T.C. is later used by the other tests to time certain functions. The successful end of this test is signified by ten (10) bells on the CTY at one second intervals.

Next the Scanner and its interface are tested. The Scanner must be connected to its interface, powered "ON" and set to "REMOTE". Both phases of the Scanner are checked in this test, the results are observed on the NIXIE Display. First the Scanner is set to address 99 and decremented down to zero at approximately one step per second. During this test, the Scanner is "jam" loaded with the address and is allowed one second to set its "Ready" flag. Secondly, the Scanner address is incremented from zero to 99 at one second intervals. The External Increment feature of the Scanner is used during this test.

Finally, the DVM and its interface are checked to ensure that all CSR bits are operational and that an interrupt does occur. At the end of this test, some dynamic digitizing is performed, with the result being typed on the CTY. The operator is asked to enter the Channel Number and type of Function on the data switches.

The program runs with RT-11 and starts at address 1000. It is called PDVM.BIN.

## APPENDIX C

### INSTRUMENTATION

The energy input into the calorimeter, the absolute temperature, the temperature differences between the calorimeter, adiabatic shield and outerguard are all required to be measured very accurately. The mass of the water sample contained in the calorimeter must also be known precisely. Consequently, very accurate instruments are employed for such measurements. Detailed descriptions of the unique instrumentation used in this research is given in earlier research reports (7,33).

The main features of the instrumentation and measuring procedures may be explained by reference to the instrumentation circuit shown in Figure C.1. Figure C.2 also shows a photograph of the instrumentation and apparatus. The instrumentation used in this research was developed with funds made available to Professor E.S. Nowak from the Atomic Energy of Canada Limited and the National Research Council of Canada.

### C.1 ENERGY MEASUREMENTS

The standard potentiometer volt-box technique is used to measure the electrical work energy added to the system. The method consists essentially of determining the D.C. current flowing through the calorimeter heater and the voltage
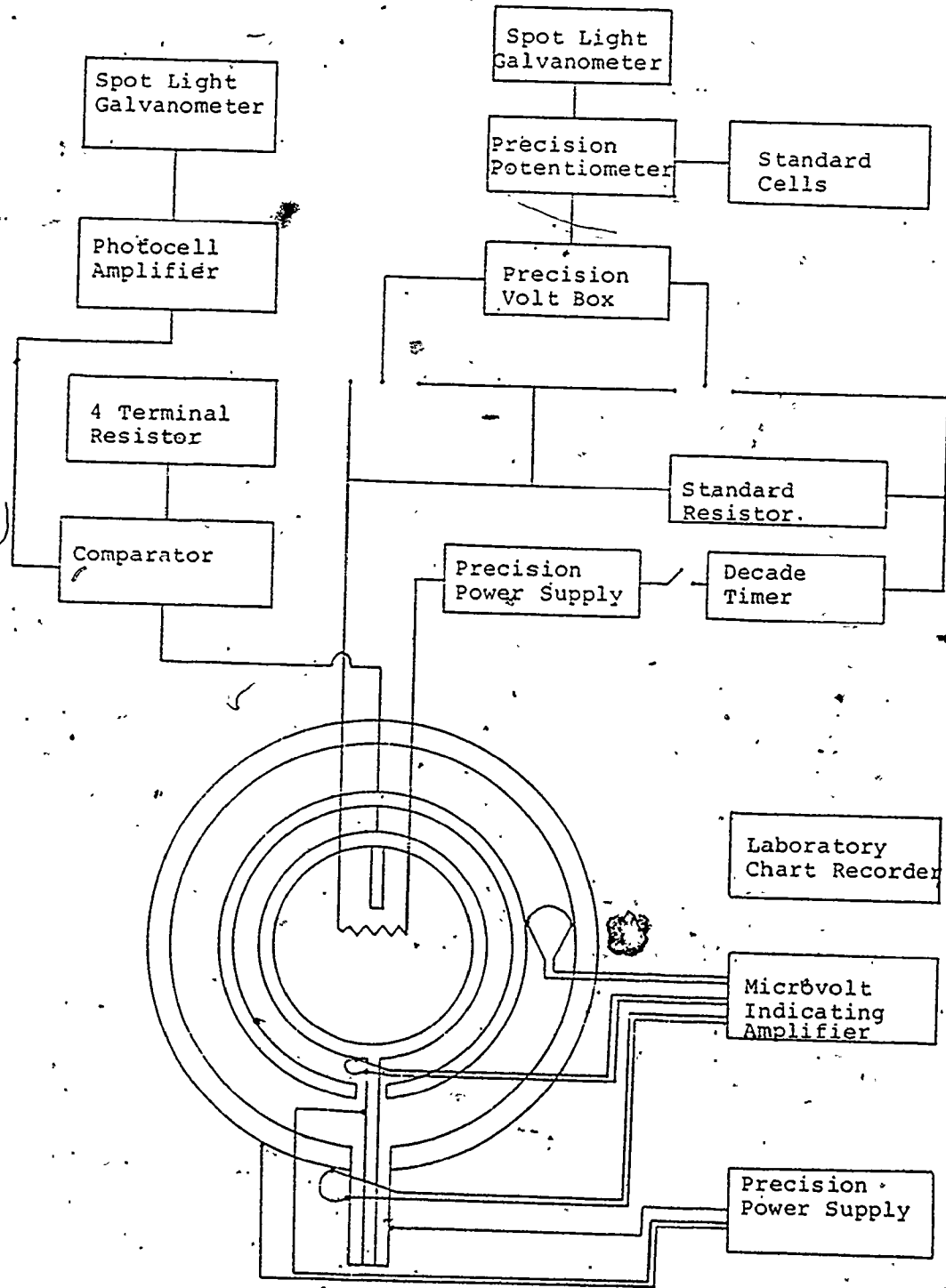
FIGURE C-1    Instrumentation circuit

FIGURE C.2  View of the instrumentations and apparatus

difference developed across the calorimeter heater. The
volt-box had a reported accuracy of $\pm 0.005\%$ (7).

Because the resistance of the calorimeter heater in-
creases during the heating period, (the temperature coeffi-
cient of resistance for Inconel is $19 \times 10^{-4}$ deg.) it was
not possible to maintain the voltage or the current at con-
stant values. The temperature change with time of the calori-
meter heater is made complex due to the effect of thermal
heat capacity of the heater and also the thermal resistance
offered to heat flow from the heater to the calorimeter
fluid contents.

In general, the temperature change with respect to time
of a calorimeter heater is characterized by an initial ther-
mal transient and then by a so-called slower steady state
change in temperature as the calorimeter temperature increases.
The initial thermal transient is governed by both the heat
capacity of the heater and the thermal resistance to heat
flow of the heater.

The resistance of the calorimeter heater of this re-
search may be described by the following expression:

$$R = R_o\{1 + a[\Delta T(1 - e^{-\tau/\tau_c})] + \beta\tau\}$$

where $R_o$ = the initial resistance

$a$ = the temperature coefficient of resistance

$$\tau_c = (M_c c_{p_c})(\text{thermal resistance})$$

$\beta$ = the heating rate

$\Delta T$ = unknown, but can be estimated for example from the temperature rise of the calorimeter and contents after the power to the calorimeter heater is turned off.

Figure C.3 is a computer plot of the voltage change during the heating period, showing that voltage increases suddenly (no doubt due to the previously mentioned resistance transient) at the beginning of the experiment and then remains essentially constant throughout. It may be seen from the curve that the total variation of voltage in the range of between approximately 3750 sec and the end of the experiment is in the order of 0.03%. However, from time zero to about 3750 sec, the sudden rise in voltage may be large which may affect the total variation and is a function of the time constant of the heater. A study of Figure C.3 reveals that for time in excess of 3750 sec, variation of voltage with time is extremely small. It could easily be speculated that the indicated variation is simply a measure of the zero drift of either the power supply or the D.C. measuring instrument.

Figure C.4 is a computer plot of current changes with time during the heating period. It is evident from this curve that the total variation of current is somewhat larger
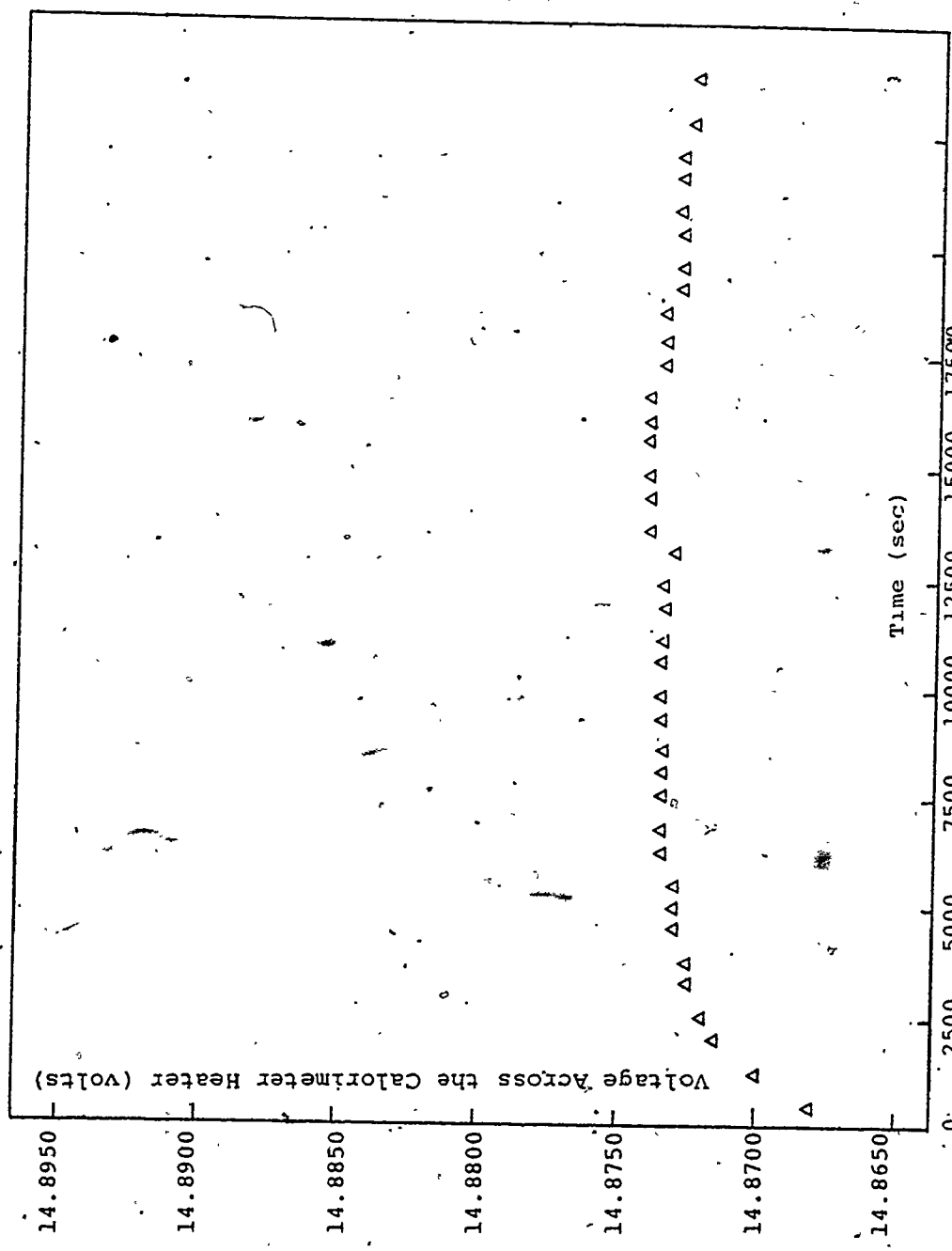
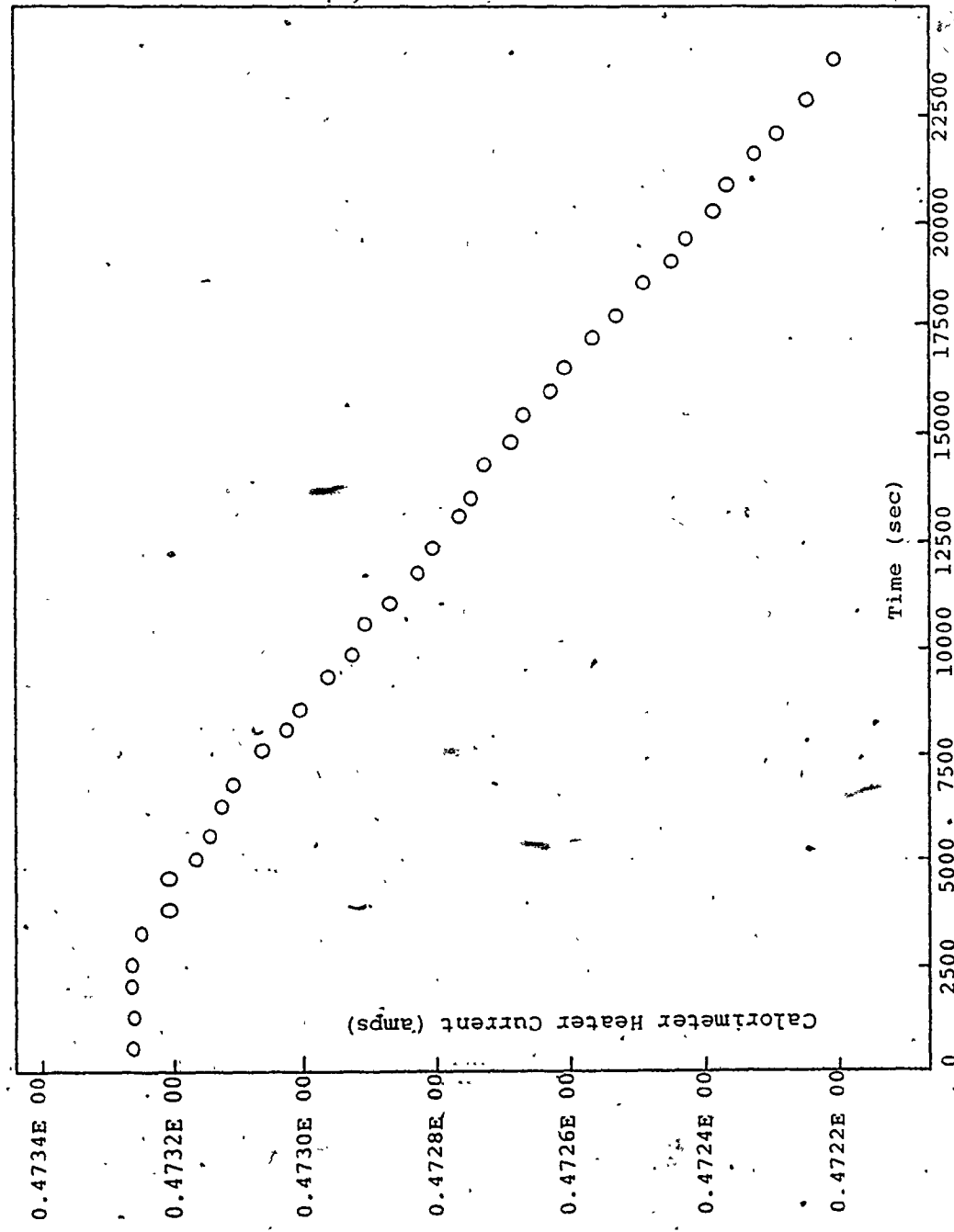FIGURE C-3   Voltage across the calorimeter heater (volts) vs time (sec)

FIGURE C-4   Variation of the calorimeter heater current (amps)
with time (sec)

than the variation in voltage and is in the order of 0.2%.

A detailed study of Figure C.4 indicates that the current decreases with time during the experiment. This is because the resistance of the calorimeter heater increases from 120 ohms to 120.15 ohms. Moreover, from Figure C.3, the voltage drop across the heater remains (essentially) constant.

The power supplied to the calorimeter can be evaluated by means of the following equation:

$$P = EI = \frac{V_H V_S}{R_S} \tag{C.1}$$

where $V_H = V_{H+S} - V_S - V_L$ is the voltage difference across the calorimeter heater (Figure C.5),

$V_{H+S}$ is the voltage drop across the calorimeter heater, the standard resistor and the power leads,

$V_S$ is the voltage difference across the standard resistor,

$V_L$ is the voltage drop across the power leads, and

$R_S$ is the resistance of the standard resistor.

The potentiometer employed in this research is accurate to 0.005% (7) and was standardized against one of a six cadmium saturated type standard cells which received an absolute calibration from the National Bureau of Standards accurate to ±0.0005% (7).
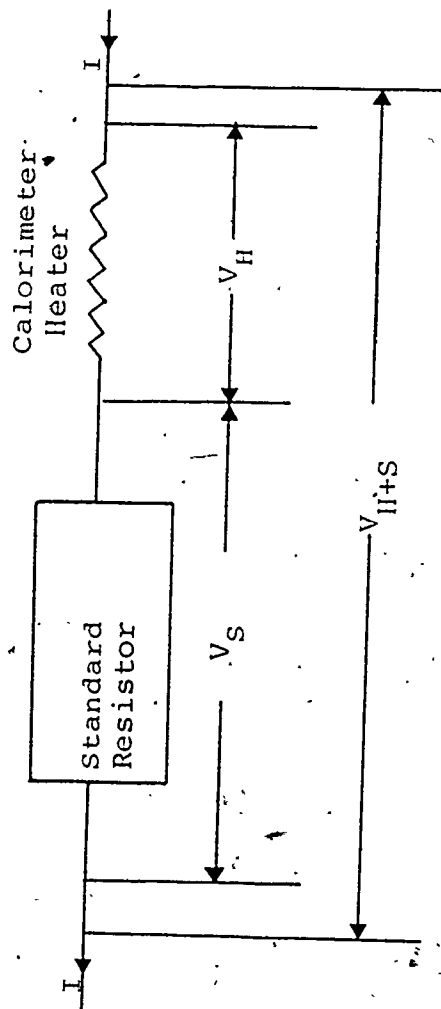
FIGURE C-5  Power measurements

It is usually not possible to take voltage and current measurements simultaneously. Therefore, readings of the current and voltage were made alternately at points equally spaced in time. More specifically, these measurements were taken every 300 seconds since it was desired to measure the input power (P) to a few hundredths of one per cent.

In calculating the input power to the calorimeter, use was made of equation (C.1) where corrections in the voltage due to the shunt resistance and the power leads were applied.

A computer plot of the power variation with time during the heating period, given in Figure C.6, shows that the input power increases suddenly when the power to the calorimeter heater is turned on and then decreases slightly with time during the experiment. It is evident from the curve that the total variation of power is in the order of 0.2%. The initial increase in power is due to the previously mentioned calorimeter heater transient. The decrease in power throughout most of the experiment is due to a decrease in current which in turn is directly linked to the increase in resistance. Over fifty degree temperature rise, the resistance increases by 0.13 per cent and consequently we would expect a power variation of at least 0.25%.
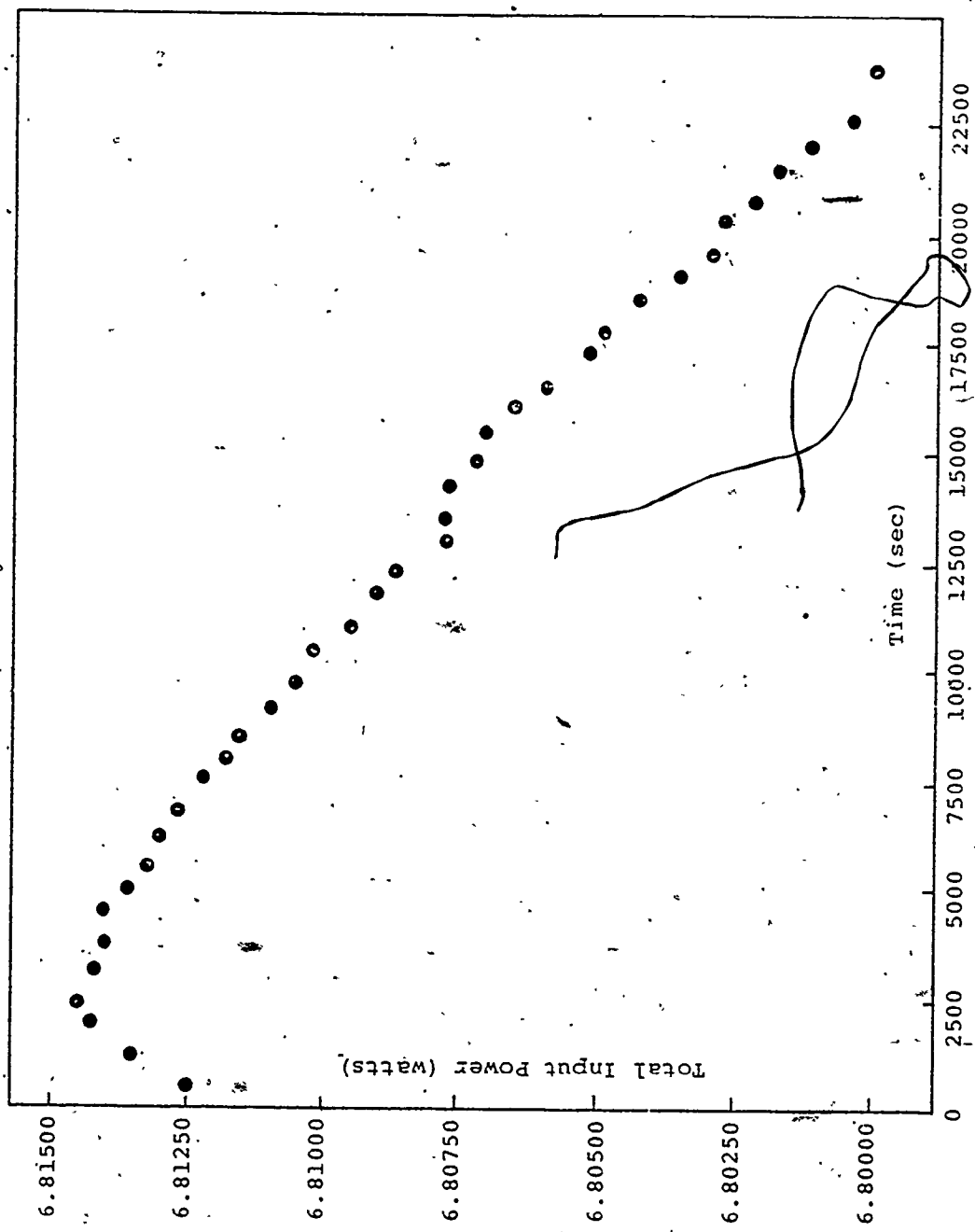
FIGURE C-6   Variation of the total input power (watts) with time (sec)

## C.2 EVALUATION OF ENERGY MEASUREMENTS

Three methods were initially employed to evaluate the so-called average value of voltage. In the arithmetic mean method, the average voltage was obtained from the individual measurements of voltage over the length of the experiment. In the graphical method, a curve was drawn through the individual points and the voltages integrated. Lastly, in the third method, a given analytical curve ($y = Ax^2 + Bx + C$, where $A = -0.32 \times 10^{-10}$, $B = 0.109 \times 10^{-5}$, $C = 14.872$) was fitted through the individual points. The result was nearly the same in all three cases – the maximum difference being less than 0.004% – as may be seen from Table C.1. The arithmetic mean method, being simplest, was thus used in all subsequent evaluations of voltage throughout the course of this research.

Calculations of the average current value were made by the same three methods outlined above, where in the least squares method, a given analytical curve ($y = Ax^2 + Bx + C$, where $A = -0.82 \times 10^{-12}$, $B = -0.38 \times 10^{-7}$, $C = 0.473$) was fitted through the individual points. These results are summarized in Table C.2 from which it can be seen that the average current determined by the three methods has approximately the same value (the maximum difference being less than 0.002%).

## TABLE C.1

### ANALYTICAL VALUES OF THE VOLTAGE MEASUREMENTS
### OF A CONSTANT MASS EXPERIMENT

(Series #1)

| Data Reduction Method | Average Voltage | % Deviation |
|---|---|---|
| Arithmetic Mean Method | 14.873 | 0.0 |
| Graphical Method | 14.8735 | +0.0034 |
| Least Squares Method | 14.87299 | -0.00007 |

## TABLE C.2

## ANALYTICAL VALUES OF THE CURRENT MEASUREMENTS
## OF A CONSTANT MASS EXPERIMENT

### (Series #1)

| Data Reduction Method | Average Current | % Deviation |
|---|---|---|
| Arithmetic Mean Method | 0.472807 | 0.0 |
| Graphical Method | 0.47281 | +0.0006 |
| Least Squares Method | 0.47280 | -0.0015 |

The average power values were calculated by the graphi-
cal, arithmetic mean and the least squares methods. In the
least squares method, a given analytical curve ($y = Ax^2 + Bx + C$, where $A = -0.32 \times 10^{-10}$, $B = -0.17 \times 10^{-7}$, $C = 6.8085$)
was fitted through the individual points. Comparison between
the results of the three methods is given in Table C.3 which
shows that the difference between the results is very small
(the maximum difference being less than 0.006%). Therefore,
the arithmetic mean method, being the simplest, was used in
the actual calculations.

## C.3 ABSOLUTE TEMPERATURE AND TEMPERATURE DIFFERENCE MEASUREMENTS

In high precision adiabatic calorimetry, one of the most
important requirements for absolute temperature and differen-
tial temperature measurements is rapid thermal response, so
that the differential temperature element may be assumed
always to indicate the same temperature as its immediate
environment. Another important requirement is that the ele-
ment and its external connections do not significantly change
the rate of heat transfer between the calorimeter shell and
the adiabatic shield. For accurately measuring the absolute
temperature of the calorimeter and its contents, only resis-
tance thermometers are used.

The platinum resistance thermometer used in this

TABLE C.3

ANALYTICAL VALUES OF THE INPUT POWER MEASUREMENTS
OF A CONSTANT MASS EXPERIMENT

(Series #1)

| Data Reduction Method | Average Power | % Deviation |
|---|---|---|
| Arithmetic Mean Method | 6.808521 | 0.0 |
| Graphical Method | 6.8089 | +0.0055 |
| Least Squares Method | 6.808423 | -0.0014 |

research is a capsule thermometer of the four-lead terminal type. It was calibrated against a long stemmed 25 ohm international primary standard platinum resistance thermometer calibrated by the National Research Council of Canada at the triple point of water, the steam point and the sulphur point. The constants in the internationally recognized resistance-temperature relationship

$$R/R_O = 1 + AT + BT^2$$

for the laboratory standard were certified by the National Research Council of Canada (6) to be as follows:

$R_O$ = ice point resistance = 25.5400 ohms

$A$ = $3.98478 \times 10^{-3}$

$B$ = $-5.8568 \times 10^{-7}$

$T$ = Temperature in °C.

In addition, the ratio of the resistance of the thermometer at steam point (100°C) to that at ice point (0°C) was found to be 1.3926.

For measuring the resistance of the thermometer, an isolating potential comparator in conjunction with a thermostated four-terminal resistor was used. A schematic diagram illustrating the principle of operation of the comparator method of temperature measurement is shown in Figure C.7. In this method, the resistance of the capsule thermometer may be
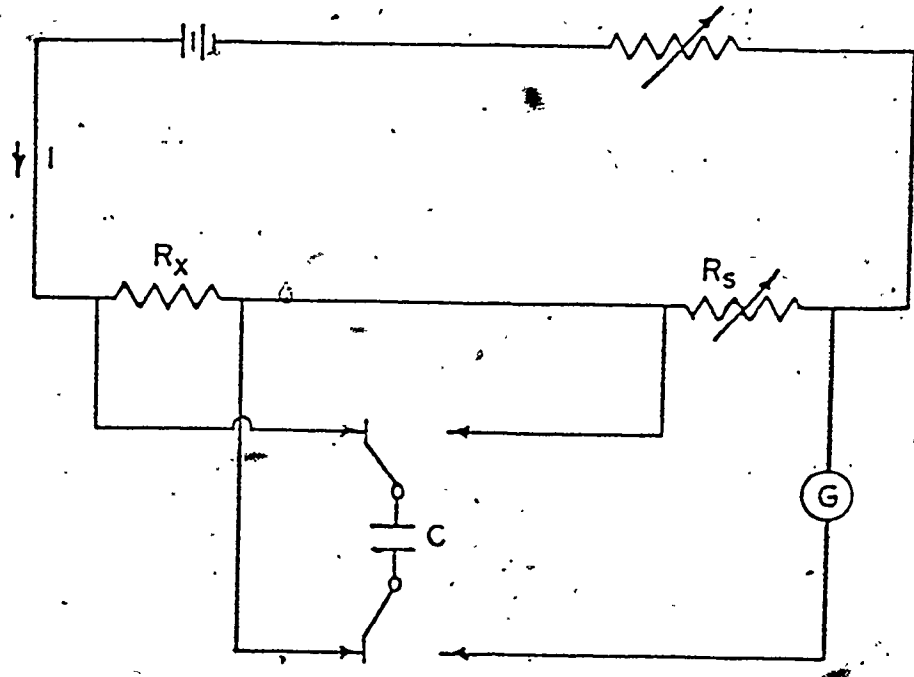
$R_s$ = FOUR TERMINAL VARIABLE RESISTOR

$R_x$ = RESISTOR UNDER TEST      I = CURRENT

G = GALVANOMETER    C = CAPACITOR

FIGURE c-7 THE ISOLATING POTENTIAL COMPARATOR
METHOD OF MEASURING RESISTANCES

measured accurately to within ±0.001%. A galvanometer con-
nected in series with one of the potential leads is used to
indicate any difference between the two potential drops in
the resistance thermometer and the variable four-terminal
resistor. The latter is adjusted to make the potential
appearing at its terminals equal to the potential across the
resistance thermometer, as established by the galvanometer
balance, indicating equality of the two resistances. The re-
sistance of the thermometer was read directly from the dial
of the variable four-terminal resistor in which a resistance
one tenth of a milliohm can be detected. This corresponds
to a temperature change of approximately one milli-degree for
a 25 ohms resistance thermometer.

In order to detect the temperature difference between
the calorimeter and adiabatic shield and between the adiabatic
shield and outerguard, two (four-junction) differential
copper-constantan thermocouples were used. Three (two-
junction) differential thermocouples* were also used to deter-
mine surface temperature variations on the calorimeter, adia-
batic shield and outerguard. The voltage outputs from the
differential thermocouples were recorded by means of a 24
point chart recorder connected to a microvolt amplifier. The

---

*The thermoelectric power of a copper-constantan thermocouple
 at 200°C is 8.3 millivolts.

voltage output from the differential thermocouples is initially amplified by the microvolt amplifier and then fed to the recorder. With this arrangement, the most sensitive range on the 10 in wide recorder chart was 25 microvolts for full scale deflection. This equipment is capable of measuring temperature difference of $\pm$ 1% accuracy. The sensitivity as indicated by the recorder chart is 5 microvolts.

## C.4  MASS MEASUREMENTS

Since the mass of water subjected to a change of state enters directly into the reduction of the data, the results can be no more reliable than the determinations of the masses will allow. Special care is therefore taken to insure that the masses of fluid sample are accurate and free from systematic errors. A precise Mettler analytical balance is thus used for weighing the water samples employed in this research. The balance has a maximum capacity of 1000 grams and it has an accuracy of 0.0001 grams. As was seen in Chapter 11, the masses used in this research are between 300 and 700 grams, consequently the maximum errors that can result through the use of this balance are no more than 0.00005%. The amounts of water samples charged to the calorimeter are not measured directly but are determined by the method of substitution. The container with the water sample was weighed before charging and then weighed again with the

remainder of the water sample. From the difference in the two weights, the mass of water charged to the calorimeter was calculated.

## C.5 TEMPERATURE CONTROL

For constant mass experiments, manual operations were used to maintain the temperature of the adiabatic shield to approximate that of the calorimeter and also for maintaining the temperature of the outerguard at a level very close to that of the adiabatic shield.

In the heat leak experiments, manual operations were also used to maintain the temperature difference offset between the calorimeter and adiabatic shield at a chosen constant value during the experiment.

With such an arrangement, the operator was able to control the temperature difference between the calorimeter and the adiabatic shield to within $\pm 0.002°C$, and the temperature difference between the adiabatic shield and outerguard to within $\pm 0.01°C$ in the constant mass experiments. In the heat leak experiments, the temperature difference offset between the calorimeter and adiabatic shield was arbitrary (as mentioned previously) and was accounted for with an accuracy of $\pm 0.001°C$.

# APPENDIX D

## THE STRAIN ENERGY EQUATIONS

### D.1 EFFECT OF TEMPERATURE ONLY

For thin shells, the relations between the stresses and the strains in radial and in tangential directions are given by (31):

$$\sigma_{11} = \frac{E}{1+\mu}(e_{11} + \frac{\mu}{1-2\mu} e) \qquad (D.1)$$

$$\sigma_{22} = \frac{E}{1+\mu}(e_{22} + \frac{\mu}{1-2\mu} e) \qquad (D.2)$$

but

$$e = e_{11} + e_{22} + e_{33}$$

and for spheres

$$e_{22} = e_{33}$$

Consequently, the relations between stresses and strains may be written in the following form after substitution and rearranging:

$$\sigma_{11} = \frac{E}{1-2\mu}[\frac{1-\mu}{1+\mu}e_{11} + \frac{2}{1+\mu}e_{22}] \qquad (D.3)$$

$$\sigma_{22} = \frac{E}{1-2\mu}[\frac{\mu}{1+\mu}e_{11} + \frac{1}{1+\mu}e_{22}] \qquad (D.4)$$

Taking into consideration the temperature effect, equations D.3 and D.4 will then read,

$$\sigma_{11} = \frac{E}{1-2\mu}[\frac{1-\mu}{1+\mu}e_{11} + \frac{2\mu}{1+\mu}e_{22} - aT] \qquad (D.5)$$

$$\sigma_{22} = \frac{E}{1-2\mu}[\frac{\mu}{1+\mu}e_{11} + \frac{1}{1+\mu}e_{22} - aT] \qquad (D.6)$$

Let R be the radial displacement of any point in the sphere. Considering the symmetry of the temperature change, there will be no other displacements, thus:

$$e_{11} = \frac{\partial R}{\partial r} \qquad (D.7)$$

$$e_{22} = \frac{R}{r} \qquad (D.8)$$

By taking an element of radius r of the sphere and with a thickness of dr and making the balance of forces as given in Figure D.1, we obtain:

$$\sigma_{11}(rd\theta) - (\sigma_{11} + \frac{d\sigma_{11}}{dr}dr)(r + dr)d\theta + 2\sigma_{22}\frac{d\theta}{2} dr = 0^* \qquad (D.9)$$

Rearranging and simplifying, we get:

$$\sigma_{11} - \sigma_{22} + r\frac{d\sigma_{11}}{dr} = 0 \qquad (D.10)$$

Upon substitution of equation D.5 and its differentiation as well as equation D.6 in equation D.10, and replacing $e_{11}$ and $e_{22}$ along with their derivatives in terms of R from equations D.7 and D.8, we obtain the following differential equation:

$$\frac{d^2R}{dr^2} + \frac{2}{r}\frac{dR}{dr} - \frac{2R}{r^2} = \frac{1+\mu}{1-\mu}\frac{d}{dr}(aT) \qquad (D.11)$$

*The total differential is taken since $\sigma_{11}$ varies only with r.
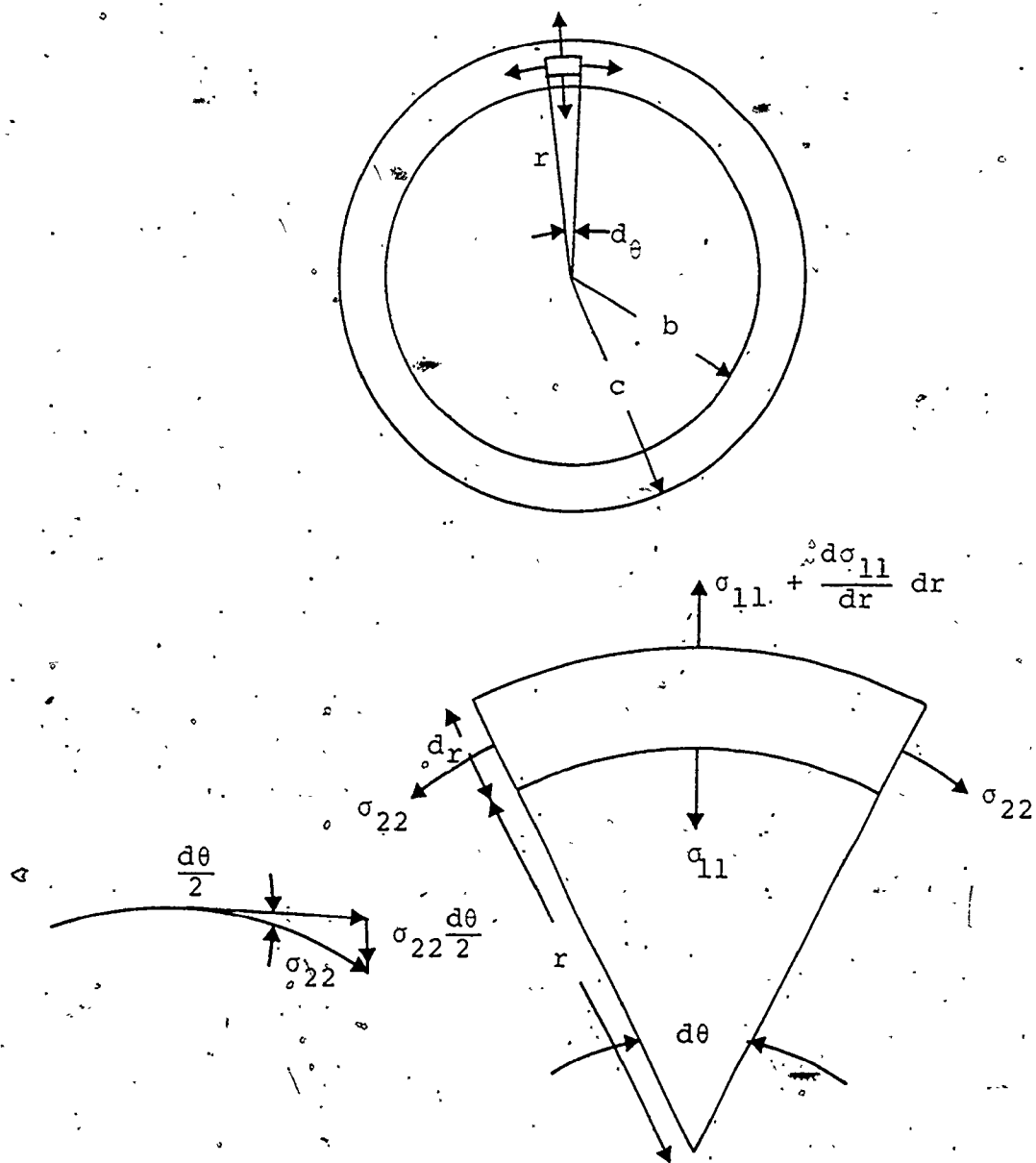
FIGURE D-1  Force balance on a spherical element

Integrating this equation twice results in:

$$R = \frac{1+\mu}{1-\mu} \int_b^r aTr^2 dr + C_1 r + \frac{C_2}{r^2} \quad\quad\quad (D.12)$$

Substitution of this expression in equations D.7 and D.8 results:

$$e_{11} = \frac{1+\mu}{1-\mu}[aT - \frac{2}{r^3} \int_{r_i}^r aTr^2 dr] + C_1 - \frac{2C_2}{r^3} \quad\quad (D.13)$$

$$e_{22} = \frac{1+\mu}{1-\mu} \frac{1}{r^3} \int_{r_i}^r aTr^2 dr + C_1 + \frac{C_2}{r^3} \quad\quad\quad (D.14)$$

Substitution of equations D.13 and D.14 into equations D.5 and D.6 results in the following expressions for the stresses:

$$\sigma_{11} = \frac{E}{1-2\mu}[C_1 - \frac{1-2\mu}{1-\mu} \frac{2}{r^3} \int_{r_i}^r aTr^2 dr - \frac{1-2\mu}{1+\mu} \frac{2C_2}{r^3}] \quad (D.15)$$

$$\sigma_{22} = \frac{E}{1-2\mu}[C_1 + \frac{1-2\mu}{1-\mu} \frac{1}{r^3} \int_{r_i}^r aTr^2 dr + \frac{1-2\mu}{1+\mu} \frac{C_2}{r^3} - \frac{1-2\mu}{1-\mu}aT] \quad (D.16)$$

To obtain the constants $C_1$ and $C_2$ in equations D.15 and D.16, the following boundary conditions are applied:

$$\sigma_{11} = 0 \quad\quad at\ r = r_i$$

$$\sigma_{11} = 0 \quad\quad at\ r = r_o$$

which results upon substitution:

$$C_1 = \frac{1-2\mu}{1-\mu} \frac{2}{r_o^3 - r_i^3} \int_{r_i}^{r_o} aTr^2 dr$$

$$C_2 = \frac{1+\mu}{1-\mu} \frac{r_i^3}{r_o^3 - r_i^3} \int_{r_i}^{r_o} aTr^2 dr$$

Consequently, and upon substitution of $C_1$ and $C_2$ back in equations D.13, D.14, D.15 and D.16, the following expressions for the stresses and strains in both radial and tangential directions are obtained:

$$\sigma_{11} = \frac{2Ea}{1-\mu} \left[ \frac{r^3 - r_i^3}{r^3(r_o^3 - r_i^3)} \int_{r_i}^{r_o} Tr^2 dr - \frac{1}{r^3} \int_{r_i}^{r} Tr^2 dr \right] \quad (D.17)$$

$$\sigma_{22} = \frac{Ea}{1-\mu} \left[ \frac{2r^3 + r_i^3}{r^3(r_o^3 - r_i^3)} \int_{r_i}^{r_o} Tr^2 dr + \frac{1}{r^3} \int_{r_i}^{r} Tr^2 dr - T \right] \quad (D.18)$$

$$e_{11} = \frac{1+\mu}{1-\mu} \left[ aT - \frac{2}{r^3} \int_{r_i}^{r} aTr^2 dr \right] + \left\{ (1-2\mu) - \frac{r_i^3}{r^3}(1+\mu) \right\}$$

$$\left\{ \frac{2}{1-\mu} \frac{1}{r_o^3 - r_i^3} \int_{r_i}^{r_o} aTr^2 dr \right\} \quad (D.19)$$

$$e_{22} = \frac{1+\mu}{1-\mu} \frac{1}{r^3} \int_{r_i}^{r} aTr^2 dr + \left\{ (1-2\mu) + \frac{r_i^3}{2r^3}(1+\mu) \right\}$$

$$\left\{ \frac{2}{1-\mu} \frac{1}{r_o^3 - r_i^3} \int_{r_i}^{r_o} aTr^2 dr \right\} \quad (D.20)$$

The strain energy is given by:

$$W_S = \int \frac{1}{2} \sigma \cdot e \cdot dV$$

Consequently, the strain energy in both radial and tangential directions is given by the following two expressions:

$$W_{S_{11}} = 2\pi \int_{r_i}^{r_o} \sigma_{11} e_{11} r^2 dr \quad (D.21)$$

$$W_{S_{22}} = 2\pi \int_{r_i}^{r_o} \sigma_{22} e_{22} r^2 dr \qquad (D.22)$$

where the value $4\pi r^2 dr$ was substituted for $dV$.

Using these facts and substituting from equations D.17, D.18, D.19 and D.20 into equations D.21 and D.22, we obtain the following expressions for $W_{S_{11}}$ and $W_{S_{22}}$.

$$W_{S_{11}} = \frac{4\pi E}{1-\mu} \int_{r_i}^{r_o} [\frac{r^3-r_i^3}{r^3(r_o^3-r_i^3)} \frac{1+\mu}{1-\mu} aT \int_{r_i}^{r_o} aTr^2 dr - \frac{1+\mu}{1-\mu} \frac{1}{r^3} aT \int_{r_i}^{r} aTr^2 dr$$

$$+ \frac{(r^3-r_i^3)\{2(1-2\mu)r^3-2(1+\mu)r_i^3\}}{r^6(1-\mu)(r_o^3-r_i^3)^2} (\int_{r_i}^{r_o} aTr^2 dr)^2$$

$$+ \frac{4r_i^3(1+\mu)-2r^3(2-\mu)}{r^6(1-\mu)(r_o^3-r_i^3)} (\int_{r_i}^{r_o} aTr^2 dr)(\int_{r_i}^{r} aTr^2 dr)$$

$$+ \frac{2}{r^6} \frac{1+\mu}{1-\mu}(\int_{r_i}^{r} aTr^2 dr)^2]r^2 dr \qquad (D.23)$$

$$W_{S_{22}} = \frac{2\pi E}{1-\mu} \int_{r_i}^{r_o} [\frac{2r_i^3(1+\mu)+2r^3(2-\mu)}{r^6(1-\mu)(r_o^3-r_i^3)}(\int_{r_i}^{r_o} aTr^2 dr)(\int_{r_i}^{r} aTr^2 dr)$$

$$+ \frac{(2r^3+r_i^3)\{r_i^3(1+\mu)+2r^3(1-2\mu)\}}{r^6(1-\mu)(r_o^3-r_i^3)^2} (\int_{r_i}^{r_o} aTr^2 dr)^2$$

$$+ \frac{1+\mu}{1-\mu} \frac{1}{r^6} (\int_{r_i}^{r} aTr^2 dr)^2 - \frac{1+\mu}{1-\mu} \frac{aT}{r^3} \int_{r_i}^{r} aTr^2 dr$$

$$+ \frac{aT\{2r^3(2\mu-1)-r_i^3(1+\mu)\}}{r^3(1-\mu)(r_o^3-r_i^3)} \int_{r_i}^{r_o} aTr^2 dr]r^2 dr \qquad (D.24)$$

The total strain energy is given by:

$$W_{S_T} = W_{S_{11}} + W_{S_{22}}$$

Thus, upon addition of equations D.23 and D.24, simplifying and rearranging, the following expression for the strain energy which results from the temperature effect only is obtained:

$$
W_{S_T} = \frac{2\pi E}{1-\mu} \int_{r_i}^{r_o} \left[ \frac{3}{r^3} \frac{2\mu r^3 - r_i^3(1+\mu)}{(1-\mu)(r_o^3 - r_i^3)} aT \int_{r_i}^{r_o} aTr^2 dr - \frac{3}{r^3} \frac{1+\mu}{1-\mu} aT \int_{r_i}^{r} aTr^2 dr \right.
$$

$$
+ \frac{8r^6(1-2\mu) - 2r_i^3 r^3(2-\mu) + 5r_i^6(1+\mu)}{r^6(1-\mu)(r_o^3 - r_i^3)^2} \left( \int_{r_i}^{r_o} aTr^2 dr \right)^2
$$

$$
+ \frac{5}{r^6} \frac{1+\mu}{1-\mu} \left( \int_{r_i}^{r} aTr^2 dr \right)^2
$$

$$
\left. + \frac{10r_i^3(1+\mu) - 2r^3(2-\mu)}{r^6(1-\mu)(r_o^3 - r_i^3)} \left( \int_{r_i}^{r_o} aTr^2 dr \right) \left( \int_{r_i}^{r} aTr^2 dr \right) \right] r^2 dr \qquad (D.25)
$$

Upon substitution of the expression of T in terms of r, numerical values for the strain energy are obtained. For the special case of the work in this research, the relationship between the temperature T and radius r is given as a linear relationship between T and heating rate where this is a case of linear heating. Such a relation is given in reference (21) as:

$$
T = \tau \frac{dT}{d\tau} + \frac{1}{6\alpha}(r^2 - r_o^2) \frac{dT}{d\tau} + \frac{r_i^3}{3\alpha r r_o}(r_o - r) \frac{dT}{d\tau} \qquad (D.26)
$$

where $\frac{dT}{d\tau}$ is the heating rate,

$\alpha$ is the thermal diffusivity,

$\tau$ is time, and

$r_i$ and $r_o$ are the inner and outer radii of the calorimeter shell.

This expression is thus substituted in equation D.25 and numerical values of strain energy are thus obtained upon substitution for the values of the given constants.

D.2   EFFECT OF PRESSURE ONLY

The relations between the stresses and strains in the radial and tangential directions are as follows (64):

$$\sigma_r = \frac{E}{1-2\mu}[\frac{1-\mu}{1+\mu} e_r + \frac{2u}{1+\mu} e_t] \qquad (D.27)$$

$$\sigma_t = \frac{E}{1-2\mu}[\frac{\mu}{1+\mu} e_r + \frac{1}{1+\mu} e_t] \qquad (D.28)$$

As previously mentioned in Section D.1, taking R as the radial displacement of any point in the sphere, and taking the force balance on an element of the sphere, the following equation is obtained:

$$\sigma_r - \sigma_t + r \frac{d\sigma_r}{dr} = 0$$

Upon substitution of $\sigma_r$, $\sigma_t$ and $\frac{d\sigma_r}{dr}$ from equations D.27 and D.28 and also substituting for $e_r$ and $e_t$ in terms of R, the following equation results:

$$\frac{d^2R}{dr^2} + \frac{2}{r}\frac{dR}{dr} - \frac{2R}{r^2} = 0$$

Integrating this equation twice, the following expression is obtained:

$$R = C_1 r + \frac{C_2}{r^2}$$

Substituting this expression as well as the expressions for strains, as previously done in Section D.1, into equations D.27 and D.28, the following expressions for the stresses may be written:

$$\sigma_r = \frac{E}{1-2\mu}[C_1 - \frac{2C_2}{r^3}\frac{1-2\mu}{1+\mu}] \tag{D.29}$$

$$\sigma_t = \frac{E}{1-2\mu}[C_1 + \frac{C_2}{r^3}\frac{1-2\mu}{1+\mu}] \tag{D.30}$$

The constants $C_1$ and $C_2$ may be obtained by applying the following boundary conditions:

$$\sigma_r = -P_i \quad \text{at } r = r_i$$

$$\sigma_r = -P_o \quad \text{at } r = r_o$$

but $P_o = 0$, since there is vacuum outside the spherical shell.

The constants are found to be:

$$C_1 = -\frac{1-2\mu}{E}\frac{r_i^3 P_i}{r_i^3 - r_o^3}$$

$$C_2 = - \frac{1+\mu}{2E} P_i \frac{r_i^3 r_o^3}{r_i^3 - r_o^3}$$

Substituting the expressions for $C_1$ and $C_2$ back in equations D.29 and D.30, the following expressions for the stresses are obtained:

$$\sigma_r = - \frac{P_i r_i^3}{r_i^3 - r_o^3} (1 - \frac{r_o^3}{r^3}) \qquad \text{(D.31)}$$

$$\sigma_t = - \frac{P_i r_i^3}{r_i^3 - r_o^3} (1 + \frac{r_o^3}{2r^3}) \qquad \text{(D.32)}$$

Upon substituting equations D.31 and D.32 into equations D.27 and D.28, the following expressions are obtained for the strains:

$$e_r = - \frac{P_i}{E} \frac{r_i^3}{r_i^3 - r_o^3} [(1-2\mu) - \frac{r_o^3}{r^3}(1+\mu)] \qquad \text{(D.33)}$$

$$e_t = - \frac{P_i}{E} \frac{r_i^3}{r_i^3 - r_o^3} [(1-2\mu) + \frac{r_o^3}{2r^3} (1+\mu)] \qquad \text{(D.34)}$$

Since the strain energy is given by:

$$W_s = \int \frac{1}{2} \sigma e \, dV$$

Substitution of the stress and strain expressions from the above equations, and substituting for the elemental spherical volume from the following relation,

$$dV = 4\pi r^2 dr$$

the following two expressions are obtained for the strain

energy in both radial and tangential directions:

$$W_{S_r} = \frac{2\pi P_i^2}{E} \frac{r_i^6}{(r_i^3-r_o^3)^2}[\frac{1-2\mu}{3}(r_o^3-r_i^3)-(2-\mu)r_o^3 \ell n \frac{r_o}{r_i}$$

$$-\frac{1+\mu}{3} \frac{r_o^6}{r_o^3-r_i^3}] \qquad (D.35)$$

$$W_{S_t} = \frac{2\pi P_i^2}{E} \frac{r_i^6}{(r_i^3-r_o^3)^2}[\frac{1-2\mu}{3}(r_o^3-r_i^3)+(2-\mu)\frac{r_o^3}{2} \ell n \frac{r_o}{r_i}$$

$$-\frac{1+\mu}{12} \frac{r_o^6}{r_o^3-r_i^3}] \qquad (D.36)$$

Combination of equations D.35 and D.36 results in the follow-

ing expression for the total strain energy which results from

the pressure effect only:

$$W_{S_p} = \frac{2\pi P_i^2}{E} \frac{r_i^6}{(r_i^3-r_o^3)^2}[\frac{2}{3}(1-2\mu)(r_o^3-r_i^3)-(2-\mu)\frac{r_o^3}{2} \ell n \frac{r_o}{r_i}$$

$$-\frac{5}{12}(1+\mu) \frac{r_o^6}{r_o^3-r_i^3}] \qquad (D.37)$$

Substitution of the constants at different pressure

values then results in numerical values of the strain energy

due to pressure effect alone.

D.3  MASS EFFECT ONLY

The stresses along the calorimeter surface are represented by a step function.  Therefore, the stresses will be found in two steps.

(i)  The Stresses Above the Supports.

With reference to Figure D.2, we may get the following relations:

$\phi = 60°$

$r = r_o \sin\phi = \frac{\sqrt{3}}{2} r_o$

$h_1 = r_o \cos\phi = \frac{r_o}{2}$

$\therefore h = r_o - h_1 = \frac{r_o}{2}$

Denoting the total volume of liquid contained in the sphere by $V_{Liq}$, we have:

$$V_{Liq} = \frac{4}{3} \pi r_o^3 - \frac{1}{3} \pi y^2 (3r_o - y) \qquad (D.38)$$

Denoting the second term in the Right Hand Side of equation D.38 by $V_1$, i.e.

$$V_1 = \frac{1}{3} \pi y^2 (3r_o - y) \qquad (D.39)$$

and since the volume of fluid below the supports is given by:

$$V_2 = \frac{1}{3} \pi h^2 (3r_o - h) \qquad (D.40)$$
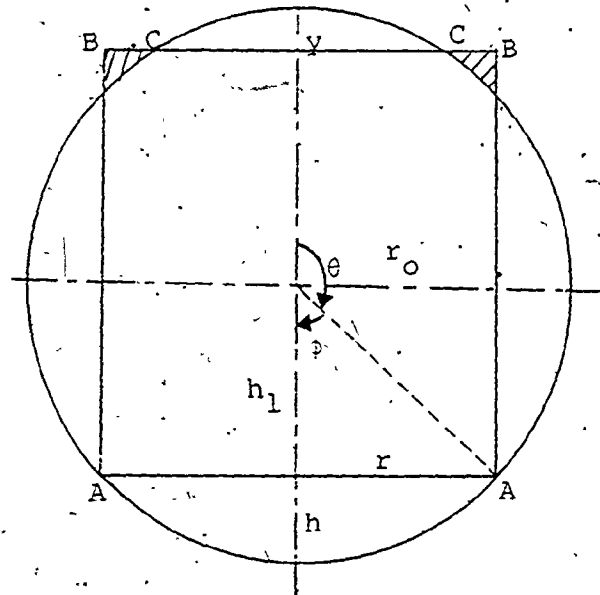
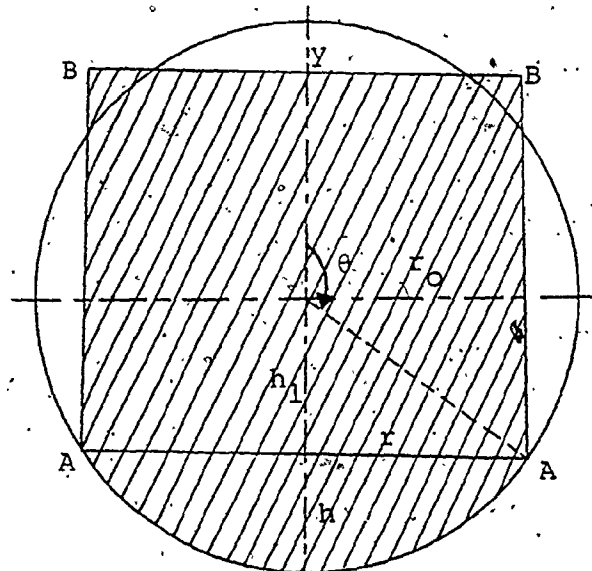FIGURE D-2   Calculations of $S_m$ and $S_t$ above the supports



FIGURE D-3   Calculations of $S_m$ and $S_t$ below the supports

Then substitution of the value for h into equation D.40 re-sults:

$$V_2 = \frac{5}{24} \pi r_o^3$$

Thus, the volume of the fluid above the supports is given by,

$$V_f = V_{Liq} - V_2$$

i.e.,

$$V_f = \frac{27}{24} \pi r_o^3 - \frac{\pi}{3} y^2 (3r_o - y) \tag{D.41}$$

The volume of the cylinder AABB is given as:

$$V_{cyl} = \pi r^2 (2r_o - h - y) \tag{D.42}$$

with the substitution of the value of h in equation D.42, we obtain:

$$V_{cyl} = \frac{3\pi}{4} r_o^2 (\frac{3}{2} r_o - y)$$

By taking the circle AA just above the supports, there-fore, the down pull W* is given by (11):

$$W^* = \text{weight of cylinder AABB} - \text{weight of liquid AACC.}$$

Thus:

$$W^* = [\pi r^2 (2r_o - h - y) - \{\frac{27}{24}\pi r_o^3 - \frac{\pi}{3} y^2 (3r_o - y)\}] \gamma \tag{D.43}$$

Rearranging and simplifying, the following expression may be written for the down pull:

$$W^* = \{\frac{\pi}{3} y^2 (3r_o - y) - \frac{3}{4} \pi r_o^2 y\} \gamma \qquad (D.44)$$

Since the meridional stress is given by (11):

$$S_m = \frac{W^*}{2\pi r t \sin\theta}$$

Therefore, substitution for $W^*$ from equation D.44, as well as for $r$ and $\sin\theta$ and arranging, the following expression is obtained for the meridional stresses above the supports:

$$S_{m_1} = \frac{2\gamma}{3r_o t} \{\frac{1}{3} y^2 (3r_o - y) - \frac{3}{4} r_o^2 y\} \qquad (D.45)$$

Also, the tangential stress is given by (8):

$$S_t = \frac{W_{cyl} + W_f}{2\pi r_o t \sin^2\theta}$$

Thus, substitution for $W_{cyl}$, $W_f$ and $\sin\theta$ and rearranging results in the following expression for the tangential stresses above the supports:

$$S_{t_1} = \frac{2\gamma}{3r_o t} \{\frac{9}{4} r_o^3 - \frac{3}{4} r_o^2 y - \frac{1}{3} y^2 (3r_o - y)\} \qquad (D.46)$$

(ii)  The Stresses Below the Supports

With reference to Figure D.3, and taking the circle AA just below the supports, we have:

$W^{**}$ is the weight of a body of liquid bounded by a cylinder $r$ from the top surface down and by the spherical container bottom below.  Consequently, the following expression

may be written for $W^{**}$:

$$W^{**} = [\pi r^2 (2r_o - h - y) + \frac{1}{3} \pi h^2 (3r_o - h)] \gamma \qquad (D.47)$$

Substituting for $h$ and $r$ and rearranging, the following equation results:

$$W^{**} = (\frac{4}{3} \pi r_o^3 - \frac{3}{4} \pi r_o^2 y) \gamma \qquad (D.48)$$

Since the meridional stress below the supports is given by (11):

$$S_{m_2} = \frac{W^{**}}{2\pi r t \sin\theta}$$

Therefore, upon substitution for $W^{**}$, $r$ and $\sin\theta$ we obtain:

$$S_{m_2} = \frac{2\gamma}{3t} \{\frac{4}{3} r_o^2 - \frac{3}{4} r_o y\} \qquad (D.49)$$

The tangential stress below the supports is given in terms of the meridional stress as follows:

$$S_{t_2} = \frac{Pr_o}{t} - S_{m_2}$$

Thus, upon substitution for $S_{m_2}$ and rearranging, the following expression for the tangential stress below the supports may be obtained:

$$S_{t_2} = \frac{3Pr_o - 2\gamma(\frac{4}{3} r_o^2 - \frac{3}{4} r_o y)}{3t} \qquad (D.50)$$

The corresponding strains are obtained by using Hook's Law (65):

$$e_r = \frac{1}{E}(S_m - 2\mu S_t)$$

$$e_t = \frac{S_t}{E}(1-\mu) - \frac{\mu}{E} S_m$$

The following expressions for strains above and below the supports for both meridional and tangential directions are obtained upon substitution of the stress-expression in equations D.45, D.46, D.49 and D.50.

$$e_{r_1} = \frac{2\gamma}{3r_o tE}[y^2 r_o(1+2\mu) - \frac{3}{4}r_o^2 y(1-2\mu) - \frac{1}{3}y^3 - \frac{9}{2}\mu r_o^3] \qquad (D.51)$$

$$e_{t_1} = \frac{2\gamma}{3r_o tE}[\frac{9}{4}r_o^3(1-\mu) - \frac{3}{4}r_o^2 y(1-2\mu) - y^2 r_o + \frac{1}{3}y^3] \qquad (D.52)$$

$$e_{r_2} = \frac{2\gamma}{3r_o tE}[(\frac{4}{3}r_o^3 - \frac{3}{4}r_o^2 y)(1+2\mu) - \frac{3P\mu r_o^2}{\gamma}] \qquad (D.53)$$

$$e_{t_2} = \frac{2\gamma}{3r_o tE}[\frac{3}{4}r_o^2 y - \frac{4}{3}r_o^3 + \frac{3P}{2\gamma} r_o^2(1-\mu)] \qquad (D.54)$$

From the definition of strain energy, we have

$$W_S = \int \frac{1}{2} S. e. dV$$

Therefore, the following expressions for strain energy may be written

$$W_{S_1} = \int \frac{1}{2} S_{m_1}.e_{r_1}.dV_1 + \int \frac{1}{2} S_{t_1}.e_{t_1}.dV_1 \qquad (D.55)$$

$$W_{S_2} = \int \frac{1}{2} S_{m_2}.e_{r_2}.dV_2 + \int \frac{1}{2} S_{t_2}.e_{t_2}.dV_2 \qquad (D.56)$$

Upon substitution of the expressions for stresses and corresponding strains in equations D.55 and D.56 and rearranging, the following expressions for strain energy above and below the supports may be obtained:

$$W_{S_1} = \frac{2\gamma^2 \pi y^2}{27 r_o^2 t^2 E} (3r_o - y) [\frac{81}{16} r_o^6 (1-\mu) - \frac{27}{16} r_o^5 y (2-5\mu)$$

$$- \frac{9}{8} r_o^4 y^2 (3+4\mu) + \frac{3}{4} r_o^3 y^3 (2-\mu) + 2 r_o^2 y^4 (1+\mu)$$

$$- \frac{2}{3} r_o y^5 (2+\mu) + \frac{2}{9} y^6] \tag{D.57}$$

$$W_{S_2} = \frac{5\pi r_o^5 \gamma}{72 E t^2} [\frac{3P^2}{2\gamma} (1-\mu) + P(\frac{3}{4} y - \frac{4}{3} r_o)(2-\mu) + \gamma(\frac{3}{8} y^2 - \frac{4}{3} y r_o$$

$$+ \frac{32}{27} r_o^2)] + \frac{5\pi r_o^5 \gamma^2}{54 E t^2} [(\frac{4}{3} r_o - \frac{3}{4} y)^2 (1+2\mu) - \frac{3P\mu}{\gamma}(\frac{4}{3} r_o - \frac{3}{4} y)] \tag{D.58}$$

The total strain energy which results from the mass effect only is obtained as the sum of the strain energies given by expressions D.57 and D.58 and is given by the following equation:

$$W_{S_m} = \frac{2\gamma^2 \pi y^2}{27 r_o^2 t^2 E} (3r_o - y) [\frac{81}{16} r_o^6 (1-\mu) - \frac{27}{16} r_o^5 y (2-5\mu) - \frac{9}{8} r_o^4 y^2 (3+4\mu)$$

$$+ \frac{3}{4} r_o^3 y^3 (2-\mu) + 2 r_o^2 y^4 (1+\mu) - \frac{2}{3} r_o y^5 (2+\mu) + \frac{2}{9} y^6]$$

$$+ \frac{5\gamma \pi r_o^5}{72 t^2 E} [\frac{3P^2}{2\gamma}(1-\mu) + P(\frac{3}{4} y - \frac{4}{3} r_o)(2-\mu) + \gamma(\frac{3}{8} y^2 - \frac{4}{3} y r_o + \frac{32}{27} r_o^2)]$$

$$+ \frac{5\gamma^2 \pi r_o^5}{54 t^2 E} [(\frac{4}{3} r_o - \frac{3}{4} y)^2 (1+2\mu) - \frac{3P\mu}{\gamma}(\frac{4}{3} r_o - \frac{3}{4} y)] \tag{D.59}$$

## APPENDIX E

## SURFACE ENERGY EQUATIONS

The change in fluid surface energy which arises due to an energy addition process conducted on a constant mass two-phase fluid sample contained in a spherical calorimeter is given by the following expression:

$$W_{S.E.} = \sigma \pi (R_2^2 - R_1^2) \qquad (E.1)$$

where $R_1$ and $R_2$ are the radii of the liquid vapour interface at the initial and final saturation states respectively.

The height of the vapour cap, h, is related to the radius of the liquid vapour interface $R_1$ by the following trigonometric relation:

$$R_1^2 = R^2 - (R^2 - 2Rh + h^2)$$
$$= 2Rh - h^2 \qquad (E.2)$$

where R is the radius of the calorimeter. The height of the vapour cap, h, in turn may be expressed in terms of the vapour volume, the total mass contained in the calorimeter and certain thermodynamic saturation quantities for the liquid and gaseous phases of the fluid sample.

Specifically, in order to evaluate h, it is necessary

to start with the following constant volume identity,

$$V = V_f + V_g \qquad (E.3)$$

where

V is the total volume of the calorimeter (which is assumed to be a constant throughout energy addition process),

$V_f$ is the total volume of liquid at a given saturation state, and

$V_g$ is the total volume of vapour at a given saturation state.

Equation E.3 may be rewritten in terms of the masses and specific volumes of the liquid and vapour saturation states.

$$V = m_f v_f + m_g v_g \qquad (E.4)$$

Since

$$M = m_f + m_g \qquad (E.5)$$

where M is the total mass and is constant for a particular filling during a given energy addition process,

$m_f$ and $m_g$ are the masses of the liquid and vapour saturation states.

It follows from equations E.4 and E.5 that the masses of liquid and vapour are given in terms of the specific volumes and the total mass by the following expression:

$$m_f = \frac{V - Mv_g}{v_f - v_g} \quad \text{and} \quad m_g = -\left(\frac{V - Mv_f}{v_f - v_g}\right) \qquad (E.6)$$

Upon substitution for V from $V = Mv$, where v is the specific volume defining the heterogenous two phase system, we obtain:

$$m_f = M \frac{v_g - v}{v_g - v_f}$$

$$m_g = M \frac{v - v_f}{v_g - v_f} \qquad (E.7)$$

Upon substitution of $m_f$ and $m_g$ from equations E.7 back into equation E.4, the following equation is obtained:

$$V = M v_f \frac{v_g - v}{v_g - v_f} + M v_g \frac{v - v_f}{v_g - v_f} \qquad (E.8)$$

Comparison of equations E.3 and E.8 results in the following expression for the total volume of vapour at initial state.

$$V_g = M v_g \frac{v - v_f}{v_g - v_f} \qquad (E.9)$$

It can easily be shown that the volume of the vapour cap is:

$$V_g = \frac{1}{3} \pi h^2 (3R - h) \qquad (E.10)$$

Equations E.9 and E.10 yield the following relationship:

$$M v_g \frac{v - v_f}{v_g - v_f} = \frac{1}{3} \pi h^2 (3R - h) \qquad (E.11)$$

For a given constant mass constant volume two phase energy addition process, the volume of the vapour cap changes as the two phase fluid sample passes through intermediate saturation states. Specifically, both the volume and height of the vapour cap are functions of the saturation temperature as well as functions of the mass loading.

Equation E.10 can be written as,

$$h^3 - 3Rh^2 + \frac{3V_g}{\pi} = 0 \qquad (E.12)$$

The solutions of this equation are:

$$h_I = R[1 + 2\cos\{\frac{1}{3}\cos^{-1}(1 - \frac{2V_g}{V})\}] \qquad (E.13)$$

$$h_{II} = R[1 + 2\cos\{\frac{1}{3}\cos^{-1}(1 - \frac{2V_g}{V}) + \frac{2\pi}{3}\}] \qquad (E.14)$$

$$h_{III} = R[1 + 2\cos\{\frac{1}{3}\cos^{-1}(1 - \frac{2V_g}{V}) + \frac{4\pi}{3}\}] \qquad (E.15)$$

In order to determine the range of validity of these solutions for different fillings, equation E.12 was arranged to read,

$$4(\frac{V_g}{V}) = 3(\frac{h}{R})^2 - (\frac{h}{R})^3$$

and if $y = \frac{h}{R}$, we have

$$y^3 - 3y^2 = -4(\frac{V_g}{V}) \qquad (E.16)$$

By differentiating the function $f(y) = y^3 - 3y^2$ twice, it was found to have a maximum at $y=0$ and a minimum at $y=2$. The following graph was thus obtained for $f(y)$ in the range of physical interest.

Testing the solutions given by equations E.13, E.14 and E.15 for the function given by Figure E.1, the following solution was found to be valid at all points and for all fillings:

$$h = R[1 + 2\cos\{\tfrac{1}{3}\cos^{-1}(1 - \tfrac{2V_g}{V}) + \tfrac{4\pi}{3}\}] \qquad (E.17)$$

The value of $h_1$ for the height of the vapour cap at the initial saturation temperature is:

$$h_1 = R[1 + 2\cos\{\tfrac{1}{3}\cos^{-1}(1 - \tfrac{2V_{g_1}}{V}) + \tfrac{4\pi}{3}\}] \qquad (E.18)$$

Similarly, the height of vapour at final temperature is:

$$h_2 = R[1 + 2\cos\{\tfrac{1}{3}\cos^{-1}(1 - \tfrac{2V_{g_2}}{V}) + \tfrac{4\pi}{3}\}] \qquad (E.19)$$

With reference to Figure E.2, we may write the trigonometric relationship,

$$R^2 = (R - h_1)^2 + R_1^2 \qquad (E.20)$$

Substitution of the value for $h_1$ from equation E.18 into equation E.20 and rearranging, results in the following expression for the radius of curvature at the initial state $R_1$.
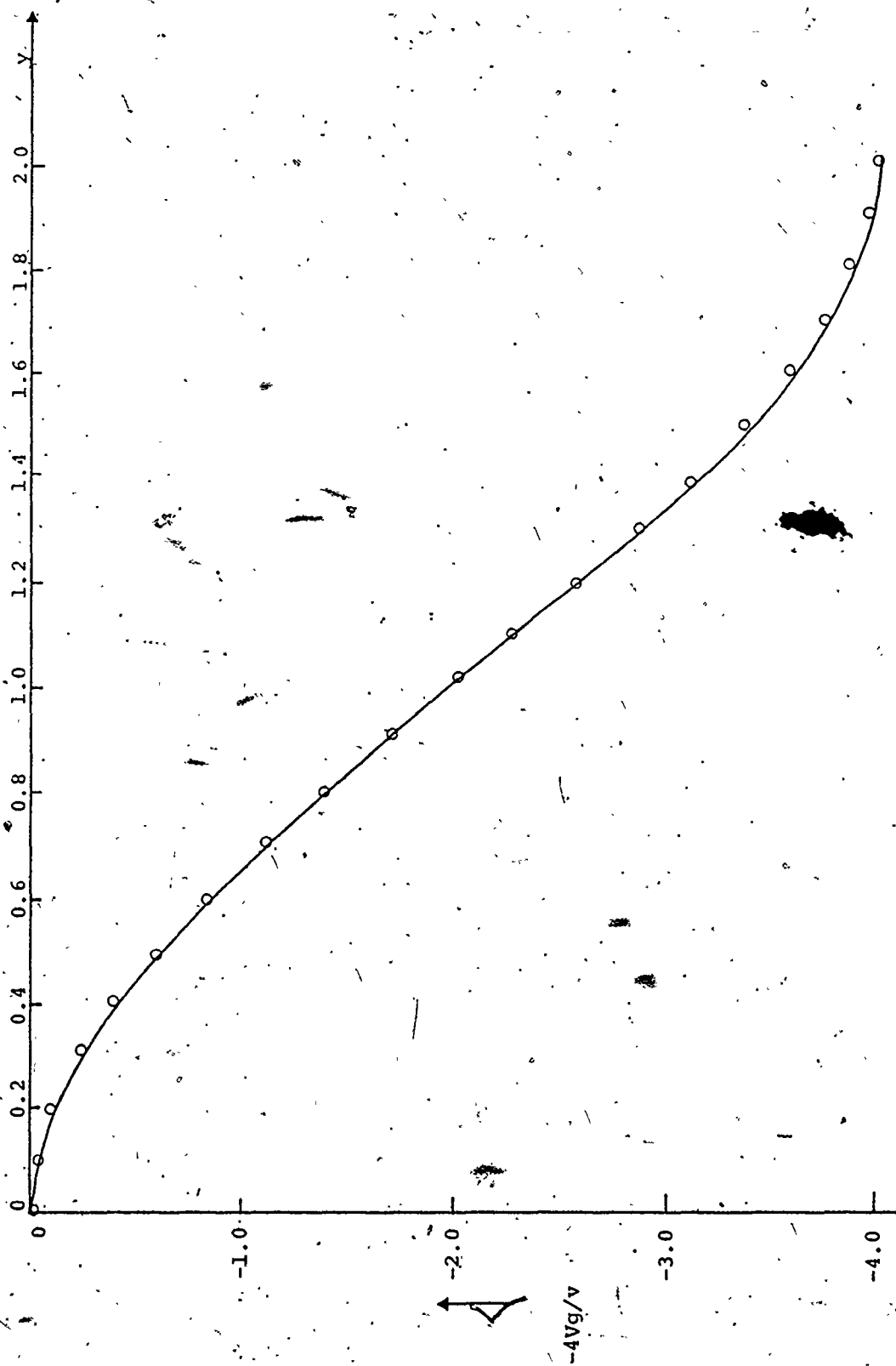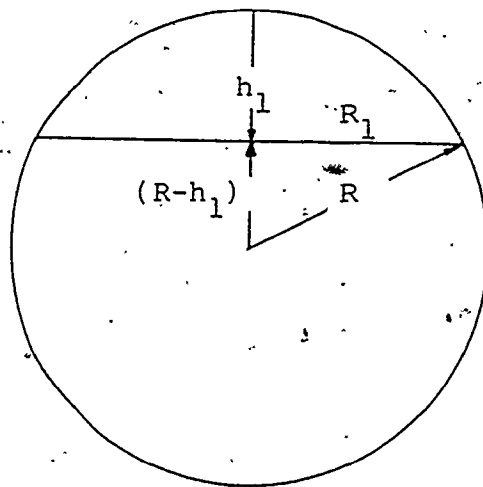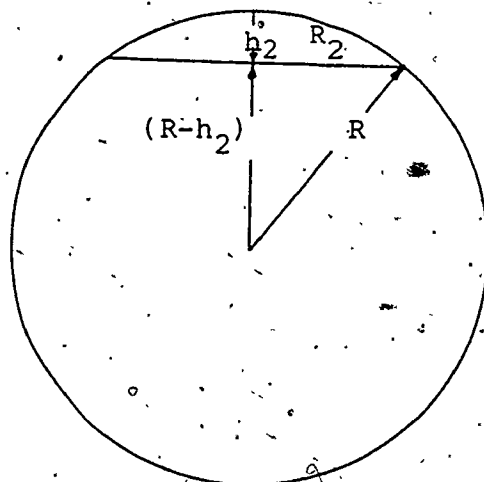
FIGURE E-1  The function $f(y) = y^3 - 3y^2$ vs $Vg/v$

(a)



(b)

FIGURE E-2    Geometric calculations of vapour heights
for vapour condensation process

$$R_1^2 = R^2 \{1 - 4 \cos^2\{\frac{1}{3} \cos^{-1}(1 - \frac{2V_{g_1}}{V}) + \frac{4\pi}{3}\}\} \qquad (E.21)$$

A similar expression is obtained for the radius of curvature at the final temperature $R_2$,

$$R_2^2 = R^2 \{1 - 4 \cos^2\{\frac{1}{3} \cos^{-1}(1 - \frac{2V_{g_2}}{V}) + \frac{4\pi}{3}\}\} \qquad (E.22)$$

Upon substitution of the expressions for $R_1$ and $R_2$ into equation E.1, the following equation for the change in the surface energy is obtained:

$$W_{S.E.} = 4\pi R^2 \sigma [\cos^2\{\frac{1}{3} \cos^{-1}(1 - \frac{2V_{g_2}}{V}) + \frac{4\pi}{3}\}$$

$$- \cos^2\{\frac{1}{3} \cos^{-1}(1 - \frac{2V_{g_1}}{V}) + \frac{4\pi}{3}\}] \qquad (E.23)$$

For the net surface energy to be obtained, two equations as equation E.23 are necessary; one for the high filling case and the other for the low filling case. Therefore, if equation E.23 represents the surface energy change for the high filling, then a similar equation represents the surface energy for the low filling, i.e.

$$(W_{S.E.})_{L.F.} = 4\pi R^2 \sigma [\cos^2\{\frac{1}{3} \cos^{-1}(1 - \frac{2V_{g_4}}{V}) + \frac{4\pi}{3}\}$$

$$- \cos^2\{\frac{1}{3} \cos^{-1}(1 - \frac{2V_{g_3}}{V}) + \frac{4\pi}{3}\}] \qquad (E.24)$$

The net surface energy equation is obtained from equations E.23 and E.24 and is written in the following general

form:

$$W_{S.E._{net}} = (W_{S.E.})_{H.F.} - (W_{S.E.})_{L.F.}$$

$$W_{S.E._{net}} = 4\pi R^2 \sigma [\cos^2(\theta_2) - \cos^2(\theta_1) - \cos^2(\theta_4) + \cos^2\theta_3] \quad (E.25)$$

where

$$\theta_1 = \frac{1}{3}\cos^{-1}(1 - \frac{2V_{g_1}}{V}) + \frac{4\pi}{3} \quad (E.26)$$

$$\theta_2 = \frac{1}{3}\cos^{-1}(1 - \frac{2V_{g_2}}{V}) + \frac{4\pi}{3} \quad (E.27)$$

$$\theta_3 = \frac{1}{3}\cos^{-1}(1 - \frac{2V_{g_3}}{V}) + \frac{4\pi}{3} \quad (E.28)$$

$$\theta_4 = \frac{1}{3}\cos^{-1}(1 - \frac{2V_{g_4}}{V}) + \frac{4\pi}{3} \quad (E.29)$$

Numerical values of net surface energy are thus obtained upon substitution of the constants as well as specific volumes in equation E.25.

APPENDIX F

## F.1 LIGHT WATER SAMPLE PURIFICATION

Ordinary distilled water taken from a communal supply
was used in the research reported here.  The water was puri-
fied and degassed by distillation in a special Corning all-
glass water distillation unit, as shown in operation in
Figure F-1.  The electrical conductivity of the triple dis-
tilled and degassed water was found to be $1.8 \times 10^{-6}$ mho per
cm.  It was measured by a water purity indicator shown in
Figure F-2.

## F.2 CHARGING PROCEDURE

After the sample was distilled and collected in a glass
container, it was degassed by boiling for approximately 10
minutes using a hot plate as shown in Figure F-3.  The glass
container was then closed, turned over and connected to the
vacuum as shown in Figure F-4 in order to be degassed com-
pletely, as indicated by the dying away of boiling activity.
The water sample was then allowed to return to room tempera-
ture, the filling valve closed and the container disconnected
from the vacuum.  The glass container with its charge of
water and filling valve was initially weighed, connected to
the filling tube of the calorimeter as shown in Figure F-5
and the calorimeter and filling tube were then evacuated to

244

FIGURE F-1. View of the Water Distillation Unit

FIGURE F-2  View of the Water Purity Indicator
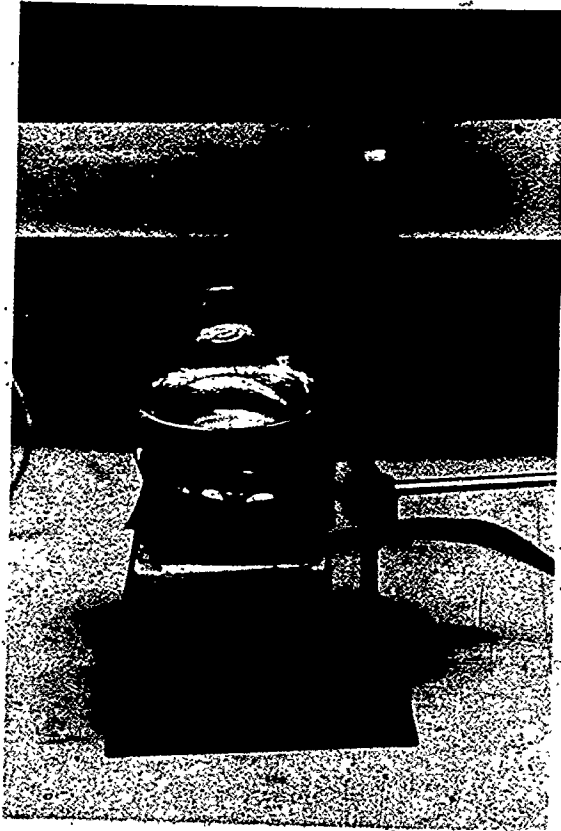
FIGURE F-3  Water Boiled for Degassing

FIGURE ⬥-4   Water Container Connected to Vacuum

FIGURE F-5   Charging Process

a pressure of about 0.003 mm. Hg.

After evacuation, the vacuum valve was closed and the filling valve opened. Placing a hot plate under the container, and with the filling valve open, the water sample was forced into the calorimeter by its vapour pressure. The high pressure valve was then closed and the container with the filling tube detached was weighed with a Mettler balance having a sensitivity of 0.0001 grams. The weight of sample charged into the calorimeter was obtained by subtracting the final weight of the container and its contents from their initial weight.

## APPENDIX G

## LIST OF EQUIPMENT

1. Absolute Temperature Measurement

   Isolating Potential Comparator, Model 9800, S/N 25889
   Guildline Instrument Company Limited.

   Four Terminal Variable Resistor, Model 9801-T, S/N 26124
   Guildline Instrument Company Limited.

   Laboratory Standard Resistance Thermometer, S/N 331
   Rosemount Engineering Company Limited.

   Photo Cell Galvanometer Amplifier, Model 9460, S/N 180641
   Guildline Instrument Company Limited.

   Spotlight Galvanometer Model 9461-A, S/N 26605 Guildline
   Instrument Company Limited.

2. Power Measurement

   Multiple Standard Resistors, Model 9200, S/N 25799,
   Guildline Instrument Company Limited.

   Spotlight Galvanometer, Model 2430-A, S/N 1693079, Leeds
   and Northrup Company Limited.

   Volt Box, Model 2851, S/N M-3545, Honeywell Control Com-
   pany Limited.

   Vernier Potentiometer, S/N C-391692, Cambridge Instru-
   ment Company Limited.

   Precision Quartz Crystal Timer, U.W.O. Shop.

3. Temperature Difference Measurement and Control

    DC Microvolt Amplifier, Cat. 9835-B, Leeds and Northrup

        Company Limited.

    Deviation Amplifier, Model 687293, Honeywell Control

        Limited.

    Electronic 16 Laboratory Recorder, S/N K 710 951 8001,

        Honeywell Control Limited.

    Silicon Control Rectifier (SCR) Model R7170A, Honeywell

        Control Limited.

4. Mass Measurement

    Mettler Analytical Balance, 0-1000 gram, Model K-4,

        Fisher Scientific Company Limited.

5. Power Supply Equipment

    D.C. Power Supply, Model QR 60-6.

    D.C. Power Supply, Model LH122A FM, Lambda Electronic

        Corporation.

    D.C. Power Supply, Model LH125A FM, Lambda Electronic

        Corporation.

    D.C. Power Supply, Model LP-531-FM, Lambda Electronic

        Corporation.

    D.C. Power Supply, Model JQE, Kepco Power Supply Inc.

    D.C. Power Supply, Model 865C, Harrison Laboratories Inc.

    D.C. Power Supply, Model SY 60-18, NJE Corporation.

6. Miscellaneous

Vacuum Pump, S/N 60038, Sargent-Welch Scientific Company.

McLeod Gage, S/N 85660, The Pennwalt Corporation.

Automatic Three Liter Water Still, S/N 0113, Corning
Company Limited.

# BIBLIOGRAPHY

1. Baker, B.L. "Heat Capacity and Thermodynamic Properties of Saturated Deuterium Oxide". AECU-4738, 1959.

2. Barber, C.R. "International Practical Temperature Scale of 1968", Nature, Vol. 222, pp. 929-931, 1969.

3. Bedford, R.E. and Thomas, H.P. "Practical Temperature Scales Between 11 K and 273 K", Metrologia, Vol. 4, No. 1, pp. 14-30, 1968.

4. Bedford, R.E. and Barber, C.R. "Relationships Between The International Practical Temperature Scale of 1968 and the NBS-55, NPL-61, PRMI-54, and PSU-54 Temperature Scales in the Range From 13.81 to 90.188 K", Metrologia, Vol. 5, No. 2, pp. 47-49, 1969.

5. Bedford, R.E. and Kirby, C.G.M. "Notes On The Application of The International Practical Temperature Scale of 1968", Metrologia, Vol. 5, No. 3, pp. 83-87, 1969.

6. Berry, R.J. "Calibration of One Platinum Resistance Thermometer", NRC Report No. APH-1322, 1965.

7. Chan, J.S. "A Calorimeter Apparatus for Studying the Thermodynamic Properties of Heavy Water and Measurements On the Enthalpy of Saturated Liquid Heavy Water", Ph.D. Thesis, Faculty of Engineering Science, The University of Western Ontario, 1970.

8. Chan, J.S. and Nowak, E.S. "The Thermal Behaviour of Saturated Heavy Water and Light Water", presented at the 6th Symposium on Thermophysical Properties, August 1973.

9. Cockett, A.H. and Ferguson, A. "The Specific Heat of Water and of Heavy Water", Philosophical Magazine and Journal of Science, Vol. 29, Series 7, pp. 185-199, 1940.

10. Condon, E.U. and Odishaw, H. "Handbook of Physics", McGraw Hill Book Co., 1958.

11. Den Hartog, J.P. "Advanced Strength of Materials", McGraw Hill Book Company, 1952.

12. Feingold, A. and Gupta, K.G. "New Analytical Approach to The Evaluation of Configuration Factors in Radiation From Spheres and Infinitely Long Cylinders", Transactions of The American Society of Mechanical Engineers, Journal of Heat Transfer, pp: 69-76, 1970

13. Fiock, E.F. "A Review of Calorimetric Measurements on Thermal Properties of Saturated Water and Steam", Transactions of the American Society of Mechanical Engineers, Vol. 52, pp. 231-242, RSP 52-30, 1930.

14. Glasstone, S. and Sesonske, A. "Nuclear Reactor Engineering", Van Nostrand Reinhold Company, 1967.

15. Gopala Rao, R.V. and Gopalakrishnan "On The Surface Tension of Liquids", Z. Phys. Chemie, Leipsiz., Vol. 247, pp. 1-7, 1971.

16. Holman, J.P. "Heat Transfer", McGraw Hill Book Company, 1976.

17. Haywood, J.H. and Wilson, L.B. "The Strain Energy Expression for Thin Elastic Shells", Transactions of The American Society of Mechanical Engineers, Journal of Applied Mechanics, pp. 546-552, 1958.

18. Hussein, F. and Nowak, E.S. "Computer Operated Fully Automatic Data Acquisition System For An Adiabatic Calorimetric Facility", Report to the Faculty of Engineering Science, 1975.

19. Ivey, C.M. "A Constant Volume - Constant Mass System for Measuring the P-V-T Properties of Heavy Water and Measurements of the Saturated Vapour Pressure of Heavy Water", Ph.D. Thesis, Faculty of Engineering Science, The University of Western Ontario, 1975.

20. Jeener, J. "Low Temperature Mixing Calorimeter For Liquids", The Review of Scientific Instruments, Vol. 28, No. 4, pp. 263-265, 1957.

21. Kent, C.H. "Thermal Stresses in Spheres and Cylinders Produced by Temperatures Varying With Time", Transactions of The American Society of Mechanical Engineers, Journal of Applied Mechanics, APM 54-18, pp. 185-196, 1932.

22. Kingery, W.D. "Property Measurements At High Temperatures", John Wiley and Sons Inc., New York, 1959)

23. Knowles, J.K. and Reissner, E. "On Stress-Strain Relations and Strain Energy Expressions in the Theory of Thin Elastic Shells", Transactions of the American Society of Mechanical Engineers, Journal of Applied Mechanics, pp. 104-106, 1960.

24. Landau, L.D. and Lifshitz, E.M. "Fluid Mechanics", Addison-Wesley Publishing Co. Inc., pp. 230-244, 1959.

25. Le Neindre, B. and Vodar, B. "Experimental Thermodynamics - Volume II", Butterworths, London, 1975.

26. Love, A.E.H. "The Stress Produced in a Semi-Infinite Solid by Pressure on Part of the Boundary", Philosophical Transactions of the Royal Society of London, Vol. 228, Series A, pp. 377-420, 1929.

27. Love, T.J. "Radiative Heat Transfer", A Bell and Howell Company, 1968.

28. Martin, D.L. and Snowdon, R.L. "Continuous Heating Adiabatic Calorimeter for the Range 300 to $475^0$K, Canadian Journal of Physics, Vol. 44, pp. 1449-1465, 1966.

29. McCormack, P.D. "A Theory of Surface Tension Based On The Interaction Between Orbiting Molecules", Surface Science - North Holland Publishing Co., Vol. 26, pp. 375-388, 1971.

30. McCullough, J.P. and Scott, D.W. "Experimental Thermodynamics - Volume I", Plenum Press, New York, 1968.

31. Novozhilov, V.V. "The Theory of Thin Shells", P. Noordhoff Ltd. - Groningen - The Netherlands, 1959.

32. Nowak, E.S. "A Rational Equation of State for Water and Water Vapour in The Critical Region", Transactions of The American Society of Mechanical Engineers, Paper 63-HT-35, pp. 320-326, 1964.

33. Nowak, E.S. "A Colorimetric Investigation of The Enthalpy of Heavy Water", CR 15 D-4609, 1969.

34. Nowak, E.S., Grosh, R.J. and Liley, P.E. "Smoothed Pressure-Volume-Temperature Data for Water in The Critical Region Derived From Experimental Measurements", Transactions of The American Society of Mechanical Engineers, Journal of Heat Transfer, Vol. 83, Series C, pp. 14-26, 1961.

35. Nowak, E.S. and Konanur, A.K. "An Analytical Investigation of Free Convection Heat Transfer to Supercritical Water", Transactions of The American Society of Mechanical Engineers, Journal of Heat Transfer, pp. 345-350, 1970.

36. Nowak, E.S. "The Enthalpy of Saturated Heavy Water Liquid", presented at the 84th Annual Meeting of the Engineering Institute of Canada, Ottawa, September 1970.

37. Nowak, E.S. and Chan, J.S. "An Experimental Investigation of the Enthalpy of Saturated Heavy Water Liquid", Transactions of The American Society of Mechanical Engineers, Journal of Heat Transfer, pp. 422-426, 1971.

38. Olcer, N.Y. "Unsteady Temperature Distribution in a Sphere Subjected to Time-Dependent Surface Heat Flux and Internal Heat Source", Transactions of The American Society of Mechanical Engineers, Journal of Heat Transfer, pp. 45-50, 1969.

39. Osborne, N.S. and Van Dusen, M.S. "Specific Heat of Liquid Ammonia", Journal of Research of the National Bureau of Standards, Vol. 14, pp. 397-431, 1917.

40. Osborne, N.S. and Van Dusen, M.S. "Latent Heat of Vaporization of Ammonia", Journal of Research of the National Bureau of Standards, Vol. 14, pp. 439-472, 1917.

41. Osborne, N.S. "An Aneroid Calorimeter for Specific and Latent Heats", Journal of Research of the National Bureau of Standards, Vol. 14, pp. 133-157, 1917.

42. Osborne, N.S. "Calorimetry of Saturated Fluids", Journal of Optical Soc. America and Rev. Sci. Inst., Vol. 8, pp. 519-540, 1924.

43. Osborne, N.S., Stimson, H.F. and Sligh, T.S. "A Flow Calorimeter for Specific Heats of Gases", Journal of Research of the National Bureau of Standards, Vol. 20, pp. 119-151, 1925.

44. Osborne, N.S., Stimson, H.F. and Fiock, E.F. "A Calorimetric Determination of Thermal Properties of Saturated Water and Steam From $0^0$ to $270^0 C$", Journal of Research of the National Bureau of Standards, Vol. 5, pp. 411-480, 1930.

45. Osborne, N.S. "Calorimetry of a Fluid", Transactions of the American Society of Mechanical Engineers, Vol. 52, Paper FSP-52-29, pp. 221-229, 1930.

46. Osborne, N.S. and Meyers, C.H. "A Formula and Tables for the Pressure of Saturated Water Vapor in the Range 0⁰ to 374⁰C", Journal of Research of the National Bureau of Standards, Vol. 13, pp. 1-20, 1934.

47. Osborne, N.S., Stimson, H.F. and Ginnings, D.C. "Calorimetric Determination of the Thermodynamic Properties of Saturated Water in Both the Liquid and Gaseous States From 100 to 374⁰C", Journal of Research of the National Bureau of Standards, Vol. 18, pp. 389-445, 1937.

48. Osborne, N.S., Stimson, H.F. and Ginnings, D.C. "Thermal Properties of Saturated Water and Steam", Journal of Research of the National Bureau of Standards, Vol. 23, pp. 261-270, 1939.

49. Osborne, N.S., Stimson, H.F. and Ginnings, D.C. "Measurements of Heat Capacity and Heat of Vaporization of Water in the Range 0⁰ to 100⁰C", Journal of Research of the National Bureau of Standards, Vol. 23, pp. 197-260, 1939.

50. Özisik, M.N. "Radiative Transfer", John Wiley and Sons Inc., New York, 1972.

51. Perry, R.H. and Chilton, C.H. "Chemical Engineers Handbook", McGraw Hill Book Company, pp. (3-240)-(3-241), 1973.

52. Popov, E.P., Penzien, J. and Rajan, M.K-S. "Stress Concentrations in Thin Spherical Shells", Transactions of The American Society of Mechanical Engineers, Journal of Engineering for Industry, pp. 231-236, 1966.

53. Rao, S.R. "Surface Studies by Thermochemical Measurements", Sci. Prog. Oxf., Vol. 59, pp. 91-108, 1971.

54. Rivkin, S.L. and Egorov, B.N. "Experimental Investigation of the Heat Capacity of Heavy Water", Atomnaya Energiya, Vol. 7, No. 5, pp. 462-465, 1959.

55. Rivkin, S.L. and Egorov, B.N. "Specific Heat of Heavy Water at High Temperatures and Pressures", Atomnaya Energiya, Vol. 14, No. 4, pp. 416-418, 1963.

56. Rohsenow, W.M. and Hartnett, J.P. "Handbook of Heat Transfer", McGraw Hill Book Co., 1973.

57. Schmidt, J.E. and Sonneman, G., "Transient Temperatures and Thermal Stresses in Hollow Cylinders Due to Heat Generation", Transactions of the American Society of Mechanical Engineers, Journal of Heat Transfer, pp. 273-278, 1960.

58. Sheindlin, A.E. and Gorbunov, N.I. "An Experimental Study of the Enthalpy of Water and Steam at Temperatures Up to $460^0 C$ and Pressures Up to 490 Bar" Teploenergetika, Vol. 11, No. 5, pp. 86-89, 1964.

59. Siegel, R. and Howell, J.R. "Thermal Radiation Heat Transfer", McGraw Hill Book Company, 1972.

60. Sparrow, E.M. and Cess, R.D., "Radiation Heat Transfer", Brooks/Cole Publishing Company, California, 1966.

61. Spiegel, M.R. "Mathematical Handbook of Formulas and Tables", McGraw Hill Book Company, 1968.

62. Stimson, H.F. "International Practical Temperature Scale of 1948", Journal of Research of the National Bureau of Standards, A - Physics and Chemistry, Vol. 65A, No. 3, pp. 139-145, 1961.

63. "The International Practical Temperature Scale of 1968", Adopted by the Comite International des Poids et Mesures, Metrologia, Vol. 5, No. 2, pp. 35-44, 1969.

64. Timoshenko, S.P. "Strenght of Materials", Part II, D. van Nostrand Company Inc., New York, 1962.

65. Timoshenko, S.P. and Goodyier, J.N. "Theory of Elasticity", McGraw Hill Book Company, 1970.

66. U.W.O. Computer Centre, "Interface Between PDP-11 and 2760 Digital Voltmeter Scanning Facility" Report to the Faculty of Engineering Science, 1977.

67. Vargaftik, N.B., Oleshchuk, O.N. and Belyakova, P.E. "Experimental Investigation of the Thermal Conductivity of Heavy Water", Atomnaya Energiya, Vol. 7, No. 5, pp. 465-468, 1959.

68. West, E.D. and Ginnings, D.C. "An Adiabatic Calorimeter for the Range $30^0$ to $500^0 C$", Journal of Research of the National Bureau of Standards, Vol. 60, No. 4, pp. 309-316, 1958.

69. West, E.D. "Heat Exchange in Adiabatic Calorimeters", Journal of Research of the National Bureau of Standards, Series A, Vol. 67A, No. 4, pp. 331-341, 1963.

70. Whalley, E. "The Thermodynamic and Transport Properties of Heavy Water", National Research Council Conference, Paper No. 4373, pp. 15-26, 1957.

71. White, W.P. "Calorimetry in Furnaces", Geophysical Laboratory, Carnegie Institution of Washington, pp. 1120-1136, 1929.

72. Wiebelt, J.A. "Engineering Radiative Heat Transfer", Holt, Rinehart and Winston Inc., New York, 1966.

73. Williamson, E.D. and Adams, L.H. "Temperature Distribution in Solids During Heating Or Cooling", Physical Review, Vol. 14, No. 2, pp. 99-114, 1919.

## VITA

NAME:              Fahmy Mahmoud Hussein

PLACE OF BIRTH:    Damietta, Egypt

YEAR OF BIRTH:     1947

POST-SECONDARY
EDUCATION AND      Alexandria University
DEGREES:           Alexandria, Egypt
                   1965-1970  B.Sc. (Nuclear Engineering)

                   Alexandria University
                   Alexandria, Egypt
                   1970-1972  B.Sc. (Physics)

                   University of Western Ontario
                   London, Ontario
                   1973-1974  M.Sc. (Physics)

                   University of Western Ontario
                   London, Ontario
                   1974-1978  Ph.D.

PUBLICATIONS:      Hussein, F.M., "Electron-Ion Recombination"
                   M.Sc. Thesis, U.W.O., 1974.

                   Hussein, F.M. and Nowak, E.S., "Computer
                   Operated Fully Automatic Data Acquisition
                   System For An Adiabatic Calorimetric
                   Facility", Report to the Faculty of
                   Engineering Science, University of Western
                   Ontario, June 1975.

                   Hussein, F.M., "Thermophysical Properties
                   Laboratory PDP 11/10 Minicomputer Pre-
                   liminary Instructions", Report to the
                   Faculty of Engineering Science, University
                   of Western Ontario, February 1977.

# END

## 5 09 78

# FIN